DOCTOR OF PHILOSOPHY

The role of pulmonary arterial stiffness in right ventricular remodelling in COPD

Weir-Mccall, Jonathan

Link to publication

The role of pulmonary arterial stiffness in right ventricular remodelling in COPD.

Jonathan Weir-McCall

A thesis submitted in fulfilment of the requirements for the

Degree of Doctor of Philosophy

Division of Molecular and Clinical Medicine,

Medical Research Institute,

University of Dundee

2017

TABLE OF CONTENTS

LIST OF TABLES

LIST OF FIGURES

ABBREVIATIONS

6MWT	6 minute walking test
BMI	Body Mass Index
BNP	Brain Natriuretic Peptide
BP	Blood pressure
CMR	Cardiac magnetic resonance
COPD	Chronic obstructive pulmonary disease
CRF	Case Report Form
DLCO	Diffusing capacity of the Lungs for Carbon Monoxide
ECG	Electrocardiogram
ECHO	Echocardiogram
FEF	Forced Expiratory Flow
FEV1	Forced expiratory volume in 1 second
FVC	Forced vital capacity
FISP	Fast imaging with steady state precession
FLASH	Fast imaging using low angle shot
GCP	Good Clinical Practice
GOLD	Global initiative for chronic Obstructive Lung Disease
HIC	Health Informatics Centre
HR	Heart Rate
hsCRP	High sensitivity C-reactive protein
HV	Healthy Volunteers
ICS	Inhaled Corticosteroid
KCO	Transfer factor for Carbon monoxide
LABA	Long Acting Beta Agonist
LAMA	Long Acting Muscarinic Antagonist
LPA	Left pulmonary artery
LV	Left Ventricle
LVEDV	Left ventricle end diastolic volume
LVEF	Left ventricle ejection fraction

LVESV	Left ventricle end systolic volume
LVMVR	Light ventricular mass to volume ratio
LVM	Left ventricular mass
LVSV	Left ventricle stroke volume
mMRC	Modified British Medical Research Council
MPA	Main pulmonary artery
MRA	Magnetic resonance angiography
MRI	Magnetic Resonance Imaging
NHV	Normal healthy volunteers
PA	Pulmonary artery
PAT	Pulmonary Acceleration Time
PC	Phase contrast
PFTs	Pulmonary Function Tests
PWV	Pulse Wave Velocity
RLV	Residual lung volume
ROI	Region of interest
RPA	Right pulmonary artery
RV	Right Ventricle
RVEDV	Right ventricle end diastolic volume
RVEF	Right ventricle ejection fraction
RVESV	Right ventricle end systolic volume
RVH	Right ventricular hypertrophy
RVM	Right ventricular mass
RVMVR	Right ventricular mass to volume ratio
RVSV	Right ventricle stroke volume
SABA	Short Acting Beta Agonist
SAMA	Short Acting Muscarinic Antagonist
SNR	Signal to noise ratio
SOP	Standard Operating Procedure
SSFP	Steady state free precession
TE	Time to echo
TLC	Total Lung Capacity

TMF/SMF	Trial/Study Master File
TR	Time to Recovery
VENC	Velocity Encoding
VMI	Ventricular mass index

AKNOWLEDGEMENTS

Entering a PhD and a world of full time research, leaving behind the clinical realm in which you have become accustomed is always challenging. Thanks to the guidance, help and support of innumerable people, this process was not only smooth but also incredibly interesting and energizing. Of the large team of people I have worked with over the last 4 years there are a few in particular whom I must thank individually:

Graeme Houston, who has not just been my supervisor in this PhD, but also my academic supervisor in my Clinical Lecturer post preceding this. Without the tireless yeas of support and numerous opportunities he has provided I would never have gained either the experience or knowledge necessary to design and undertake this study. His encouragement and advice over these last few years has been instrumental to the completion of this.

Allan Struthers and Brain Lipworth for their constant guidance and support over the last 4 years of my PhD and for the year prior to that when applying for the funding. Without their guidance and advice, none of this would have been possible.

Rory McCrimmon for his suggestion that I apply for the Scottish Translational Medicine and Therapeutics Initiative Wellcome Trust fellowship, and his help in the subsequent application process.

Declaration

I, Jonathan Weir-McCall, declare that this thesis is based on results obtained from investigations which I have personally carried out, and that the entire thesis is my own composition. I have consulted all the references cited within the text of this thesis. Any work other than my own is clearly stated in the text and acknowledged with reference to any relevant investigators or contributors. This thesis has never been presented previously, in whole or in part, for the award of any higher degree.

Signed:……………………………………………………………...

Dated:…………………………

SUPERVISOR STATEMENT

I, Professor Graeme Houston, confirm that Jonathan Weir-McCall has done this research under my supervision and that I have read this thesis. Also, the conditions of ordinance and relevant regulations of the University of Dundee have been fulfilled, thereby qualifying him to submit his thesis in the application for the degree of Doctor of Philosophy.

Signed:…………………………………………………………..

Dated:…………………………

SUMMARY

COPD is the second most common cause of pulmonary hypertension, and is a common complication of severe COPD with significant implications for both quality of life and mortality. Pulmonary arterial stiffening occurs early in the disease process before the development of overt pulmonary hypertension. Early detection would open this up as a potential therapeutic target before end stage arterial remodeling occurs. Traditionally the assessment of the arterial stiffness required right heart catheterization, however recent advance in MRI are yielding new opportunities to undertake this assessment non-invasively. Pulse wave velocity is one of the most commonly used techniques in the systemic circulation but has been poorly explored in the pulmonary circulation. This thesis was undertaken to test the hypothesis that pulmonary PWV would be elevated in COPD, and that this would correlate with right ventricular mass, and predict future adverse remodeling.

Two commonly used techniques are available for measuring PWV with MRI: the transit time technique and the flow-area technique. These techniques were applied in a cohort of young healthy volunteers (n=10) and older healthy volunteers (n=20). These techniques were repeated using on-table repetition and repetition at 6 months. These were also assessed during exercise in the young healthy volunteers. PWV did not differ between the two age groups (YHV 2.4±0.3 ms^{-1}, OHV 2.9±0.2 ms^{-1}, p=0.1). Using a high temporal resolution sequence through the RPA using the flow-area technique accounting for wave reflections yielded consistently better within-scan, interscan, intraobserver and

interobserver reproducibility. Exercise did not result in a change in PWV (mean (95% CI) of the differences: 0.10 (−0.5 to 0.9), p=0.49) despite a significant rise in heart rate (65±2 to 87±3, p<0.0001), blood pressure (113/68 to 130/84, p<0.0001) and cardiac output (5.4±0.4 to 6.7±0.6 L/min, p=0.004).

58 participants with COPD underwent pulmonary function tests, six-minute walk test, and cardiac MRI. These were compared with a cohort of 20 healthy controls. Cardiac MRI was used to quantify right and left ventricular mass and volumes, with phase contrast imaging of the main pulmonary artery in order to calculate pulmonary PWV and of the ascending and abdominal aorta in order to calculate the aortic pulse wave velocity. Those with COPD demonstrated evidence of pulmonary arterial stiffening and pulmonary vascular remodeling with higher pulmonary artery area at end diastole (COPD: 2.36 ± 0.56 cm^2/m$^{1.7}$ vs. HC: 2.14 ± 0.28 cm^2/m$^{1.7}$, p=0.027), reduced pulsatility (COPD: 24.88 ± 8.84 % vs. HC: 30.55 ± 11.28 %, p=0.021), reduced PAT (COPD: 104.0 ± 22.9 ms vs. HC: 128.1 ± 32.2 ms, p<0.001) and higher PWV (COPD: 2.62 ± 1.29 ms^{-1} vs. HC: 1.78 ± 0.72 ms^{-1}, p=0.001). Those with an elevated PWV did not demonstrate any difference in subjective breathlessness, exercise capacity, or any difference in right ventricular systolic function. Cardiac remodelling in COPD was instead that of a reduced preload with a lower RV end diastolic volume (COPD: 53.6±11.1 ml vs. HC: 59.9±13.0 ml,p=0.037) and RV stroke volume (COPD: 31.9±6.9 ml/m2 vs. HC: 37.1±6.2 m/m2l,p=0.003). Those with COPD had a non-significantly higher aortic PWV (COPD: 8.7 ± 2.7 ms^{-1} vs. HC: 7.4 ± 2.1 ms^{-1}, p=0.06), with aortic PWV correlating with left ventricular remodeling (rho=0.34, p=0.01).

34 participants with COPD underwent repeat imaging at 1 year. While there was a significant increase in pulmonary PWV (Baseline 2.30 ± 0.97, Follow-up: 3.39 ± 1.4 ms^{-1}, p<0.001) there was no significant change in ventricular mass or volumes.

This thesis has therefore proven its original hypothesis that pulmonary PWV is elevated in those with COPD. However we have seen that this elevation in PWV has no significant association with right ventricular remodeling either at baseline or at one-year follow-up. Instead we observed a pattern of ventricular remodeling that was more consistent with an under filled condition rather than an overloaded condition. Future work in COPD should thus be targeted at better understanding of the underpinning pathophysiological process behind this.

CHAPTER 1: Background and Literature Review

1 INTRODUCTION

Chronic obstructive pulmonary disease (COPD) is the fourth leading cause of morbidity and mortality in the UK, with this predicted to become the third most common cause of death by 2020, both in the UK and worldwide.(1,2) It is the only leading cause of mortality that is increasing in prevalence, with approximately 30,000 people in the UK dying each year from COPD.(3) Despite rapid advances in medicine over the past few decades and a fall in the general population mortality rate of 40%, no such improvement has been witnessed in patients with COPD, with static mortality rates in those with moderate and severe disease.(4) Despite the high mortality associated with the primary disease, 25-50% of COPD patients will die from cardiovascular complications rather than their underlying lung disease.(1) It is not just cardiac mortality that patients with COPD are at increased risk of, they are also at increased risk of cardiac morbidity with unrecognised heart failure in 20%, ischaemic heart disease in 30% and atrial fibrillation in 13%.(5,6)

Reduced FEV1 has been shown to be one of the strongest indicators for future cardiac death, second only to smoking and above that of blood pressure and cholesterol.(7) Poor FEV1 is also a strong predictor of ventricular arrhythmia, myocardial infarction, and heart failure, with the rate of decline in FEV1 independently predicting all cause and cardiac mortality.(7–11) While shared aetiologies, in particular smoking, could be suggested as

confounding factors, the association between FEV1 and cardiac mortality persists even after accounting for smoking status.(7)

A variety of models have been proposed for the interaction between COPD and cardiovascular disease which can be loosely grouped into 4 categories:(1)

Inflammation model

Lung hyperinflation model

Shared genetics model

Pulmonary hypertension model

The focus of this review will be on the pulmonary hypertension model, however, we will briefly review the merits of the other models prior to this.

1.1 INFLAMMATION MODEL

The inflammatory model is based on the premise that inflammatory mediators generated in the lung are carried in the circulation to the coronary arteries and systemic arteries where they promote atherosclerosis – itself a known inflammatory process.(12) An excellent overview can be found on the topic by Sinden and Stockley.(13) Circulating VEGF, hsCRP, TNFα and fibrinogen are all elevated in patients with COPD consistent with an inflammatory process,(14–18) and alveolar macrophages reacting to particulate inhalation have been shown to upregulate systemic inflammation. The ability of proteins to move across from the lung surface to the systemic circulation has been documented in

animals and humans, both in healthy lungs and in those with COPD, thereby providing evidence of the possibility of inflammatory mediator migration.(19–21) Furthermore the discovery of circulating microparticles and microRNAs, known to modulate endothelial function, make this an attractive theory.(22)

Indirect evidence of this is provided by evidence of arterial and endothelial dysfunction in patients with COPD. Arterial stiffness is increased in patients with COPD compared with controls matched for age and smoking status.(23)   The degree of arterial stiffening correlates with the extent of emphysematous changes within the lungs, IL-6 levels and hsCRP levels.(23–25) Furthermore a study by Dransfield et al. showed an improvement of PWV with inhaled fluticasone-salmetrol, although this was limited to those with elevated arterial stiffness at baseline.(26) Arterial stiffness is important as increased stiffness is a known marker of future cardiovascular risk due to its effects of increasing afterload and impairing diastolic coronary blood flow.(27) It also contributes to end organ damage by transmitting the high pressure fluctuations present in the central vessels to the less resilient microvasculature.(28) This may explain the association between low FEV1 and microvascular damage.(29) Endothelial function is also impaired in COPD compared with healthy volunteers and smokers without COPD.(30,31)   The importance of peripheral endothelial function has been ascribed to the correlation between the peripheral and coronary endothelial function(32,33), however this link has been called into doubt.(34,35) Despite the apparent lack of correlation, endothelial dysfunction remains a strong and independent predictor of future cardiovascular events.(36) However, despite the apparent strong link between COPD and vascular function, Barr et al. found no correlation between

lung function or emphysema and coronary artery atherosclerosis as measure by CT calcium score in early COPD.(37)

1.2 PULMONARY HYPERINFLATION MODEL

Pulmonary hyperinflation occurs due to lung parenchymal destruction with loss of lung elasticity combined with expiratory airflow obstruction.(38) This in turn causes an increase in intrathoracic (and therefore intrapleural) pressures due to a high intrinsic positive end-expiratory pressure.(39) Left ventricular hypertrophy has been noted in patients with COPD and hyperinflation(40,41), and has been posited to be due to these effects of raised intrapleural pressures increasing left ventricular transmural pressure thereby augmenting shear stress.(42) The increase in left ventricular mass of 5% per SD rise in %emphysema within the lungs is comparable the per SD rise in systolic blood pressure.(41) This is of importance as a 5% rise in LV mass is associated with a 7% increased risk of cardiovascular death and a 20% increased risk of developing heart failure.(43) However, a study by Jorgensen et al. showed no evidence of increased diastolic stiffness in patients with severe COPD on invasive LV pressure measurements.(44) Indeed several studies have shown that apparent diastolic dysfunction with low left ventricular end diastolic volumes in patients with hyperinflation is due to a low preload secondary to impaired filling rather than left ventricular stiffness causing impaired relaxation.(44–47) While early studies demonstrated a strong independent predictive value of hyperinflation on mortality,(48) more recent studies have shown this to be lost when the transfer co-

efficient is taken into account weakening the prospect of a significant mechanistic link.(49,50)

1.3 SHARED GENETICS MODEL

The concept of shared genetics is similar to that of shared aetiologies, and stands on its own as well as feeding into the other models. Despite smoking being a well acknowledged risk factor for emphysema, the extent of emphysema varies widely among smokers and response to smoke inhalation varies by genetic strain in mice models.(51,52) Emphysema and arterial stiffening are both due to connective tissue degradation: In the pulmonary parenchyma elastin degradation causes loss of alveolar attachments, decreased compliance and increased emphysema;(53) while in the arteries elastin degradation is associated with increased collagen deposition and arterial stiffening.(54) The possibility of a genetic linkage is well demonstrated in Marfan syndrome where aortic root stiffening is a cardinal feature, and emphysema occurs even in the absence of a smoking history.(55,56) Furthermore, a decrease in skin elasticity is present in COPD independent of smoking or age,(57) a finding similar to that seen in the Klotho mouse model (a model of accelerated aging) where atherosclerosis, emphysema and decreased skin elasticity are all present.(58) The work of genetic studies is rapidly growing, with useful reviews on COPD and coronary artery disease readily available.(59,60) In a recent review of GWAS in cardiovascular disease, out of 33 genetic risk variants identified, only 10 mediate their risk through known mechanisms, leaving a wide range of possible genetic linkages.(59) Finally as mentioned in the inflammatory model chronic bronchitis and atherosclerosis are both inflammatory

conditions - itself a pathway with genetic influences.(61) However, despite several promising avenues, at present the effects of the identified susceptibility loci are still dwarfed by the effects of smoking in COPD.(62)

1.4 PULMONARY HYPERTENSION MODEL

COPD is the second most common cause of pulmonary hypertension after left sided heart disease.(63) Pulmonary hypertension (Cor Pulmonale when associated with right heart failure in COPD) is relatively common in severe COPD and is present in >50% of patients awaiting lung transplantation.(64) The incidence increases with increasing severity of COPD, with pulmonary hypertension present in 5% of moderate (GOLD stage II), 27% of severe (GOLD stage III) and 53% of very severe (GOLD stage IV) COPD.(65) The true incidence in mild to moderate COPD however is poorly appreciated due to the absence of large scale epidemiological studies.(66) In comparison to other causes of pulmonary hypertension the pulmonary pressure elevations are modest, however survival is poor and correlates better with the pulmonary pressures and pulmonary vascular resistance than with the severity of airflow obstruction.(67–70)

Pulmonary hypertension is defined as a mean pulmonary arterial pressure (mPAP) greater than or equal to 25mmHg at rest.(71) The gold standard for the assessment of pulmonary pressures is through direct measurement of the pressures within the pulmonary arteries during right heart catheterization. During this process pulmonary vascular resistance, right atrial pressure, pulmonary capillary wedge pressure, pulmonary saturations and

cardiac index can also be measured, with useful information both on the aetiology of the pulmonary hypertension and also on prognosis provided by these additional measures.(72) No other technique can currently conclusively diagnose pulmonary hypertension, however there are several options for assessing for its presence. Both echocardiography and MRI can measure the pulmonary artery systolic pressure (PASP) through measurement of the velocity of the tricuspid regurgitant jet using the modified bournelli equation ($\Delta P = 4v^2$) and combing this with the right atrial pressure (RAP) with PASP = ΔP + RAP. RAP is estimated based on the diameter of the vena cava and its change in diameter during inspiration, although some groups have suggested it is more accurate to calculate PASP assuming a constant RAP of 10mmHg.(73) The crucial limitation of PASP is that it measures systolic pressure rather than mean pulmonary pressure which is what is used for the diagnosis of pulmonary hypertension, with PASP frequently inaccurate in those who are acutely unwell or with advanced lung disease.(72,74) One final technique is using CT with the ratio of the pulmonary artery diameter to the aortic diameter, with a ratio of >1 demonstrating reasonable sensitivity and specificity for the presence of pulmonary hypertension in those with COPD and other lung conditions.(75,76)

However: Pulmonary vascular changes occur in mild COPD before pulmonary hypertension occurs(77); Right ventricular dysfunction has been observed in normoxaemic COPD patients with normal pulmonary arterial pressures(78); and right ventricular hypertrophy is one of the earliest cardiac changes and is present even in mild COPD.(79–81) Additionally in both mice and guinea pig models, vascular remodeling occurs even before the onset of emphysema.(82–84) The notion of an elevated rest pressure as a cut-off is also

restrictive in evaluating the role of the pulmonary arteries and right heart as even minimal exertion causes marked elevations in mPAP and oxygen desaturation in COPD, with exercise induced pulmonary hypertension present in 35%-58% of patients with normoxaemia or mild hypoxia.(67,85–87) See Figure 1-1.

Figure 1-1: Diagram of the gradually progressive changes in the right ventricle and pulmonary arteries that precede the development of outright pulmonary hypertension

Normal pulmonary pressures
- mPAP <25mmHg at rest and exercise
- Right ventricle: Impaired relaxation and reduced longitudinal strain
- Pulmonary vessels: Endothelial dysfunction

Exercise - induced pulmonary hypertension
- mPAP <25mmHg at rest and >25mmHg on exercise
- Right ventricle: Worsening strain and filling with development of hypertrophy
- Pulmonary vessels: Muscularised arterioles and intimal fibrosis

Pulmonary Hypertension
- mPAP >25mmHg at rest
- Right ventricle: Progressive hypertrophy, cavity dilation and reduced ejection fraction
- Pulmonary vessels: End stage remodelling with marked luminal narrowing.

Therefore the pulmonary hypertension model, whereby right ventricular failure occurs once pulmonary hypertension exists, is a misnomer, and an alternate should be considered - the right ventriculo-arterial model.

1.4.1 Vascular changes

Vascular remodeling within COPD develops secondary to intimal hyperplasia, with muscularisation of the arterioles and with rather little change in the tunica media.(88,89) This hyperplasia is induced by proliferation of smooth muscle cells and the deposition of elastic and collagen fibers.(90,91) Originally hypoxia was held to be the driving force behind this remodeling, however similar arterial changes are present in smokers with and without COPD, and arterial changes can be observed in mild COPD when hypoxia is yet to develop.(77,90,92) The vascular remodeling in COPD is most likely due to endothelial dysfunction and apoptosis which in turn causes remodeling, capillary loss and small vessel thrombosis.(12) This is likely due to a combination of local inflammatory mediators released from the endothelial dysfunction in the adjacent pulmonary parenchyma, and direct effects from the inhaled cigarette smoke on the vascular endothelium.(12,91) However an experimental study by Ferrer et al. in guinea pig models shows hypoxia still plays a contributory role, as a hypoxic environment after cigarette exposure induced significantly greater changes in pulmonary arterial pressures and pulmonary vascular remodeling than cigarette smoking or hypoxia alone.(84) More recently the pulmonary vascular sympathetic nerves which control the pulmopulmonary baroreceptor reflex originating at the pulmonary trunk has been proposed to be of significant importance in the development of pulmonary arterial hypertension.(93) This is evidenced by a rise in

pulmonary arterial pressures and pulmonary vascular resistance (PVR) induced by stretching the branch pulmonary arteries.(93–96) In a single study by Chen et al.(97) on 21 patients with significant pulmonary hypertension despite maximum medical therapy, intravascular pulmonary artery denervation with cessation of medical therapy resulted in significant improvement in pulmonary pressures and exercise capacity. However the role of this reflex in humans is still controversial and has also yet to be evaluated in COPD induced pulmonary hypertension.(98)

1.4.2 The right ventriculo-arterial model

1.4.2.1 Right ventricle

The right ventricle (RV) got off to an inauspicious start in the 1940s and 50s when a series of papers showed no significant alterations in the pulmonary arterial or systemic pressures following open ablation of the right heart in a dog model (see Figure 1-2), leading one of the authors to conclude that "a normal, contractile right ventricular wall is not necessary for the maintenance of a normal circulation".(99–101)

Figure 1-2: Example of the ventricular charring and lack of change in systolic systemic and venous pressures
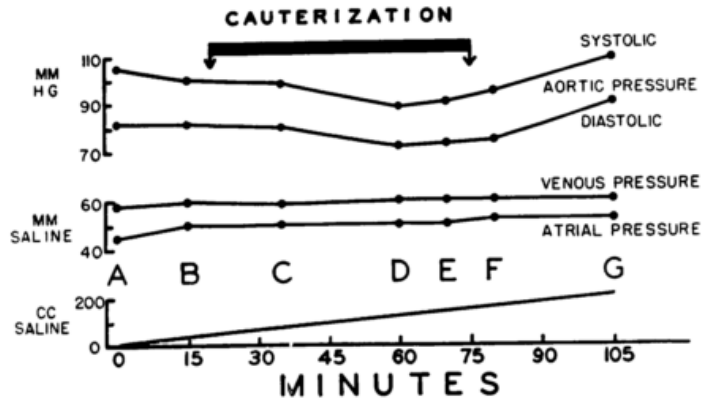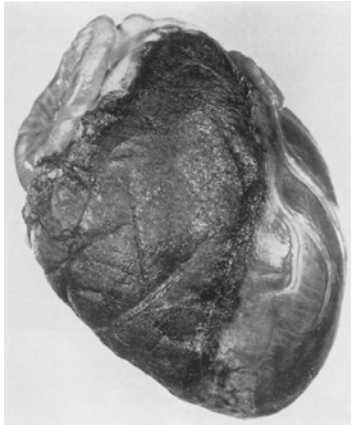
Adapted from Bakos ACP, Circulation and Kagan A, Circulation.(100,101)

Despite this apparent swan song for a significant role of the right ventricle, a paper in 1982 demonstrated that the open pericardial model did not accurately represent the functional haemodynamics of the heart.(102) Goldstein et al. demonstrated that when the right coronary artery was infarcted within an intact pericardium there was a profound and rapid fall in left ventricular pressures due to a fall in left ventricular (LV) preload, equalisation of RV and LV pressures and elevated intrapericardial pressures which did not occur when they repeated their experiment after pericardiectomy. Thus there is a marked ventricular interdependence due to the shared pericardial compartment, shared interventricular septum and the dependence of the left heart preload on the output of the right.(46,103–108)

Recent work has shown the importance of the right heart in health and disease. In health the right ventricle responds to exercise, obesity and traditional cardiovascular risk factors

in a manner similar to, but independent of, the left ventricle.(109–111) A decreased RV mass is associated with an increased risk of developing dyspnoea, and an increased RV mass is associated with an increased risk of future congestive cardiac failure and cardiovascular mortality in a healthy population.(112,113) In patients with COPD, right ventricular remodeling is apparent even early in the disease with right ventricular hypertrophy and diastolic dysfunction present in mild and moderate COPD with systolic impairment occurring in severe COPD.(79,80) This has significant implications with right ventricular dysfunction associated with poorer exercise capabilities and increased mortality independent of pulmonary function tests.(114,115)

1.4.2.2 Pulmonary artery

There has been a great deal of recent interest in systemic arterial stiffening in COPD due to the mechanistically plausible link this provides between COPD and the excess cardiovascular mortality associated with this condition.(116)   In comparison to the systemic arterial circulation there are several key differences in the nature of the vascular tree between that of the pulmonary and systemic circulation. The pulmonary artery is a low pressure, high distensibility system which acts to transform the highly pulsatile right ventricular output into the near steady flow at the capillary level.(117) The distal pulmonary vascular bed is also comprised of highly distensible vessels that, through distension and recruitment of the microvascular bed, are able to accommodate large increases in volume such as during exercise. This response is the opposite of that experienced in the systemic circulation where exercise induces vasoconstriction in the

majority of the vascular tree other than the vessels supplying the muscles. This inbuilt reserve means that resting pulmonary arterial pressures will only rise relatively late in a disease process when 60-70% of the bed is obstructed.(118) The peripheral distensibility of the vessels also differs from the systemic circulation where only the proximal arteries act as capacitance vessels, expanding and contracting with each beat of the heart, while the peripheral vessels are responsible for resistance. Due to the dual function of the vessels, there is an inverse relationship between the resistance and capacitance of the pulmonary circulation, with the product of the two (the resistance-compliance time constant) remaining the same in both health and disease.(119)

The pulmonary arteries and microcirculation have distinct effects on the right ventricular afterload which can be split into two key components – the steady component required to drive and maintain forward flow and the oscillatory component required to overcome the pulsatile component of flow (see Figure 1-3). The steady component is a function of peripheral vascular resistance whereas the oscillatory component is a function of both proximal and distal pulmonary arterial stiffness.(120) Even in the healthy adult, 30% of the right ventricular output is spent on generating pulsations (compared with only 10% in the systemic circulation).(121) This energy is considered wasted in terms of ventricular power output, but is crucial in acting as a blood reservoir and maintaining steady flow through the pulmonary tree.(122) As the pulmonary artery stiffens the oscillatory component of the workload increases, although remains as a constant of the total energy expenditure of the right ventricle.(123,124) As the artery stiffens it also starts to dilate and become less compliant, and the dilation of this in relation to the aorta has been shown to be a useful

clinical marker in COPD, with a PA:Aortic ratio>1 an independent predictor of future acute exacerbations, exercise capacity, pulmonary hypertension and mortality.(125–128)

Figure 1-3: The role of pulmonary arterial stiffening in peripheral and proximal vascular remodeling and impact on tight ventricular function. From Tan et al, Pulm Circ 2014.(129)
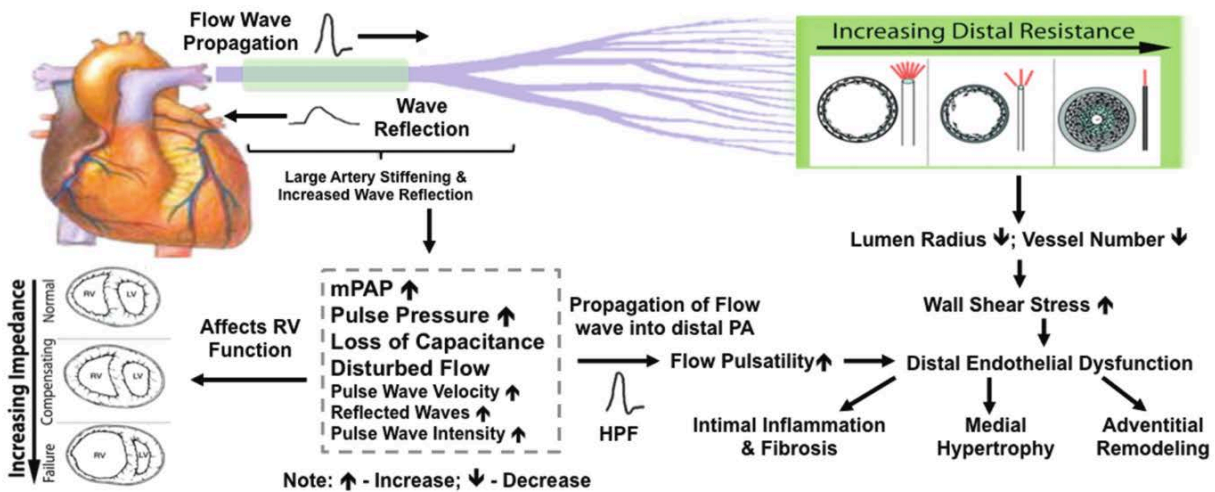
The compliance of the pulmonary artery is a key component in decoupling the right ventricle from the pulmonary bed, allowing the right ventricle to work at maximum efficiency and protecting the microcirculation from large pressure gradients.(117,130) Indeed the stiffness of the pulmonary artery is a strong determinant of right ventricular function,(131) and increased stiffness causes distal pulmonary arterial endothelial dysfunction and inflammation.(132,133) Increased stiffness is independently associated with reduced functional capacity,(134) and higher mortality than the pulmonary artery pressures or pulmonary vascular resistance.(135–139) While vascular distensibility is partly dependent on underlying distending pressures,(119,140) multiple studies have

shown the intrinsic stiffness of the arterial walls to be increased in pulmonary hypertension independently of these.(141–145)

1.4.2.3 Right ventriculo-arterial model

Optimal ventriculo-arterial coupling occurs when there is maximal transference of potential energy from one elastic chamber to another, e.g. from the ventricle to the artery. This is dependent on the elastance – the change in pressure for a given change in volume – of the two chambers.(146) The ventricular elastance (E_{ES}) is a load independent measure of the ventricular contractility combined with the modulating effects of the geometric and structural properties of the ventricle.(147) It relies on measuring the response of the ventricular pressure to increasing volumes (see Figure 1-4). The arterial elastance (E_A) is an index incorporating the elements affecting arterial load including pulmonary vascular resistance, arterial compliance, characteristic impedance, and systolic and diastolic time interval.(148,149) The E_A/ E_{ES} calculates the extent of ventriculo-arterial coupling.

At rest the ventricle and pulmonary artery are coupled so that the right ventricle is working at optimal efficiency which occurs when the stroke work is maximal with minimal oxygen consumption.(120,150–152) This has been shown to occur when E_A is half E_{ES}.(152–154) In exercise this moves towards optimal coupling when there is maximal cardiac efficiency which is where there is maximum flow generation with minimal energy loss ($E_A=E_{ES}$).(155–157) Interestingly the optimal values for energy efficiency and cardiac efficiency are similar throughout a variety of studied mammals suggesting it has been conserved throughout mammalian evolution.(158,159) During exercise, arterial stiffness

has a progressively and intensity-dependent greater impact on E_A than PVR with the result that E_A increases on exercise despite a fall in PVR in a manner paralleling the rise in arterial stiffness.(160–162) A similar relationship is present in pulmonary hypertension whereby pulmonary stiffness has a 1.2-18 fold greater contribution to right ventricular workload than PVR.(119,141,163) In the systemic circulation, age and hypertension (two known factors associated with increased arterial stiffness) result in an exaggerated increase in E_A during exercise increasing the pulsatile load on the heart and in turn decreasing left ventricular efficiency.(155,164) This exaggerated response secondary to arterial stiffening may explain the rapid rise in mPAP observed in COPD during exercise despite a stable or minimal rise in PVR.(85) Indeed in a study by Hilde et al., an increase in pulmonary arterial stiffness was observed during exercise with a greater contribution from this to changes in mPAP than PVR.(65) Further indirect evidence comes from a study by Kubo et al. which showed the pulmonary arterial wall thickness to be related to exercise pulmonary pressures rather than resting pulmonary pressures, and to correlate highly with change in pressure from rest to exercise.(165)

Figure 1-4: Calculation of EA:EES in the right ventricle and pulmonary artery. Ventricular end systolic pressure-volume is linear and characterised by the slope Ees and is generated by measuring pressure-volume loops under gradated preload and afterload conditions
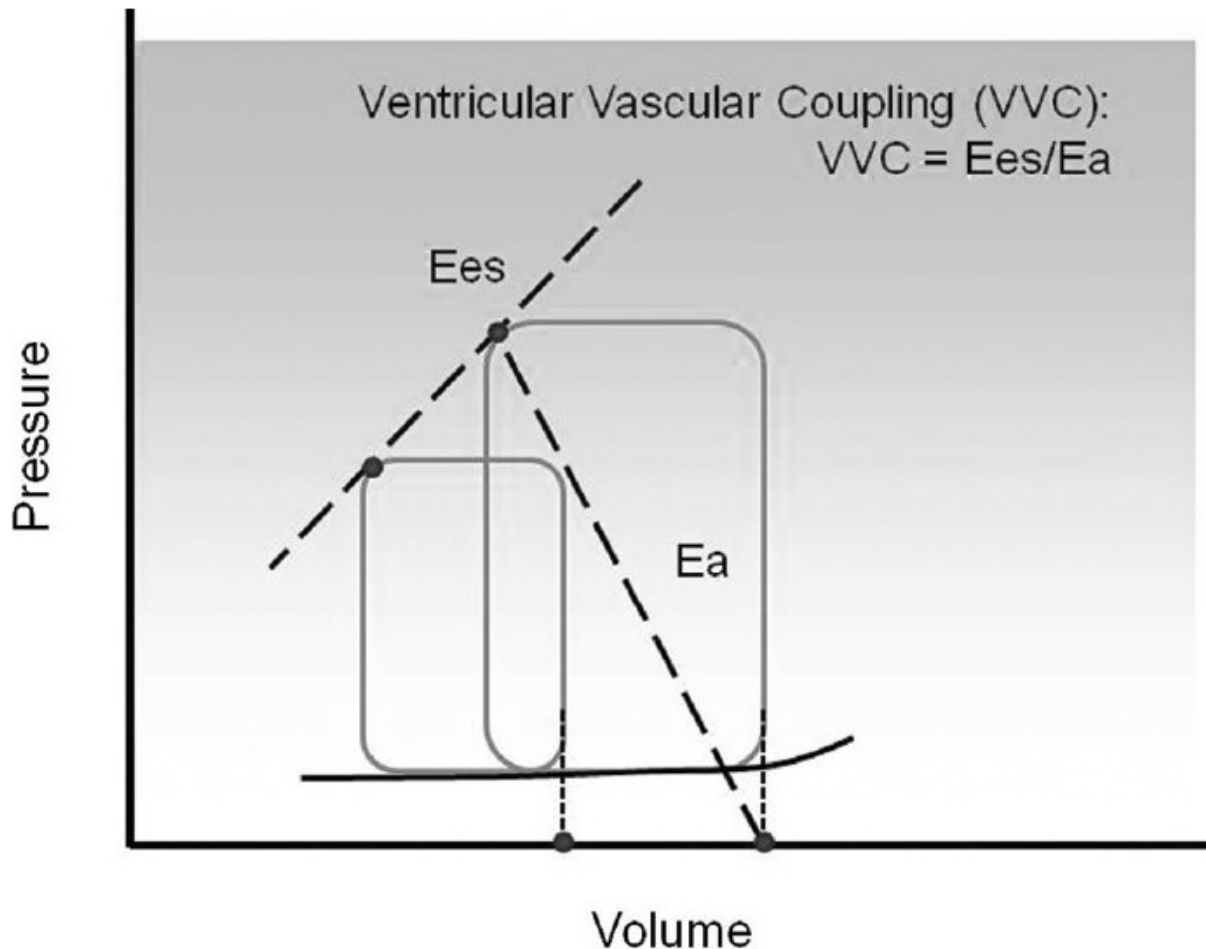
Reproduced from Wang et al. 2011.(166). Ea = Arterial elastance; Ees = Ventricular elastance.

When the E_A increases so that the $E_A:E_{ES}$ is consistently above 0.5 the ventricle adapts to the increased workload by inducing hypertrophy.(167) This increases the E_{ES} thereby returning the ventriculo-arterial system to its most energy efficient state, albeit at a slightly higher energy consumption than previously.(168–170) As E_A continues to rise the right

ventricle eventually fails to adapt with a resultant decrease in the E_{ES} and thereby a rapid increase in E_A/E_{ES} indicating uncoupling and reduced myocardial efficiency.(152,171)

Fourie et al. demonstrated that myocardial efficiency reached a maximum when the E_A reached 1mmHgml^{-1} (corresponding to an mPAP of 20mmHg), while maximum stroke work corresponded to an E_A of 2 mmHgml^{-1} (corresponding to a MPAP of 30-40mmHg).(117) This corresponds with observations that at approximately 40mmHg the pulmonary artery reaches it maximum dimension and minimal distensibility.(143,171,172) Consistent with this, Stevens et al. demonstrated that in patients with pulmonary hypertension there was a curvilinear relationship between RV function and PA distensibility with marked loss of pulmonary artery distensibility without commensurate loss of ventricular function until only minimal distensibility remained when a rapid decompensation of the right ventricle occurred.(141) A similar curvilinear relationship has also been observed in COPD between pulmonary arterial stiffness and peripheral vascular resistance, with a rapid rise in PVR only occurring after significant stiffening of the pulmonary arteries has occurred.(78) Pulmonary stiffness is increased early in pulmonary hypertension development, and is increased even in those with exercise induced pulmonary hypertension, both in mixed pulmonary arterial hypertension studies and in COPD.(65,78,143,172) This combination of features suggest pulmonary arterial stiffness as a promising biomarker for detection of early disease and as a potential therapeutic target before end stage arterial remodeling occurs with dire consequences for the right ventricle.

1.5 MEASURING PULMONARY ARTERY STIFFNESS.

The stiffness of the pulmonary artery can be quantified using a variety of metrics, with these measuring stiffness locally, regionally or systemically. Table 1-1 summarises the various methods of measuring arterial stiffness and the common methods for acquiring these. As can be seen from the table the majority of these require knowledge of the arterial pressures to calculate the stiffness. In the arterial circulation this is not a significant issue as the brachial arterial pressures are readily obtained with a sphygmomanometer, as mean BP and diastolic BP are relatively constant throughout the large arteries.(173) However in the pulmonary arteries this provides a significant hurdle as an external measurement of the pressures is not readily available. Despite numerous attempts to quantify pulmonary arterial pressures and vascular resistance using echocardiography, CT and MRI, none of these have yet proven accurate enough to negate the need for invasive measurement with right heart catheterisation.(73,174–180)

1.5.1 Right heart catheterisation

Right heart catheterisation can be used to calculate several metrics of arterial stiffness, including capacitance, PWV and elastance, although the latter two require dedicated catheters and equipment not routinely available in the catheter laboratory. In addition, it can be combined with techniques for the visualisation of the pulmonary artery cross sectional area such as MRI or intravascular ultrasound, to derive a wide range of metrics of arterial stiffness and ventriculo-arterial coupling. Table 1-2 summarises the studies looking at invasive assessment of pulmonary arterial stiffness. Despite its utility, RHC has

numerous disincentives including its invasive nature, cost, and exposure to ionising radiation. While the combination of MRI and right heart catheterisation allows catheter guidance without exposure to ionising radiation and simultaneous acquisition of anatomical and pressure measurements, it does not negate the invasive or costly nature of the study.(181,182) Of the measures of arterial stiffness, only pulsatility and pulse wave velocity can be derived entirely non-invasively.

1.5.2 Pulsatility

Multiple studies have shown reduced pulsatility in pulmonary hypertension.(134,135,145,172,183–185) A single echocardiography study has shown reduced pulmonary artery pulsatility in COPD, which correlated with right ventricular functional parameters.(186) A single abstract using cardiac MR has also described decreasing pulsatility with increasing severity of COPD.(187)(Table 1-3) However, as discussed above, the pulmonary stiffness is dependent not only upon distending pressures, but also upon the intrinsic elasticity of the pulmonary vessel wall, thus a fall in pulmonary pulsatility does not differentiate a fall in pulsatility due to a fall in stroke volume or in distending pressures from that of a rise in arterial stiffness.

Table 1-1: Measures of arterial stiffness - Calculations, definitions and alternate means of assessment.

	Calculation	Definition	Method of assessment
Local			
Pulsatility (%)	(maxA – minA)/minA X 100	Relative change in lumen area during the cardiac cycle	MRI Echocardiography IVUS
Compliance (mm²/mmHg)	(maxA – minA) / PP	Absolute change in lumen area for a given change in pressure	RHC plus MRI/Echo/IVUS
Distensibility (%/mmHg)	[(maxA – minA)/PP X minA] X 100	Relative change in lumen area for a given change in pressure	RHC plus MRI/Echo/IVUS
Elastic modulus (mmHg)	PP X minA/(maxA – minA)	Pressure change driving a relative increase in lumen area	RHC plus MRI/Echo/IVUS
Stiffness index (N/A)	Ln(sPAP/dPAP) / [(maxA – minA)/minA]	Slope of the function between distending arterial pressure and arterial distension	RHC plus MRI/Echo/IVUS
Young's elastic modulus	[3(1+minA/WCSA)]/Distensibility	Wall thickness for a given distensibility	RHC plus IVUS
Regional			
Capacitance (mm³/mmHg)	SV/PP	Change in volume associated with a given change in pressure	RHC
PWV (ms⁻¹)	Δd/Δt (TT technique) ΔQ/ΔA (Flow-area technique)	Speed of transmission of pressure wave	RHC MRI
Systemic			
Elastance (mmHgml⁻¹)	E_A/ E_{ES} = (ESP/SV) / (ESP/ESV-V0)	Change in pressure for a given change in volume	RHC with flow-volume loops

A= area; d = distance; dPAP = diastolic pulmonary artery pressure; EA = Arterial elastance; Echo = echocardiography; EES = Ventricular elastance; IVUS = intravascular ultrasound; maxA = maximum cross sectional area; mina = minimum cross sectional area; MRI = magnetic resonance imaging; PP = pulse pressure; PWV = pulse wave velocity; Q=Flow over a single heart beat; RHC = right heart catheter; sPAP = systolic pulmonary artery pressure; SV = stroke volume; t = time; WCSA = Wall cross sectional area.

Table 1-2: Summary of studies looking at invasive measurement of pulmonary arterial stiffness.

Study	Population	No	Method	Finding
Milnor et al(188)	Mixed PH	7	RHC	Increased impedance in PH
Nakayama et al(189)	Mixed PH	62	RHC	Increased augmentation index and earlier inflection time in PH
Castelain et al(142)	Mixed PH	14	RHC	Increased augmentation index and earlier inflection time in PH
Mahapatra et al(136)	Mixed PH	104	RHC	Capacitance strongest predictor of mortality in PH. On multivariate analysis, capacitance was the only statistically significant predictor of mortality.
Hilde et al(78)*	COPD	98	RHC	PA compliance greatly reduced in COPD Gold 2,3 and 4
Hilde at al(65)*	COPD	98	RHC	PA compliance fell with exercise in patients with and without PH, with similar elevations in mPAP during exercise between the two groups.
Muthurangu et al(190)	IPAH	17	RHC with MRI	Inverse relationship between compliance and PVRI and mPAP. A fall in compliance was evident in 7/17 following nitric oxide inhalation
Kuehne et al(152)	Mixed	12	RHC with MRI	Increased elastance in PH, with resultant ventriculo-arterial uncoupling
Kopec et al(191)	IPAH	26	RHC with IVUS	PWV high in IPAH (mean PWV 10ms^{-1}) with excellent correlation with compliance (β= -0.81) and reasonable correlation with mPAP (β =0.48)
Lau et al 2012(144)	IPAH	8	RHC with IVUS	Increase in all measure of pulmonary arterial stiffness. Inverse curvilinear relationship between mPAP and compliance and distensibility. No change in PA stiffness following 6 months of bosentan therapy.
Rodes-Cabau et al(138)	IPAH	20	RHC with IVUS	Reduced pulsatility in PH, with reduced pulsatility predictive of future mortality. Epoprostenol infusion increased pulsatility by 53%.
Lau et al 2014(192)	IPAH	5	RHC with IVUS	High PWV in IPAH (mean PWV 10.6ms^{-1}) with the reflected backward compression wave carrying 31% of the energy of the forward compression wave

*Drawn from the same population
‡ Different calculation for %pulsatility so not directly comparable
COPD = chronic obstructive pulmonary disease; CoV = Coefficient of variation; EIPH = Exercise induced pulmonary hypertension; FEV1 = Forced expiratory volume in one second; HV = Healthy volunteers; IPAH = Idiopathic pulmonary arterial hypertension; NYHA = New York heart association; PASP = Pulmonary artery systolic pressure; PH = Pulmonary hypertension; PWV = pulse wave velocity; QA= flow by area; TT = transition time; 6MWT = six minute walking test.

1.5.3 Pulse wave velocity

Pulse wave velocity (PWV) is the speed at which the pressure wave, generated by ventricular contraction, is transmitted through the arterial tree. This is directly related to vessel wall elasticity, with increased stiffness leading to increased PWV.(193) A reflected pressure wave is present which is generated when the pressure wave is reflected from the termination of the arteries, with alterations in the smallest arteries increasing the size of the reflected wave while large artery stiffening increases the PWV.(188) In health this reflected wave only represents a tiny fraction of the total output energy, and arrives in diastole and reduces preload of the subsequent ventricular contraction.(157,188,194,195) However in pulmonary hypertension this can reach 30% of the forward wave energy. With an increased PWV resulting in the earlier arrival of the reflected wave during systole thereby increasing the afterload of the heart and thus cardiac workload.(142,189,192,196–198)

PWV is an established marker of arterial stiffness in the systemic circulation with aortic pulse wave velocity shown to be associated with future cardiovascular events, and to improve risk stratification.(199) Transcutaneous waveform analysis methods are the gold standard for aortic PWV measurement including pressure,(200) distension,(201) and flow waveform.(202) However a transcutaneous approach is not possible for the pulmonary arteries. While PWV can be measured invasively on right heart catheterisation,(188) magnetic resonance imaging is a possible alternative for non-invasive assessment of the pulmonary arteries using flow waveforms.(203) It is performed by the acquisition of ECG gated phase contrast sequences which measure flow the in proximal main pulmonary

artery and in the mid right or left pulmonary arteries. A distance can be calculated between the two imaging planes (Figure 1-5), and the pulse wave timed from when it leaves the main pulmonary artery until it arrives in branch pulmonary arteries thus allowing a speed between the two points to be generated.(203)

Figure 1-5: Measurement of PWV using MRI
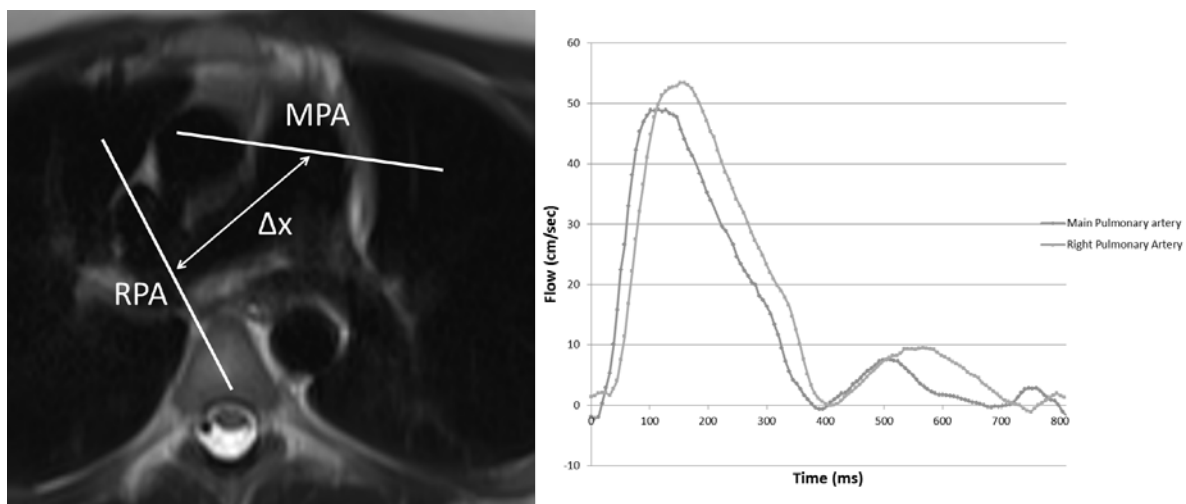
The locations of the two-phase contrast planes are delineated on the left image (a) with the distance between them measured. The two separate waveforms are traced on the right (b) relative to the triggering R-wave used to start image acquisition. The time between the waves arriving at the two consecutive locations can then be measured allowing calculation of the speed of the pulse wave.

MRI derived pulse wave velocity has been previously validated against both invasive and non-invasive techniques in the aorta.(204–206) Several studies have shown this to be a feasible and reproducible technique in the pulmonary arteries in healthy volunteers,(203,207) with the observed pulse wave velocity of 1.96-2.3ms^{-1} similar to that obtained invasively.(188,194) Pulse wave velocity is raised in pulmonary hypertension

using both invasive RHC and MRI assessment (See Table 1-2).(191,208) To date there have

been no studies assessing pulmonary PWV in COPD.

Table 1-3: Summary of studies looking at non-invasive measurement of pulmonary arterial stiffness.

Study	Population	No	Method	Finding
Pulsatility				
Bogren et al (209) ǂ	Mixed PH	4	MRI	Pulsatility 23% in HV and 8% in PH
Paz et al (210)	HV	9	MRI	No difference in pulsatility between the main pulmonary artery, right pulmonary artery and left pulmonary arteries.
Gan et al (135)	Suspected PH	70	MRI	Right pulmonary artery pulsatility showed a curvilinear relationship with mortality. Pulsatility <16%
Jardim et al (185)ǂ	IPAH	19	MRI	<10% pulsatility predicts non-responders to acute vasodilator testing with 100% sens and 56% spec.
Sanz et al (184)*	Suspected PH	59	MRI	Pulsatility 41% in non-PH and 17.4% in PH. No difference in pulsatility between different causes of PH.
Sanz et al (143)*	Suspected PH	94	MRI	No difference in pulsatility between group without PH and EIPH. Pulsatility <40% predicted PH with 93% sens. and 63% spec.
Kang et al (134)	Mixed PH	35	MRI	Pulsatility correlated with 6MWT (R2=0.61, p<0.001). <20% pulsatility predicted poor function (6MWT <400m) with 82% sens. and 94% spec.
Stevens et al (141)*	Suspected PH	124	MRI	Pulsatility correlates with right ventricular function
Stevens et al(211)	Suspected PH	43	MRI	Pulsatility correlated with exercise capacity while RHC pressures did not.
Swift et al (172)	Suspected PH	134	MRI	Pulsatility elevated even in very mild elevations in PVR. Pulsatility predicted mortality.
Revel et al (212)ǂ	Suspected PH	45	CT	Pulsatility of 16.5% predicted PH with sens 86% and spec 96%.
Pasierski et al (145)	Suspected PH	19	Echo	Pulsatility reduced in pulmonary hypertension with a linear relationship between pulsatility and PASP
Mahapatra et al (137)	Suspected PH	54	Echo	Capacitance was the strongest predictor of mortality including invasive pressure measurements
Ertan et al (186)	COPD	54	Echo	Right pulmonary artery pulsatility reduced in COPD patients, with significant differences between NYHA functional classes.
Liu et al (187)	COPD	135	MRI	Pulsatility falls with increasing severity of COPD, with a positive association with %predicted FEV1 and inversely correlated with %emphysema
PWV				
Peng et al (207)	HV	17	MRI	PWV 1.96±0.27 with high intra-scan and inter-scan reproducibility (5.5% and -10.9% respectively)
Bradlow et al (203)	HV	10	MRI	No significant difference in PWV using the left or right pulmonary arteries. CoV 12% for both intra and inter-observer assessment.
Ibrahim et al (208)	Heterogeneous	33	MRI	PWV raised in pulmonary hypertension. Comparable measurements between TT and QA methods.

*Drawn from the same population, ǂ Different calculation for % pulsatility so not directly comparable to other studies. COPD = chronic obstructive pulmonary disease; CoV = Coefficient of variation; EIPH = Exercise induced pulmonary hypertension; FEV1 = Forced expiratory volume in one second; HV = Healthy volunteers; IPAH = Idiopathic pulmonary arterial hypertension; NYHA = New York heart association; PASP = Pulmonary artery systolic pressure; PH = Pulmonary hypertension; PWV = pulse wave velocity; QA= flow by area; TT = transition time; 6MWT = six minute walking test.

1.6 PULMONARY ARTERIAL STIFFNESS AS A TREATMENT TARGET

Traditional treatments of pulmonary hypertension such as phosphodiesterase inhibitors and endothelin-1 receptor antagonists have yielded disappointing results, despite their success in treating the underlying pulmonary hypertension in the COPD cohorts with significant reductions in mPAP and PVR with therapy with sildenafil and bosentan.(213–216) However by counteracting the natural vasoconstrictive response of the blood vessels to the hypoxic state of severely damaged lung tissue, these medications simply divert blood away from the best oxygenated segments of the lung to those that are most severely disease, thereby worsening the ventilatory-perfusion mismatch,failing to improve the hypoxic and hypercapnic driven symptoms in severe COPD cohort.(217) However these treatments have all focused on altering the peripheral vasculature. Given the greater impact of pulmonary stiffness on remodeling, drugs to target and ameliorate this process may be a novel route to target. Due to the relatively recent identification of the importance of pulmonary arterial stiffness in right ventricular remodeling, there have been relatively few studies targeted at its treatment. Despite this there are several studies suggestive of promising avenues for further exploration.

Statins have been proposed as a route to reduce systemic arterial stiffness,(218) although a meta-analysis showed mixed response with two studies showing improvement, one showing no change and another showing progression of stiffening.(219) Statins in guinea pigs and mice with emphysema have been shown to reverse arterial remodeling and halt the formation of emphysema.(220,221) Indirect evidence of the benefits from statins in COPD related pulmonary hypertension come from observational studies showing lower

pulmonary arterial pressures in patients on statins prior to right heart catheterisation.(222) Furthermore a study on pulmonary arterial stiffness showed that other than mPAP, the only other factors independently associated with pulmonary arterial stiffness was LDL cholesterol and BMI.(191) Statins are also associated with increased exercise capacity and reduced mortality in COPD,(223–225) however due to the observational nature of these studies the underpinning mechanisms are still in debate.(226,227)

Xanthine oxidase inhibitors have been shown to improve endothelial function and arterial stiffness in the systemic circulation.(228–232) They have also been shown to reduce endothelial dysfunction induced by smoking and obstructive sleep apnoea (233–235) – a condition similar to COPD in its effects of intermittent hypoxia.(236) Additionally allopurinol inhibits hypoxia induced pulmonary vasoconstriction, pulmonary hypertension, endothelial dysfunction and vascular remodeling in hypoxic animal models of pulmonary hypertension.(237–241) It has been shown to reduce airway reactive nitrogen species production in COPD, however its effects on smoking induced pulmonary vascular damage has not been assessed.(242)

As with xanthine oxidase inhibitors, mineralocorticoid receptor antagonists have been shown to improve systemic endothelial function and arterial stiffness.(243–245) In 2 separate mouse models of pulmonary hypertension, mineralocorticoid receptor antagonists prevented or reversed adverse pulmonary vascular remodeling with improved pulmonary vascular resistance, pulmonary artery pressure, and remodeling of the right

ventricle.(246) A group in Bethesda, USA are currently recruiting patients with pulmonary hypertension without right heart failure to evaluate its efficacy in humans in modulating pulmonary vascular remodeling.(247) Its use in COPD has not currently been assessed.

Long term oxygen therapy improves survival in severe COPD and reduces pulmonary arterial pressures and vascular resistance while improving cardiac output.(68,248) It has also been shown to reduce peripheral arterial stiffness in COPD, however its effects on the pulmonary arterial stiffness has not been evaluated.(249)

There are also several new classes of pharmaceutical agents currently being designed that specifically target the processes causing arterial stiffening. Currently these are all being targeted at systemic vascular remodeling and are in the pre-clinical stages, however should they prove successful at preventing or reversing systemic arterial remodeling they would be promising agents for evaluation in pulmonary remodeling. The most promising of these are TGF-B1 antagonists, and drugs targeting the advanced glycation end products (AGEs).(54)   TGF-B1 is responsible for extracellular matrix remodeling and vascular fibrosis in chronic inflammatory conditions, whilst AGE form irreversible cross-links with collagen and elastin, reducing the elasticity of the arterial wall.(54)

1.7 CONCLUSIONS

Given the poor mortality in COPD, which has been largely static over the past few decades despite leaps forward in the understanding of the underlying pathophysiology, a new avenue of exploration is warranted. Pulmonary arterial stiffness holds a crucial role in

right ventricular dysfunction in pulmonary hypertension, and demonstrates promise as a useful biomarker in the development of this disease. While little is understood about the role of pulmonary arterial stiffness in COPD, the findings to date agree with the observations made in pulmonary hypertension. Further work is needed to explore this promising new path.

CHAPTER 2: Physics of Cardiac MRI

2   INTRODUCTION

Nuclear induction (the act of deposition of radiofrequency energy in the nuclei of matter which is then re-emitted) was first described by Bloch and Purcell in the 1940s. This was readily taken up in the field of chemistry where it was used to determine structural and chemical properties of molecules.(250) Indeed Paul Lauterbur (who was later awarded the Nobel prize in conjunction with Peter Mansfield for the translation of this technique into biomedical imaging), was himself a chemist. The underlying principle of the use of radiofrequency energy and magnetic gradients to produce an MRI image remain central to magnetic resonance imaging (MRI) to this day, albeit with significant subsequent advances and adaptations to this since. This chapter will look at the central principles of MRI imaging, and their current use and application within imaging of the cardiovascular system.

2.1 MRI SYSTEM COMPONENTS

In its most basic guise a magnetic resonance imaging scanner can be broken down into 3 key electromagnetic constituent elements: the main magnet, the gradient coils and the radiofrequency (RF) transmitter coil (see Figure 2-1). The main magnet is responsible for generating a constant background magnetic field (B_0). The strength of this magnetic field describes the operating strength of the magnet, and in modern clinical scanners this is typically in the order of 1.5 Tesla (symbol T, with 1T equating to approximately 20,000

Diagrammatic representation of the electromagnetic components and their spatial distribution within an MRI system (a) and the alignment of the reference co-ordinate axis in relation to B_0 which is generated by the main magnet coils (b). Adapted from Ridgway(251).

times the strength of the earths magnetic field) and 3T. Although, 7T scanners are rapidly becoming more commonplace in a research environment, and 11T pre-clinical scanners are also in development, these are still some way off becoming routinely used in the clinical environment. The gradient coils each generate much weaker (being measured in the order of milli-Tesla) transient magnetic gradients, with 3 gradient coils used in order to generate gradients in the x, y and z planes. The final component – the RF transmitter coil – generates the weakest magnetic field, and is located closest to the patient. Using a combination of these three elements, magnetic gradients can be generated in a specific pattern and order

that allow the production of a magnetic resonance signal within the body that can be spatially localized and used to build up the MR image.

2.2 MRI SIGNAL GENERATION

2.2.1 The nuclei

The entirety of MRI is built on the premise that the components of the atomic nuclei (protons and neutrons) each exhibit an intrinsic property known as spin. The ability to produce signal from this spin requires for the nucleus of the atom to have a net spin, which therefore requires an odd number of protons and neutrons so that the spin of each of these do not cancel each other out. Several elements within the body exhibit just such a property including, but not limited to, hydrogen (1H), carbon (13C), sodium (23Na), fluorine (19F) and phosphate (31P). As hydrogen is one of the most abundant elements within the body, being incorporated into water, fat and protein it is a natural choice to use for magnetic induction.

The nuclear spin gives rise to a small magnetic field (or magnetic moment). In the natural environment these are all directed in random directions, however when these are then exposed to the external magnetic field of the main magnet (with field strength B_0) they align towards or away from the magnetic field, reaching an equilibrium whereby there is a small net direction of the protons in the direction of the main field, although this is typically in the magnitude of only a few protons excess per million. This net magnetization is along the z-axis in parallel to B_0, and is known as M_0. The stronger the main magnet (and thus

B_0), the greater the excess of protons aligned in parallel to the main field (and as a consequence an increase in M_0). As M_0 increases so does the maximum signal intensity that can be generated in order to produce images thus improving the signal to noise ratio of the resultant image.

In order to use this net magnetization to produce a MR signal, the RF transmitter coil must be used to deliver energy to this group of protons. To allow for the transmission of energy that will be absorbed by the protons, a resonant frequency must be used. This resonant frequency is known as the Larmor frequency (ω_0), and can be calculated using the Larmor equation:

$$\omega_0 = \Upsilon \times B_0$$

where Υ is a gyromagnetic constant specific to each particle dependent on its mass, size and spin. For hydrogen protons this is 45.27MHz/T, therefore the Larmor frequency of hydrogen for 1.5T imaging is 67.91MHz, while at 3T this is 135.81MHz.(252)

2.2.2 Flip angles, repetition time and echo time

Prior to magnetic induction by the RF pulse the net magnetization, M_0, is aligned in parallel with B_0. By using knowledge of the Larmor equation and the magnet being used, the RF coils can be used to emit RF waves at the Larmor frequency. This induces the magnetization of the spinning protons to move from their thermal equilibrium into the transverse plane (Figure 2-2). The longer the pulse is applied for or the greater the

amplitude of the RF pulse, the further into the transverse plane the magnetization will be moved. The degree of this movement from the z-axis into the x-y plane is known as the flip angle (FA), which determines the amount of energy the precessing protons contain in both the z-axis and in the x-y axis. At a FA of 90° all the longitudinal energy has been transferred into transverse energy while at FAs of <90° the protons contain some energy in the z axis and some in the xy plane. As soon as the RF pulse is turned off the protons once again resume their precession around the z-axis, inducing a current in the same RF coils that emitted the RF pulse, which can be detected and used to generate the signal from which the MRI image is generated.

Figure 2-2: Spin magnetization
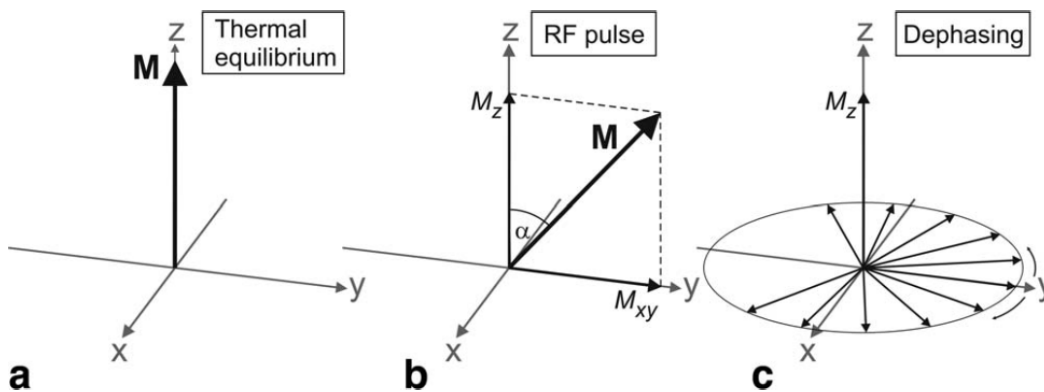
Figure 2-2: Spin magnetization: **(a)** during thermal equilibrium (M_0); **(b)** after excitation by radiofrequency induction to flip the magnetization into the horizontal plane; and (when the RF pulse is removed) **(c)** dephasing of the transverse magnetization Mxy occurs.

2.2.3 Relaxation

As the precessing protons emit this detectable signal they lose their energy relaxing back to their native equilibrium where they once again align along B_0.   Just as the flipped magnetization has both a horizontal and transverse component, the relaxation phase has both a horizontal and transverse component.

The horizontal relaxation is an exponential process and is referred to as T1 and is affected by the molecular structure in which the hydrogen protons are bound and deposit their energy. Medium sized molecules, such as fat, 'tumble' in such a way that this rate coincides with the Larmor frequency resulting is an incredibly rapid release of energy from the spinning hydrogen protons into the adjacent lattice in which they are held. Both small molecules (such as water) and large molecules (such as proteins) tumble much faster or slower than the Larmor frequency hindering efficient energy transfer thus resulting in a slow T1 relaxation. It is due to this process of transfer of energy from the spinning protons to the tumbling lattice in which they are held that T1 relaxation can be considered as spin-lattice relaxation.

In comparison, the transverse relaxation occurs due to the loss of coherence of the precessing protons. When the RF pulse is first stopped, all the hydrogen protons are precessing in coherence with one another, generating a large amplitude signal. However every atom and molecule containing the hydrogen protons are moving at random, each with their own magnetic field. As the magnetic fields of the spinning protons within these atoms interact with one another they cause tiny shifts in the Larmor frequency, resulting in

an exponential loss of coherence of the precessing protons. This can be seen as an exponential decay in the signal detected by the RF coils, known as free induction decay (FID). The rate of this decay is the T2 relaxation value and, as it is caused by the interactions of individually spinning protons with one another, it is also known as spin-spin relaxation. Molecular structures such as proteins, which hold a large number of protons in relatively close proximity to each other, facilitate a more rapid and consistent interaction between the spinning protons thus accelerating this spin-spin relaxation. In comparison, water molecules are small and widely spaced meaning they interact relatively infrequently, as a result of which spin-spin relaxation is much slower. This results in water having a long T2 relaxation time and thus a high T2 signal. One added complexity when considering T2 relaxation is that it is not just changes in the magnetic field induced by adjacent spinning protons that alter T2 relaxation rates. Inhomogeneities in the magnetic field itself (a major problem in older solid state MRI scanners but less of an issue in modern superconducting magnets) will cause more rapid relaxation, as will interfaces between tissues which have very different magnetic susceptibilities (such as seen between the lungs and adjacent heart, or between the iron in haemosiderin and tissue parenchyma). These two factors cause more rapid dephasing of the protons leading to a steeper relaxation curve which is referred to as T2*.

2.3 MR IMAGE GENERATION

So far we have discussed how it is possible to generate an MR signal, however in order to generate an image this signal must be localized. This is done through the sequential application of three magnetic gradients – the slice selection gradient, the phase encoding

gradient and the frequency-encoding gradient. Each of these is generated by the 3 directional gradient coils, and applied at right angles to each other to determine the x, y and z planes of the image stack. Through the use of these three gradients, specific tissue planes can be excited, with the resultant frequency and phase of the returned MR signal affected in such a way that spatial localization of the signal origin can be determined.

2.3.1 Slice selection

The slice selection gradient applies a magnetic gradient across the body, which adds to or detracts from the strength of B_0. Since the Larmor frequency is determined by B_0, changing this across the body will increase or decrease the Larmor frequency as the distance from the center point of the gradient increases. Thus when the radiofrequency pulse is generated it will only excite the protons at the level of the null point of the gradient, which retain the original Larmor frequency. By choosing the location of this null point, the slice of tissue to be imaged is selected.

2.3.2 Phase encoding

Once the slice selection gradient has been applied and the RF pulse has excited the slice of interest, the phase encoding gradient is applied. This causes an increase or decrease in the frequency of precession of the protons with the magnitude of this change determined by their location on the gradient and the length of time the gradient is applied for. When the gradient is turned off, the protons will return to their normal frequency of precession, however they will now be out of phase with each other with the phase of their current frequency determined by their location in the phase encoding direction.

2.3.3   Frequency encoding

The frequency-encoding gradient is subsequently applied at right angles to the phase encoding gradient and works on the same principles that the gradient changes the frequency of precession across the gradient, with the magnitude in change of the frequency determined by the protons location along the frequency-encoding axis. The frequency-encoding gradient is applied during the process of signal readout meaning the received RF signal will be composed of a range of frequencies, each of which describes the location of the signal within the frequency encoding direction.

2.3.4   Image reconstruction

The generated MR signal detected by the RF coils will now be composed of a range of frequencies, describing phase and frequency data from the emitting protons. Standard Fourier transform can only extract the frequency data from this, thus the above three gradients have to be repeatedly applied, with the slice selection and frequency encoding gradient kept constant while slight incremental changes in the strength and duration of the phase encoding gradient are applied. Once multiple readouts have been performed using this technique, a 2D Fourier transform can be applied to extricate both the phase and frequency data from the signal to generate the image. The greater the number of times this is repeated, the greater the spatial resolution that can be achieved, but at the cost of the added time required to repeat the necessary gradients and obtain the extra readouts.

2.3.5   K-space

The fact that every readout from the RF coils contains both frequency and phase data (which in turn represents x- and y- co-ordinates of the location of the origin of the signal)

leads to the need for the concept of k-space. Each line of k-space represents a single readout from the end of the pulse sequence. As the number of lines of k-space is built up the spatial data is pulled from all lines of k-space simultaneously through the aforementioned 2D Fourier transform. The parts of k-space that are filled by the signal produced following the shortest and weakest phase encoding gradients generate the highest amplitude signal due to the minimal loss of cohesion of the preceding protons, and thus generate the contrast of the tissues. In comparison the parts of k-space filled by the signal produced following the greatest strength and length of phase encoding gradients experience the greatest loss of cohesion of the protons generating the MR signal producing a low amplitude signal with very little contrast information but instead containing the edge definition and fine spatial detail.

2.4 MRI SEQUENCES

There are only two fundamental types of MR pulse sequences, with all other sequences being variations of these. These two building blocks are Spin Echo (SE) and Gradient Echo (GRE) sequences.

2.4.1.1 Spin echo

When the 90° RF pulse is applied and turned off the protons immediately start dephasing with loss of signal according to their spin-spin relaxation rate and the inhomogeneities of the field they are in. Through the application of a $180°$ transverse RF pulse the dephasing protons are refocused so that the field inhomogeneities are reversed and therefore nullified

(see Figure 2-3). This allows the larger T2 signal to be measured rather than the smaller T2* signal.

2.4.1.2 Gradient echo

In comparison to spin echo which are refocused by a transverse 180° RF pulse, gradient echoes are refocused through the use of an applied gradient. As this does not reverse the effects of magnetic field inhomogeneities, the produced signal is T2* dependent. This means the signal decays much quicker in GRE sequences than SE sequences. However the hindrance of this loss of signal is counterbalanced by the fact that a spin echo does not have to be waited for and thus this imaging is much quicker than SE sequences - a fact capitalized on by the majority of cardiac imaging sequences.

Figure 2-3: Signal formation for spin echo (top) and gradient echo (bottom) imaging.
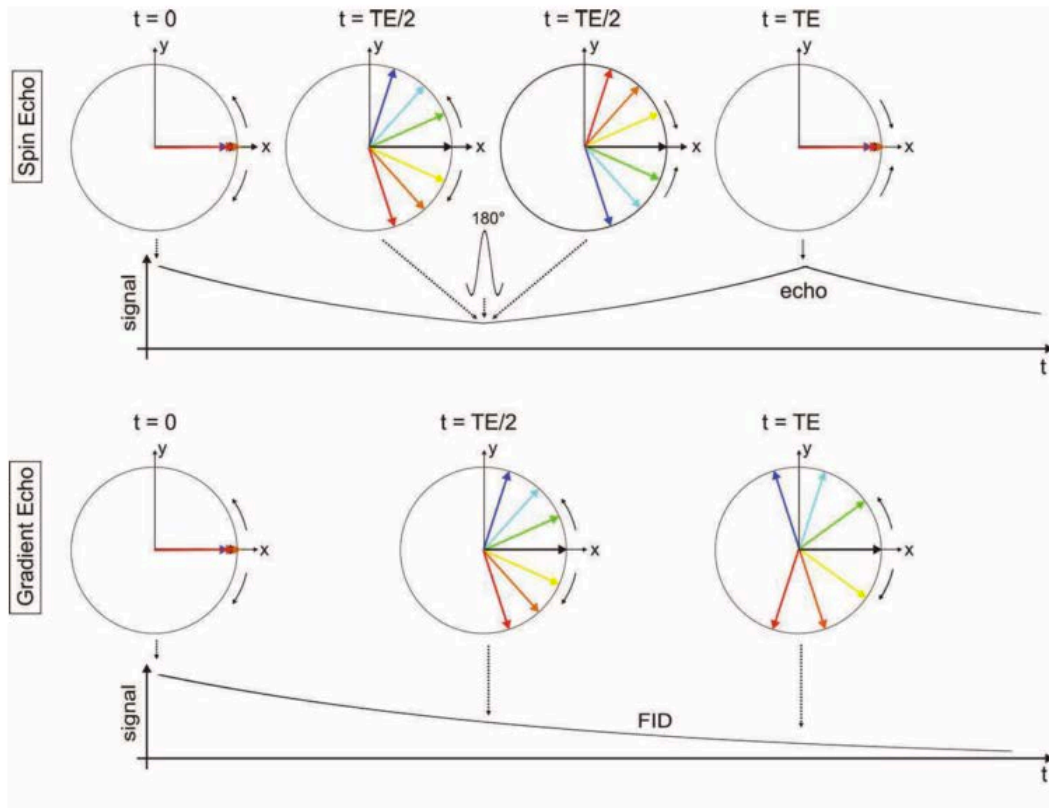
Top: The 180° refocusing pulse for spin echo imaging flips over magnetization and reverses the rotation direction of the transverse magnetization resulting in a compensation of dephasing caused by the T2' effect meaning the magnetization is rephased at echo time TE.

Bottom: For gradient echo imaging, the dephasing is not reversed. Signal and contrast are determined by both T2' and T2* effects. As a result shorter echo times are necessary for detectable gradient echo signal intensity

2.4.1.3 Tissue signal

All MRI signal is composed of a combination of T1 and T2 signal. The weighting of these two components is dependent on the sequence acquisition parameters, in particular the time to recovery (TR) between pulse sequences, and the time to echo (TE). A rapid TR with a rapid TE combines to produce a signal which is predominantly T1 weighted, while a pulse

sequence with a long TR and long TE will produce a predominantly T2 weighted image. Combining a long TR with a short TE produces a signal neither T1 or T2 weighted, and is instead predominantly affected by the number of excited protons producing any signal, and is therefore known as 'proton-density' weighting.

2.5 CARDIAC MRI

Cardiac MRI produces numerous challenges in MRI acquisition. The heart is in constant motion, not just due to the regular contraction of the atria and ventricles, but also due to the movement of the diaphragm, on which it sits, during respiration. Thus standard sequences, which take several minutes to acquire, cannot be used. Secondly, blood itself produces numerous artifacts. Fast blood flow, as seen through stenotic valves and vessels, causes dephasing of protons leading to signal drop out, while slow flowing blood (typically seen between the trabeculae of the ventricular apex) produces a signal not dissimilar from that of the ventricular wall itself. Finally the flow of blood generates its own magnetic field inhomogeneity causing artifacts, a problem exacerbated by the requirement to use fast gradient echo sequences in order to capture the heart in motion. Each of these problems can be overcome, but explain the need for higher specification scanners compared to conventional anatomical imaging, and the relatively delayed uptake of cardiac MRI compared to imaging of other regions of the body.

2.5.1 Commonly used sequences

Numerous cardiac sequences exist which allow for a detailed and thorough interrogation of the anatomical structure and function of the heart. For anatomical imaging these range

from black blood T1 and T2 weighted images, which most closely resemble conventional MRI imaging elsewhere in the body, through to tissue mapping which is revolutionizing our ability to perform a 'virtual biopsy' of the myocardium. On a functional front cine imaging provides visualization of the heart throughout the cardiac cycle allowing assessment of motion abnormalities, while perfusion sequences provides functional information on the haemodynamic flow of blood to the myocardium. However for the purpose of this thesis this chapter will focus on two of the most useful sequences for the quantification of myocardial function and blood flow: cine imaging and flow quantification

2.5.1.1 Cine sequences

As with almost all cardiac imaging, cine imaging requires the use of ECG gating in order to time the data acquisition to specific phases of the cardiac cycle. To compensate for respiratory motion, the easiest way to do this is through breath-hold acquisition. Given that a breath-hold beyond 20s is unfeasible for most patients with cardiovascular disease and that the cardiac cycle is typically in the order of 800-1000ms, image acquisition has to be fast. To achieve this gradient echo sequences must be used. These are acquired using either a spoiled gradient echo sequence or a balanced steady state free precessional (bSSFP) sequence. Both sequences use extremely rapid TRs typically in the order of magnitude of <10ms to achieve the temporal resolution and speed of image acquisition required to perform cardiac imaging. In spoiled gradient echo imaging, a low flip angle is combined with a rapid TE to provide a preserved signal while allowing rapid imaging. As the TR is smaller than the T2* relaxation of the excited tissue this means some transverse magnetization remains at the end of the sequence requiring a final gradient to be applied to remove this. This final gradient is known as the spoiling gradient which gives rise to the

name of the sequence. bSSFP on the other hand capitalizes on the residual transverse magnetisation. It instead applies a balanced gradient echo so that at the time of application of the next RF pulse the transverse magnetisation is in phase and preserved albeit with some T2* decay. This means the next RF pulse has a larger transverse magnetisation than the former with this building with each RF pulse. This results in a much larger returned signal improving image quality, albeit with a slightly unique tissue weighting which is neither T1 or T2 weighted but dependent on the square root of the ratio between the two. This incremental gain in signal and resultant improvement in signal is less susceptible to slow flowing blood providing better visualization of the blood-myocardium interface and thus more accurate myocardial delineation and quantification.(253) However this improved signal and efficiency of imaging comes at a cost. Any inhomogeneities in the magnetic field will be compounded as the transverse magnetization is amplified resulting in a significant band like signal drop out artifact in the images at the sites of these inhomogeneities. It is for this reason that bSSFP has only recently become widely used in 3T imaging as the effect of these inhomogeneities is amplified by the higher field strength and thus requires higher quality magnets with less variation in the magnetic field or more advanced shimming techniques to account for any magnetic field variation.

2.5.1.2 Flow sequences

Flow quantification can be achieved through the use of phase contrast sequences. A phase contrast sequence utilizes two bipolar gradient echo pulses, which are identical in length and amplitude varying only by their direction. As the phase shift a proton undergoes is dependent upon its location within the magnetic gradient, all stationary tissues will experience the same two opposed phase gradients, which will cancel each other out.

However any tissue moving in parallel with the opposed gradients will experience different degrees of dephasing then rephasing so will thus retain signal (see Figure 2-4). The magnitude of this phase shift is proportional to how far the proton has moved between the two gradient pulses. By varying the length of the pulses and the timing between these a direct correlation between velocity and signal can be obtained thus allowing quantification of the velocity within each voxel within the image. By combining the velocity data of each voxel with the number of voxels within a specified region of interest, such as a blood vessel, the total flow can be calculated.

Figure 2-4: Diagrammatic representation of the gradients applied in order to produce a phase contrast sequence – from Nayak et al.(254)
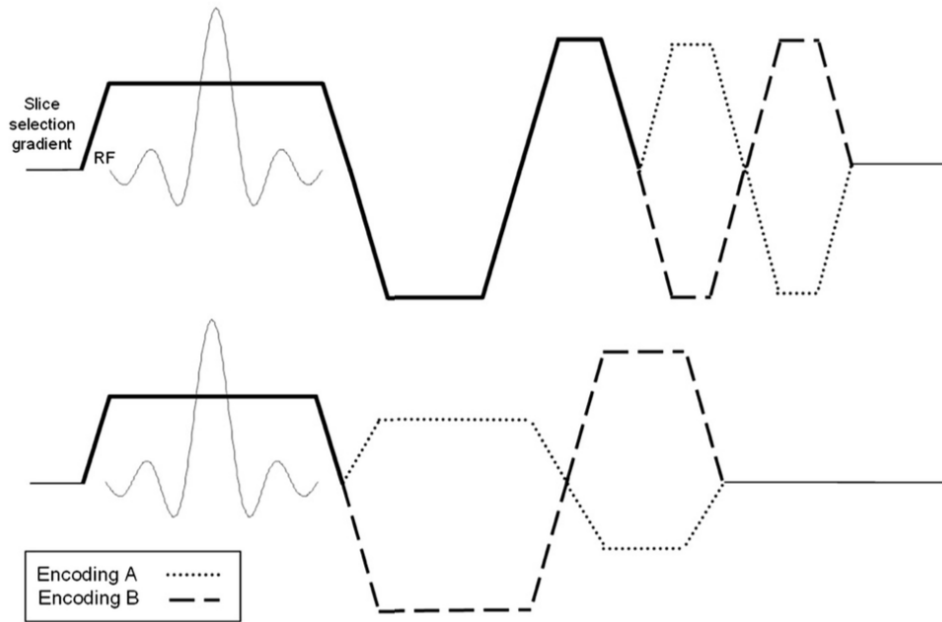
MR images are sensitized to measure the through-plane component of velocity by applying a flow-encoding gradient to the slice-selection axis of the pulse sequence. The flow encoding gradient can be added as (top) a bipolar pair to a flow-compensated slice selection waveform, or (bottom) to reduce minimum TE, combined with other gradient lobes

2.6 CONCLUSION

We have seen in this chapter that using a series of magnetic gradients applied in specific pulse sequences allows: selective excitation of a slice of tissue of interest; localization of the signal within the tissue; and weighting of the signal produced according to the type of tissue we best wish to detail. By varying and tweaking these gradients in a myriad of ways we can produce the wide range of sequences that are a daily feature within modern medical practice.

CHAPTER 3: Materials and Methods

3   INTRODUCTION

In this Chapter we will discuss the study design, the conductance of the study procedures and the acquisition of the MRI scans

3.1 STUDY DESIGN

3.1.1 Study Description

- The main body of work for the PhD (Chapters 5-7) comprises a single centre prospective observational cohort study of patients aged 40-85 years with stable COPD, with 1 year follow up.

Patients with COPD were recruited between June 2013 and May 2016. They were recruited from a combination of local COPD clinics, participants identified in screening for other studies, previous study participants and the *Tayside* Allergy & Respiratory disease Information System (TARDIS) database.

As well as a cohort of COPD patients a cohort of healthy volunteers was also recruited, the purpose of which was two fold. The first was to act as a comparator group to those with COPD using an approximately age and sex matched cohort. The second was to examine variables which might affect the measurement of PWV such as age, technique and cardiac outputs. These healthy volunteers had no history of cardiovascular or respiratory disease and were recruited via local recruitment process involving advertising in University of Dundee pay slips and the weekly University electronic newsletters.

Potential participants received an invite letter, a written 'Participant Information Sheet' (PIS) detailing the requirements of the study and the extent of their participation. An opt-

in form and pre-paid addressed envelope were included in the letter sent out. Participants were given at least 24 hours to read the PIS. Participants opting into the study were then contacted with details for their screening visit.

All study visits were held at Ninewells Hospital and Medical School.

3.1.1.1 Screening Visit

A member of the research team discussed the PIS with the participant, answered any questions posed and then obtained written informed consent. A detailed medical history was taken including and documented in a written case report form.   Heart rate, blood pressure and oxygen saturations were all obtained and where a recent eGFR was not available, blood was also taken to assess renal function for safety of contrast injection. An echocardiogram was performed during the screening visit on all potential COPD recruits, with a practice six minute walk test (6MWT) also undertaken to familiarize the patient with the procedure.

3.1.1.2 Visit 1 (Baseline)

This occurred over a half day visit to the Clinical Research Centre at Ninewells hospital.

COPD cohort:
- Pulmonary function tests: Spirometry including forced and relaxed vital capacity, gas transfer co-efficient, and impulse oscillometry on air was performed as per ATS guidelines.(255)
- MRI scan (see below for a description of acquisition and analysis and the Appendix for the MRI study SOP).
- Bloods were taken at the same time as cannulation and saved for future biomarker and genomic analysis.
- 6MWT as per ATS guidelines.(256)

Healthy volunteers

- MRI scan (as above).
- Bloods were taken at the same time as cannulation and saved for future biomarker and genomic analysis.

3.1.1.3 Visit 2 (Follow-up)

This involved a half day visit to the Clinical Research Centre at Ninewells hospital.

COPD cohort:

- Pulmonary function tests: Spirometry including forced and relaxed vital capacity, gas transfer co-efficient, and impulse oscillometry on air will be performed.
- MRI scan (see appendix A). Bloods will be taken at the same time as cannulation.
    - Bloods will be saved for future biomarker and genomic analysis.
- 6MWT

Healthy volunteers were not required to re-attend.

Figure 3-1 and Table 3-1 demonstrate the study visits and study flow plan.

Figure 3-1: Study flow chart for the COPD cohort
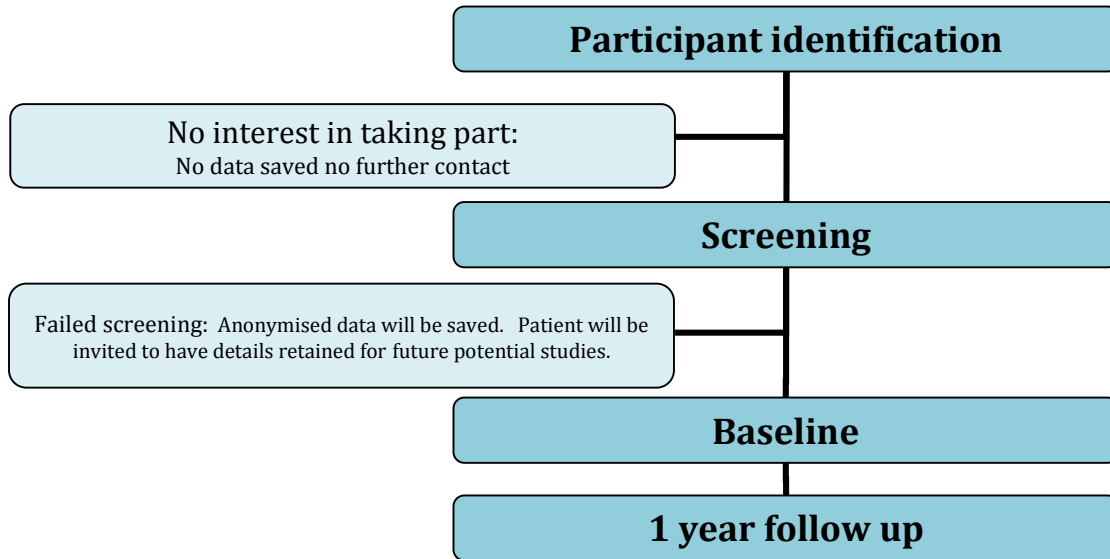
Table 3-1: Study matrix of the three study visits as undergone by the COPD cohort

Time	Screening	Baseline	1 year
Inclusion/Exclusion criteria	X		
Consent	X		
History	X		X
HR/BP/Oxygen saturations	X	X	X
Echocardiogram	X		
PFTs		X	X
6MWT		X	X
MRI		X	X
Bloods		X	X

3.2 STUDY POPULATION

3.2.1 Patient Inclusion Criteria

- Male and female volunteers aged 40-85 years with stable COPD
- Previous spirometry/PFTs documenting FEV1/FVC ratio <70%
- Smoking history ≥10 pack-years.
- GOLD 1 criteria: FEV1 >80% predicted
- GOLD 2 criteria: 50% < FEV1 <80% predicted
- GOLD 3 criteria: 30% < FEV1 <50% predicted
- GOLD 4 criteria: FEV1 <30% or FEV1<50% plus chronic respiratory failure predicted
- Stable defined as no exacerbation in previous 2 months.

3.2.2 Patient Exclusion Criteria

- History of cardiac condition, including but not limited to ischaemic heart disease, valvular disease(mild functional regurgitation allowed), arrhythmia, cardiomyopathy, congestive cardiac failure or congenital cardiac disease
- Previous cardiac or thoracic operation
- Other co-existent lung condition
- Connective tissue disease or systemic vasculitis.
- Severe renal impairment: eGFR ,30ml/min
- Moderate or severe LV systolic dysfunction (EF <40%)
- Any absolute contra-indication to MRI
- Participation in an interventional clinical trial
- Pregnancy
- Inability to provide informed consent

3.2.3 Healthy Participant Inclusion Criteria

- Asymptomatic
- Able to provide informed consent

3.2.4 Healthy Participant Exclusion Criteria

- History of cardiac condition, including but not limited to ischaemic heart disease, valvular disease (mild functional regurgitation allowed) , arrhythmia, cardiomyopathy, congestive cardiac failure or congenital cardiac disease
- Previous cardiac or thoracic operation
- Lung condition including but not limited to COPD
- Connective tissue disease or systemic vasculitis.
- Severe renal impairment: eGFR ,30ml/min
- Moderate or severe LV systolic dysfunction (EF <40%)
- Any absolute contra-indication to MRI
- Participation in an interventional clinical trial
- Pregnancy

3.2.5 Ethical approval

Ethical approval was sought and approved by the East of Scotland Research Ethics Committee 2 (reference 14/ES/0034, granted 14/04/2014 - see appendix) prior to the start of patient identification and recruitment. All research was conducted in accordance with the declaration of Helsinki.

3.2.6 Screening For Eligibility

As described above a screening visit was undertaken to assess eligibility. This was both to consent patients as well as to perform an echocardiogram to ensure there was no significant left ventricular systolic impairment (ejection fraction <45%) or the presence of

significant valvular pathology prior to progression with the rest of the study (see Table 3-2).

Table 3-2: Echocardiographic results obtained during screening visit

Parameter	Mean (SD)
LVIDd (mm)	46.4 ± 6.6
LVIDs (mm)	32.1 ± 7.6
LVEF* (%)	62.5 ± 8.2
PASP (mmHg)	12.8 ± 9.9
PAT (ms)	117.0 ± 28.9

*based on biplanar modified simpsons technique

3.2.7 Ineligible and non-recruited participants

All participants who failed screening did not progress any further with the study. Anonymised details were retained for future comparison with the study group to assess for the presence of potential skewing in the study. This was included in the consent documentation during the screening visit.

3.2.8 Withdrawal procedures

All participants were free to withdraw from the study at any time. If they withdrew prior to the baseline visit, all data pertaining to that patient was removed. If they withdraw after the baseline visit then their data was saved unless they requested otherwise.

Data collected from study visits up to the point of withdrawal and any safety visit was available for analysis. If a participant withdrew consent for use and retention of data and/or samples collected, this was complied with and documented.

3.3 STUDY VISIT PROCEDURES

All study procedures were performed on the same visit. For the COPD participants this included pulmonary function testing, a six minute walk test (6MWT) and a cardiac MRI.

3.3.1 Pulmonary Function Testing

All pulmonary function tests were performed using a VMax Encore V22 bodybox (CareFusion, Basingstoke, UK). Spirometry, lung diffusion and body plethysmography were all performed at the same time during the study visit prior to the six-minute walk test. Patients were instructed to abstain from using their inhalers for the day of, and the day before, their study visit. All measures were performed by one of three experienced pulmonary physiologists. Measurements were performed as per ERS/ATS guidelines.(255)

3.3.2 Six-Minute Walk Test

The six minute walk test was performed as per ATS guidelines.(256) The only deviation from these guidelines was the use of a 25m straight line course as opposed to a 30m course. While in theory this has the potential to reduce the observed distance walked by the individuals due to a greater frequency of having to alternate direction, in practice variations in course length between 15 and 50m have been shown to not significantly affect the total distance walked.(257) All 6MWT were performed by myself. Pre and post test oxygen saturations, heart rate and blood pressure were all obtained. The course and route were demonstrated before the test started. Predefined phrases of encouragement were used every minute in conjunction with informing the participant of the time remaining. The 6MWT was always performed after the pulmonary function tests to ensure that these measures were not influenced by tiredness from the exercise.

3.4 MRI IMAGE ACQUISITION

3.4.1 Patient preparation

All patients were informed about the MRI using both the PIS and a detailed explanation during the screening visit. A safety questionnaire was performed during screening, and again by a radiology department assistant on the day of attendance for their MRI. Details of this were confirmed by the MRI radiographer prior to progression for their MRI scan. Patients were changed into hospital gowns on their upper body and all external metal work removed as per standard safety procedures. A cannula was then inserted into the antecubital fossa before the patient was taken through to the MRI scanner.

All MRI scans performed in this thesis were acquired with a 32 RF cardiac receiver channel coil, on a 3 Tesla MRI scanner (Magnetom Trio, Siemens, Erlangen, Germany). Patients were positioned supine on the bed with their head positioned towards the bore of the magnet. Pillows and foam leg supports were used as appropriate to ensure the patient was comfortable during the examination. An MRI compatible blood pressure cuff was applied around the upper arm of the upper limb contralateral to the site of the cannula. A spirometric probe was placed on the index finger of the same arm.

3.4.2 Ventricular image acquisition

A three-plane localiser was obtained, following which 4 chamber, 2 chamber and short axis localisers of the heart were obtained. An axial half-Fourier acquisition turbo spin echo (HASTE) stack was acquired of the chest.

Using these sequences a 4 chamber, and 2 chamber long axis cine sequences were obtained. From these a short axis stack was planned aligned to the atrioventricular groove. A balanced steady state free precession (bSSFP) stack was acquired in breathold from the atrioventricular ring to the apex (Slice thickness=6 mm, interslice gap 4mm, TR/TE=47.6/1.49 ms, no. averages=1, phases=25, bandwidth/pixel=446 Hz, flip angle=53°,

field of view (FOV) = 360 × 360mm2, FOV phase = 84.4%, matrix=256 × 256), parallel acceleration factor = 2).

3.4.3 Pulmonary PWV image acquisition:

Using the short axis bSSFP and HASTE stack, a bSSFP view of the right ventricular outflow tract was planned following which an orthogonal plane was acquired to optimally visualise the main pulmonary artery and valve. Localisers along the length of the right and left pulmonary artery were then obtained. From these phase contrast imaging was acquired in three planes - through the main pulmonary artery (MPA), right pulmonary artery (RPA), and left pulmonary artery (LPA) to provide a true cross section through each of the three arteries. The MPA slice was located in the proximal main pulmonary artery as close to the valve as possible in order to maximise the distance for the TT technique while also avoiding the valve throughout the cardiac cycle. The RPA and LPA were placed as close to the hila as possible while remaining proximal to the origins of the first visualised branch (See Figure 3-2).

Figure 3-2: Planning of the short axis views of the pulmonary arteries.
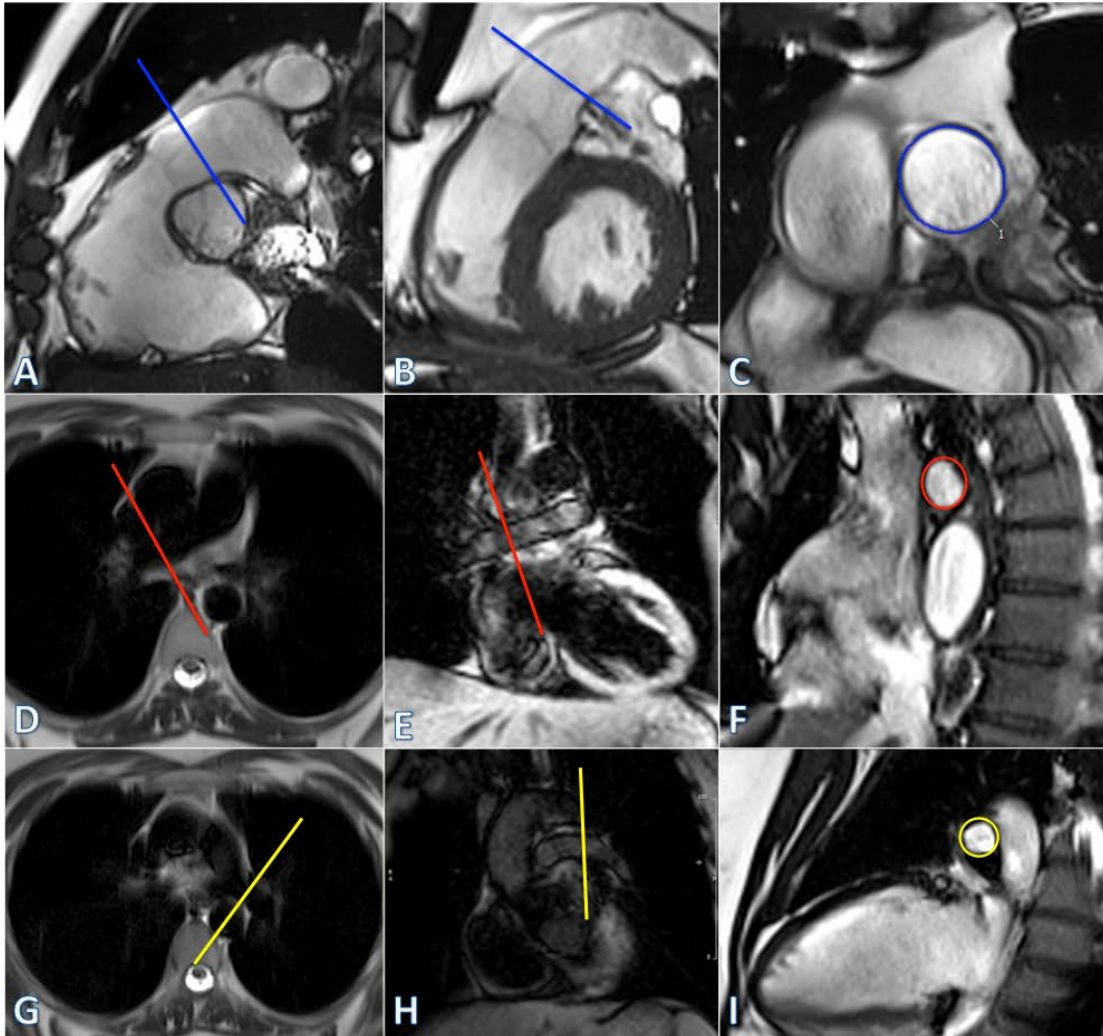
Planning of the main (A-C), right (D-F) and left (G-I) pulmonary arteries using a combination of right ventricular outflow views (A-B), the HASTE axial stack (D and G) and dedicated scout views of the branch pulmonary arteries (E and H). The linear lines represent the planes planned for the final short axis view as demonstrated in C, F and I.

3.4.3.1 High temporal resolution sequences

For the high temporal resolution scan the acquisition parameters of the phase contrast sequence were as follows: Slice thickness=6 mm, TR/TE=7/4 ms, no. averages=1, phases=128, velocity encoding=150 cm/s, bandwidth/pixel=340 Hz, flip angle=15°, field of

view (FOV) =320 × 320mm2, matrix=256 × 256. This provided a temporal resolution of 7ms (based on a TR of 7ms with a single read out and no view sharing) and a spatial resolution of 1.25 x 1.25 x 6mm.

3.4.3.2 High spatial resolution sequences

For the high spatial resolution scan, the acquisition parameters were: Slice thickness=6 mm, TR/TE=12/4 ms, no. averages=1, phases=80, velocity encoding=150 cm/s, bandwidth/pixel=340 Hz, flip angle=15°, field of view (FOV) = 320 × 320mm2, matrix=512 × 512. This provided a temporal resolution of 12ms, spatial resolution of 0.625 x 0.625 x 6mm. Both sequences were free breathing, with an acquisition time of approximately 4 minutes depending on heart rate.

3.5 IMAGE ANALYSIS

All images were anonymised and allocated a randomized study number before being exported to a dedicated workstation with image analysis performed using CVI 42 (Circle Cardiovascular Imaging Inc., Calgary, Alberta, Canada) with all analysis being performed by myself.

3.5.1 Ventricular quantification:

Epicardial and endocardial contours were drawn around the right and left ventricles at end systole and end diastole (see Figure 3-3) as per SCMR guidelines.(258) The only deviation from these guidelines was that the right ventricular trabeculae were included in the mass measurement and excluded from the volume calculation. The rationale for this is two-fold: Firstly, the SCMR guideline do not provide guidance on right ventricular mass measurement with their guidelines centered on the optimization of the volume reproducibility rather than mass quantification; and secondly, previous work has shown that right ventricular papillary and trabecular mass comprises a greater percentage of the right ventricular mass in those with pulmonary hypertension than in healthy controls, and

that changes in papillary and trabecular mass better reflect changes in pulmonary haemodynamics than right ventricular free wall mass alone.(259) The septum was treated as belonging to the left ventricle and was excluded from the right ventricular mass. Mass and volumes were normalised to height^1.7.

Figure 3-3: Short axis image of the right and left ventricles with epicardial, endocardial, and trabecular borders drawn.
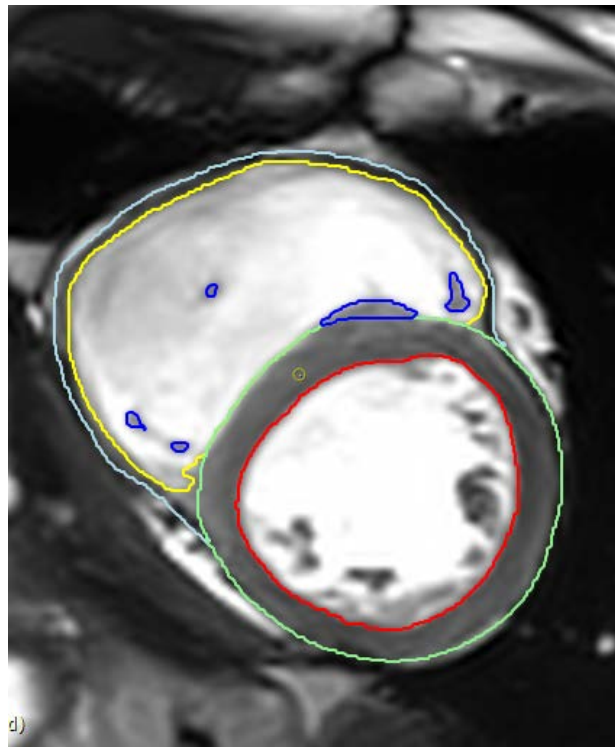
Pale blue line – Right ventricular epicardial border; Yellow line – right ventricular endocardial border; Green line – Left ventricular epicardial border; Red line – Left ventricular endocardial border; Dark blue line – Right ventricular trabecular outlines.

Intra-observer repeatability was tested in n=20 COPD participants randomly selected from the main study. Agreement was excellent for all volumetric measures (See Table 3-3) although the limits of agreement were consistently wider for the right ventricle measures than for the left. No significant difference was observed between the two measures when compared using a paired sample t-test (p>0.05 for all). Bland-Altman plots are provided in Figure 3-4 and Figure 3-5.

Table 3-3: Absolute agreement average measure intraclass correlation coefficients for

repeated measures of right and left ventricular volumes and function.

Ventricular metric	ICC	95% CI	p
LVEDV	0.99	0.99-1.0	<0.001
LVESV	0.99	0.96-0.99	<0.001
LVSV	0.97	0.93-0.99	<0.001
LVEF	0.94	0.85-0.98	<0.001
LVM	0.97	0.93-0.99	<0.001
RVEDV	0.99	0.96-0.99	<0.001
RVESV	0.94	0.87-0.98	<0.001
RVSV	0.96	0.91-0.99	<0.001
RVEF	0.84	0.64-0.93	<0.001
RVM	0.86	0.69-0.94	<0.001

Figure 3-4: Bland-Altman plots of intra-observer differences between left ventricular
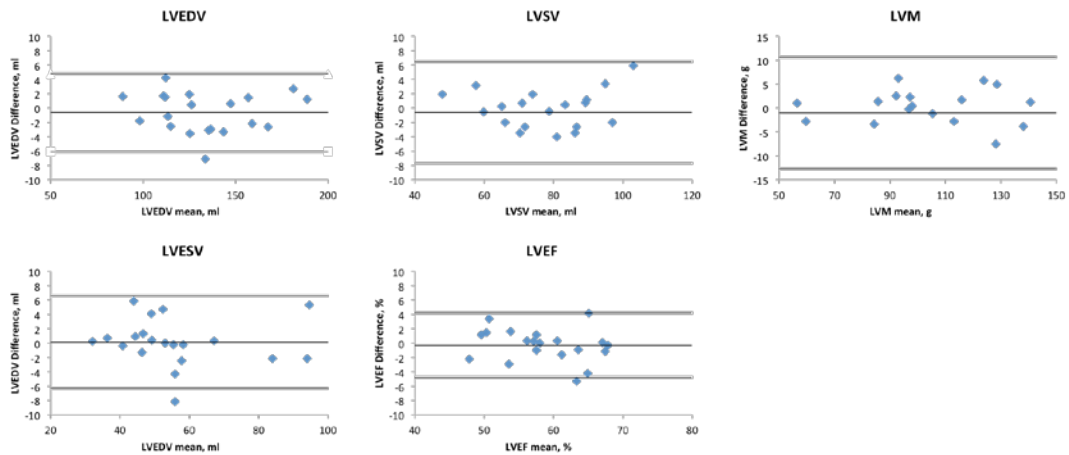
Figure 3-5: Bland-Altman plots of intra-observer differences between right ventricular measures.
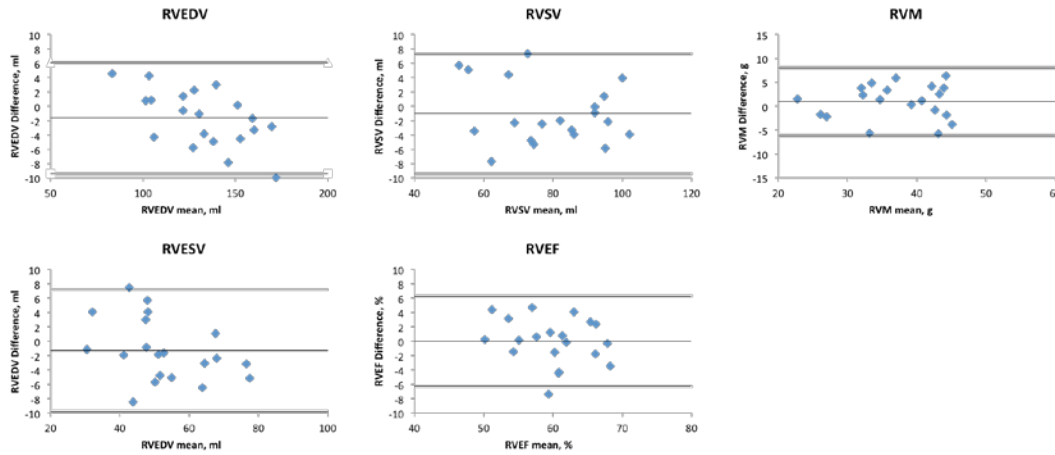
3.5.2 Pulmonary PWV Image analysis

3.5.2.1 Transit time technique

For the transit time (TT) method both distance and time data need to be measured. For the distance, the HASTE axial images were used to measure the distances between the imaging planes following the centre-line of the vessel. Where the right or left pulmonary artery lay on different slices from the main pulmonary artery a vertical height was calculated from the slice thickness and number of slices. Using this vertical height and horizontal length measured on the axial slices the final distance was calculated using Pythagoras theorem. For the time component the phase and magnitude images were pulled up side by side. A contour was manually drawn around the perimeter of the vessel on the magnitude image. This was then automatically propagated throughout the remainder of the images, and manually corrected where malposition occurred. The program then automatically calculated area, flow and velocity data, which was exported to Excel 2010 (Microsoft, US). The flow curves from the MPA, RPA and LPA were plotted, and the time to the systolic upstroke of the waves then calculated. The arrival time of the flow wave was identified as the intersection between the systolic upstroke and baseline flow. The systolic upstroke

was calculated as the line through the data points that lay between 20% and 80% levels of the maximum flow rate. The use of which was determined based on previous work by a previous PhD student at our institution (Deirdre Cassidy, Unpublished) and the work of Dogui et al.(260) The baseline was the horizontal line at minimum velocity before systole. Pulse wave was calculated for both RPA and LPA using equation 1:

$$TT\ PWV = \frac{\Delta d}{\Delta t} \tag{1}$$

Where Δd is the distance between the planes and Δt is the difference in the time to foot between the MPA and RPA/LPA (See Figure 3-6).

Figure 3-6: Transit time technique for calculation of PWV
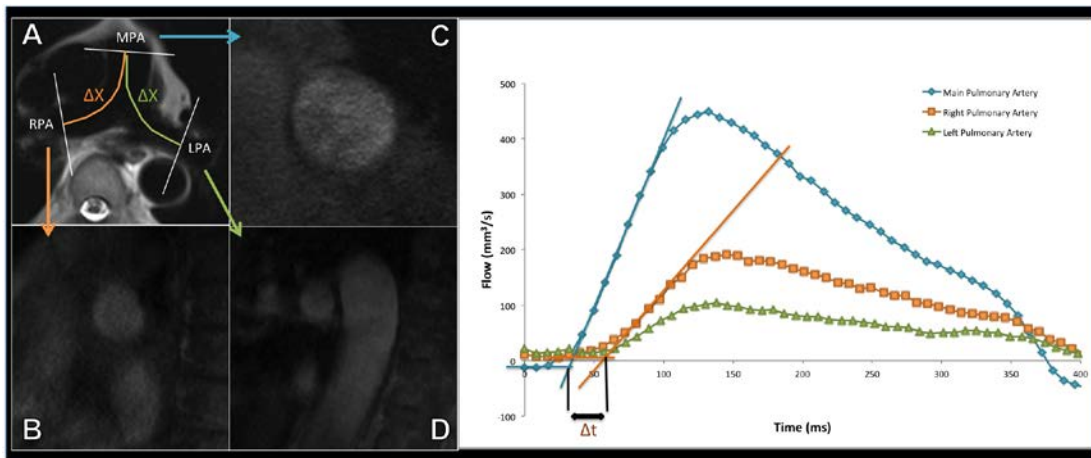
A – Axial HASTE through the pulmonary trunk bifurcation; B – short axis RPA; C – short axis MPA; D – short axis LPA; E – flow curves from the three pulmonary arteries. Time delay between the arrival of the three flow curves can then be derived, while the distance is measured from the axial HASTE image.

3.5.2.2 Flow area technique

For the flow-area (QA) method the phase and magnitude images were pulled up side by side. A contour was manually drawn around the perimeter of the vessel on the magnitude image on each image for the first 200ms of the cardiac cycle. From this the programme

calculated the total area and flow within the cross section of the pulmonary vessel. The area and flow were then plotted against one another during early systole. Early systole was defined as the time period in systole during which both the vessel area and flow were simultaneously increasing. Three techniques have been described for the calculation of QA PWV with all being variations on the basic premise of equation (2):

$$QA\ PWV = \frac{\Delta Q}{\Delta A} \qquad (2)$$

Where Q is the flow and A is the area through the pulmonary artery. The first is as described by Peng et al.(207) whereby the gradient of the line is fitted through these points using a minimum squared difference technique hereby known as QA_{Trad} (Figure 3-7). The technique proposed by Quail et al.(261) follows the same principle but restricts analysis to the first 3 data points of the systolic upstroke in order to avoid the influence of reflected waves (QA_3). Finally, Davies et al.(262) have proposed a technique that accounts for the effects of reflected waves thereby allowing usage of more data-points than the Quail et al. technique whilst maintaining accuracy. This was originally described for pressure and velocity data derived from invasive catheter measurements, however has been adapted to give equation (3):

$$PWV = \sqrt{\frac{\sum \Delta Q^2}{\sum \Delta A^2}} \qquad (3)$$

This used all datapoints in early systole, similar to the QA_{Trad} technique. This technique for calculating PWV shall be entitled QA_{INV} for the remainder of this chapter.
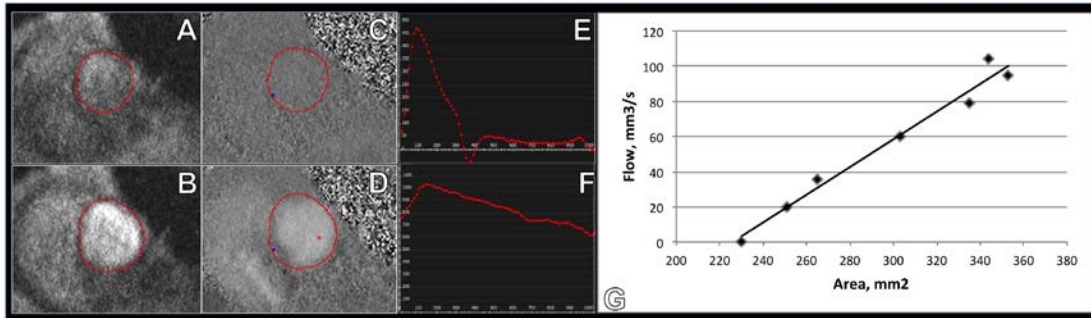
A and C demonstrate the magnitude and phase contrast images at the start of systole, while B and D demonstrate the magnitude and phase images at peak systolic flow. Reproducibility of both techniques is discussed in detail in Chapter 4.

3.5.2.3 Aortic PWV analysis:

A retrospective ECG-gated gradient-echo pulse sequence with velocity encoding was applied to measure the through plane flow at two predefined locations in the ascending and abdominal aorta. The first slice was positioned through the aortic arch at the level of the pulmonary bifurcation, and the second slice was placed axial through the proximal abdominal aorta just distal to the aortic hiatus. The same phase contrast sequence was used as for the pulmonary PWV measurement. To determine the distance between the two aortic slices, a 2D gradient echo FLASH (fast low angle shot) was acquired of the aorta in a 'candy stick' double-oblique orientation. TR/TE 40/1.2 ms; flip angle 15°, slice thickness of 8 mm, 23 cardiac phases, 1 averages, a pixel size of 1.5 x1.5 mm2, bandwidth of 475 Hz/ pix and breath hold scan time of average 9 seconds. The distance was measured along the aorta between the two analyses planes (Δx value) using candy stick FLASH and the time delay calculated as the time delay between the arrival of the foot of the pulse wave at the ascending aorta and abdominal aorta (See Figure 3-8).

Figure 3-8: Aortic pulse wave velocity calculated using the transit time technique.
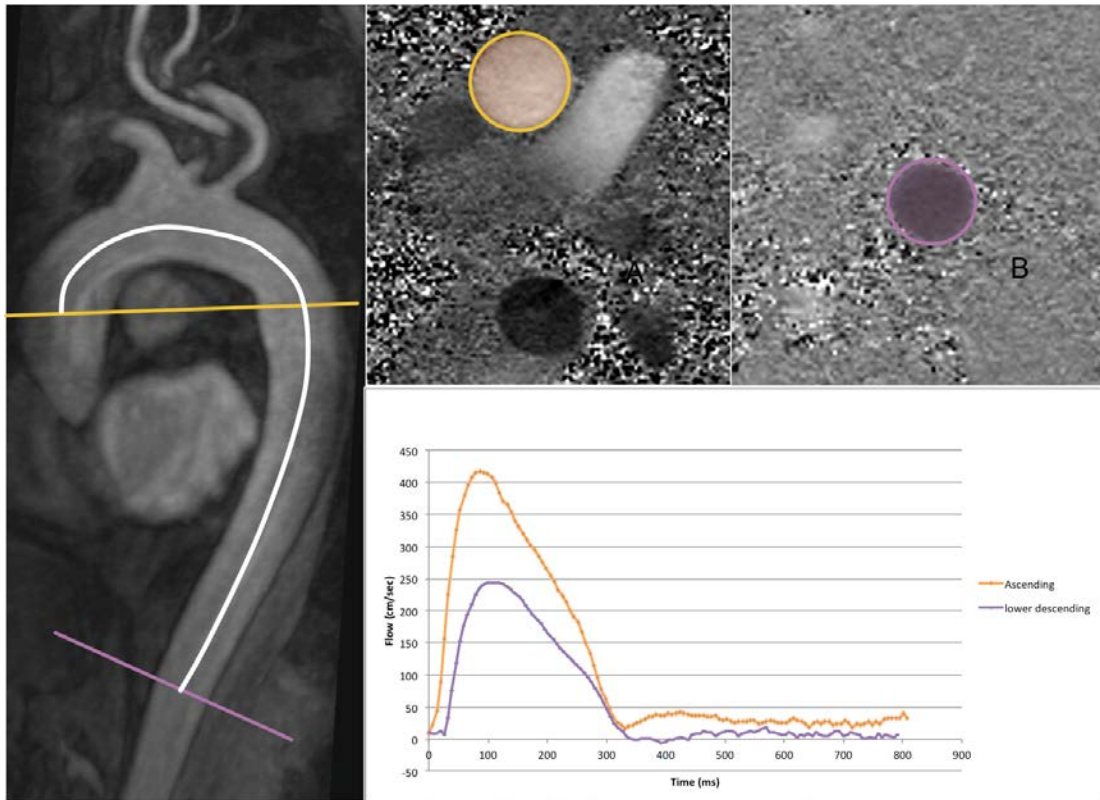
The flow curves from the ascending thoracic aorta and the abdominal aorta were plotted, and the time to the systolic upstroke of the waves then calculated. The arrival time of the flow wave was identified as the intersection between the systolic upstroke and baseline flow. The systolic upstroke was calculated as the line through the data points that lay between 20% and 80% levels of the maximum flow rate. The baseline was the horizontal line at minimum velocity before systole. Pulse wave was calculated using equation (1).

3.6 SAMPLE SIZE CALCULATION

Calculations were based on the typical RV mass in severe COPD – 57.6 ± 4.1 g/m^2.[80] No data exists on the expected progression rates of right ventricular mass in COPD. Therefore progression rates in mass in placebo groups in interventional studies for pulmonary hypertension have had to be used as a substitute. These describe an increase in mass of 5-8g (change in right ventricular mass detected over 4-36 months in groups of 21 and 44 participants respectively).[263,264]

Based on these factors, n=17 will allow detection of a 4g change with study power of 80% and a p=0.05. Further work by Bradlow et al. has shown a group size of 17 will allow detection of 10ml change in RV end diastolic volume which correlates with changes of 9-15ml seen in the placebo arm of drug intervention studies.(263–265)

Based on variability in healthy volunteers and patients with established pulmonary hypertension (207,208), n=26 will allow detection of a PWV difference of 0.64m/s between the groups with a study power of 80% and a p=0.05. n=30 will be recruited to account for potential dropouts and patients unable to tolerate the MRI scan. Ideally 30 patients will be recruited into those with mild, moderate and severe COPD to allow comparison of PWV between varying degrees of COPD severity.

CHAPTER 4: Assessment of proximal pulmonary arterial stiffness using magnetic resonance imaging: Effects of technique, age and exercise.

4 INTRODUCTION

The compliance of the pulmonary artery is a key component in decoupling the right ventricle from the pulmonary bed, allowing the right ventricle to work at maximum efficiency and protecting the microcirculation from large pressure gradients.(117,130,266) We have seen in Chapter 1 that the pulmonary stiffness has significant implications for right ventricular function,(131) functional capacity,(134) and mortality.(135–139) Its curvilinear relationship with RV function and its presence even in those with isolated exercise induced pulmonary hypertension(65,78,143,172) suggest pulmonary arterial stiffness as a promising biomarker for detection of early disease and as a potential therapeutic target before end stage arterial remodeling occurs with dire consequences for the failing right ventricle.

While the majority of measures of pulmonary arterial stiffness require right heart catheterisation to derive pulmonary pressures pulse wave velocity (PWV) is an entirely non-invasive technique for measuring arterial stiffness that does not require knowledge of the arterial pressures. This can be measured using MRI using one of two methods: the transit time (TT) technique which measures the time it takes for the pulse wave to travel between two separate points along the vessel; and the flow-area (QA) technique which measures the change in cross sectional area and flow across the vessel at this point to derive the pulse wave velocity. The results of these techniques have been

shown to correlate well with one another in the pulmonary circulation(208), and each individual technique has been shown to have good same day interscan reproducibility.(203,207) However the reproducibility of the two techniques has not been directly compared in the pulmonary circulation. In addition the effects of age or physiological flow states on both these two measures of PWV has not been elucidated.

The aim of this study is thus to assess and compare the reproducibility of the two MRI methods for measuring PWV in healthy volunteers, and to assess the effects of age and exercise on these measures.

4.1 MATERIALS AND METHODS

4.1.1 Population

Two separate study populations were studied:

1. Young healthy volunteers (YHV): Ten healthy volunteers under 40 (3 Males, 7 females, Mean age 31.5 ± 2.4 years) with no history of cardiovascular or lung disease were recruited to the study. All individuals underwent high temporal resolution phase contrast scans of their main pulmonary artery and branch pulmonary arteries at baseline, during exercise, and at 6 months follow-up.

2. Older healthy volunteers (OHV): 20 healthy volunteers over the age of 55 (9 male, 11 female, mean age 60.2 ± 1.1 years) with no history of cardiovascular or lung disease were recruited to the study. All individuals underwent high temporal resolution phase contrast scans of their main pulmonary artery and branch pulmonary arteries followed by a high spatial resolution phase contrast scan of their main pulmonary artery. All 4 sequences were repeated during the same scanning session.

4.1.2 MRI

The high spatial resolution and high temporal resolution phase contrast sequences of the pulmonary artery were acquired as described in section 3.4. Aortic PWV was similarly performed as described. The pulmonary PWV was analysed using the transit time technique, and the traditional, 3 point technique and Davies technique for flow-area PWV calculation.

4.1.2.1 Exercise

Isometric exercise was performed by the volunteer by crossing their feet and then forcefully plantarflexing the superior foot while dorsiflexing the inferior foot against each other. The participant was instructed that if any discomfort developed they should swap the positions of the feet and to continue the exercise. Image acquisition began after five minutes of this exercise with the exercise continued throughout the duration of the image acquisition. Gentle encouragement was given to ensure sustained effort throughout the process.

4.1.3 Statistics

Descriptive statistics were used for the analysis of the demographic and clinical features of the cohorts with data expressed as mean ± SEM. Normality and equality of variances of the variables was tested. A dependent sample t-test was used to compare the difference between the first scan and the repeated measure, inter-scan measure and the exercise measure. ANOVA was used to compare PWV between the two cohorts. Bland-Altman plots were used to further investigate the inter-scan and inter-observer reproducibility. All data were analysed using SPSS statistical package (version 21.0, SPSS Inc. Chicago, Illinois). Significance was assumed when $p < 0.05$.

4.2 RESULTS

4.2.1 PWV measurements

Using the TT technique PWV was measurable in all individuals, however in 5 individuals, one of the sides produced grossly inaccurate results (PWV excessively high or negative), this error was slightly more common on the left (n=3) than the right (n=2). Using the high temporal resolution QA technique, PWV was measurable in 29/30 of the study participants at the MPA, 29/30 at the RPA, and 29/30 at the LPA. Using the high spatial resolution QA technique, PWV was measurable in 29/30 participants.

Using the TT technique MPA-RPA PWV was 2.7 ± 0.1 ms^{-1} while the MPA-LPA PWV was 3.3 ± 0.2 ms^{-1}. There was a significant difference between the PWV using the right pulmonary artery and the left pulmonary artery: mean (95% CI) of the differences -0.55 (-1.1 - -0.03), P=0.038.

The results of the three QA techniques for both the high temporal resolution and low temporal resolution sequences are described in Table 4-1. Using the high temporal resolution sequences the QA_{Trad} produced significantly higher results than the QA_3 (p<0.001) or the QA_{Inv} (p<0.001), whilst there was no difference between the QA_3 and QA_{Inv} techniques (p=0.41). Similar findings were observed with the high spatial resolution sequence with the QA_{Trad} produced significantly higher results than the QA_3 (p=0.004) or the QA_{Inv} (p<0.001), whilst there was no significant difference between the QA_3 and QA_{Inv} techniques (p=0.47). There was no difference in PWV between the two sequences using QA_{Trad}, however the higher temporal resolution yielded consistently lower PWV than the high spatial resolution sequence for both the QA_3 (p=0.028) and QA_{Inv} (p=0.001). Using the QA_{Trad} method the PWV was 1.99 ± 0.14 ms^{-1} in the MPA, 1.49 ± 0.11 ms^{-1} in the RPA and 1.37 ± 0.11 ms^{-1} in the LPA. The PWV was significantly higher in the MPA compared to the RPA (mean (95%

94

CI) of the differences: 0.49 (0.15-0.89), P=0.006) and the LPA (mean (95% CI) of the differences 0.63 (0.36-0.89), P<0.001). There was no significant difference between the RPA and LPA (mean (95% CI) of the differences 0.12 (-0.11-0.34), P=0.29).

Table 4-1: Comparison of PWV between the two phase contrast sequences and 3 post processing techniques

	QA_{Trad}	QA_3	QA_{Inv}
High Temporal resolution	1.98 ± 0.13	1.0 ± 0.11	1.1 ± 0.08
High Spatial resolution	2.11 ± 0.17	1.55 ± 0.16	1.67 ± 0.13

4.2.2 Within scan reproducibility

Within scan reproducibility was assessed in the 20 OHVs. Bland-Altman plots of the between scan differences are shown in Figure 4-1.

Figure 4-1: Bland-Altman plots comparing PWV repeatability during the same visit.
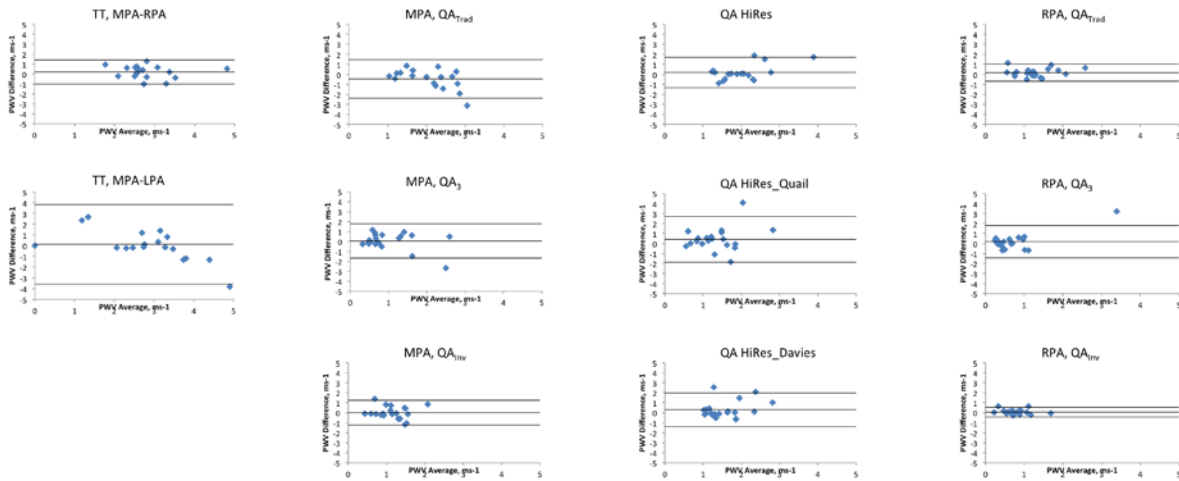
The middle line represents the mean difference while the upper and lower lines represent the $\pm 2SD$ limit.

Using the TT technique, the MPA-RPA PWV had better precision but lower accuracy than the MPA-LPA PWV (mean (95% CI) of PWV differences = 0.21 (-1.01-1.42) ms^{-1} and 0.13 (-3.57-3.83) ms^{-1} for the MPA-RPA and MPA-LPA respectively). Using the QA technique, the QA$_{Inv}$ technique again consistently yielded improved accuracy and precision over the QA$_{Trad}$ and QA$_3$ technique (mean (95% CI) of PWV differences = -0.46 (-2.39-1.47) ms^{-1}, 0.05 (-1.68-1.77) ms^{-1}, and 0.01 (-1.23-1.25) ms^{-1} for the QA$_{Trad}$, QA$_3$, and QA$_{Inv}$ of the MPA respectively; 0.17 (-0.68-1.02) ms^{-1}, 0.19 (-1.43-1.81) ms^{-1} and 0.06 (-0.42-0.55) ms^{-1} for the QA$_{Trad}$, QA$_3$, and QA$_{Inv}$ of the RPA respectively; and -0.29 (-0.91-0.32) ms^{-1}, -0.01 (-0.78-0.76) ms^{-1} and -0.06 (-0.69-0.56) ms^{-1} for the QA$_{Trad}$, QA$_3$, and QA$_{Inv}$ of the LPA respectively). The high spatial resolution yielded poorer reproducibility than the high

temporal resolution sequence (mean (95% CI) of QA$_{Inv}$ PWV differences = 0.01 (0.63) ms^{-1}, and 0.3 (0.86) ms^{-1} respectively). A combination of a high temporal resolution sequence through the RPA combined with the QA$_{Inv}$ post processing yielded the best reproducibility.

4.2.3 Inter-scan reproducibility

The scans were repeated at 6 months in 9 of the 10 YHVs. This resulted in reproducible results with no significant differences in the two measurements (P>0.5). Bland-Altman plots of the between scan differences are shown in Figure 4-2.

Figure 4-2: Bland-Altman plots comparing PWV repeatability on separate visits.
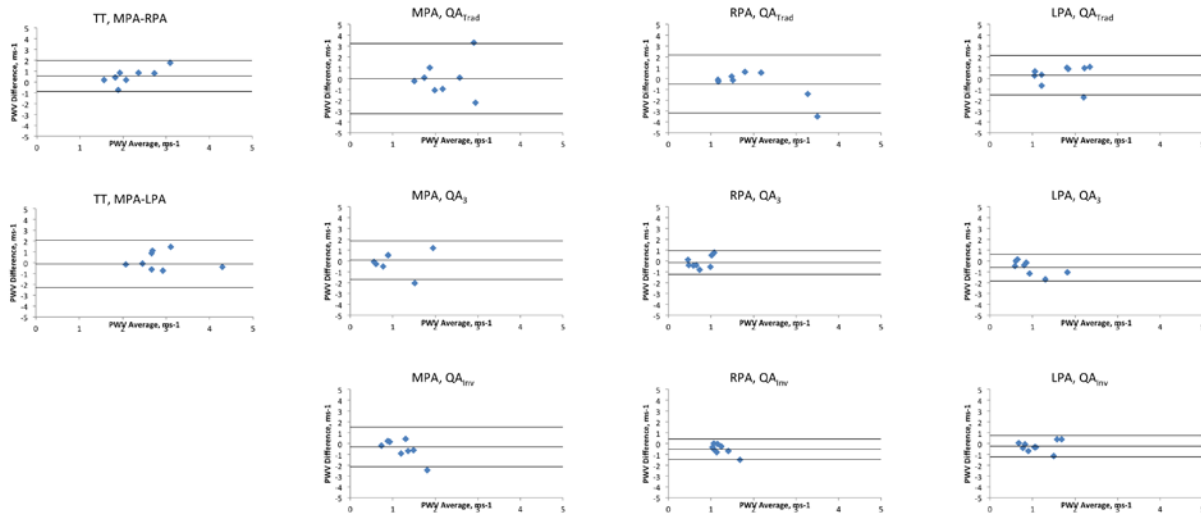
The middle line represents the mean difference while the upper and lower lines represent the $\pm$2SD limit.

Using the TT method, the MPA-RPA PWV had better precision but lower accuracy than the MPA-LPA PWV (mean (95% CI) of PWV differences = 0.56 (-0.86-1.99) ms^{-1} and 0.19 (-1.47-1.84) ms^{-1} for the MPA-RPA and MPA-LPA respectively). Using the QA technique, the QA$_{Inv}$ technique again consistently yielded improved accuracy and precision over the QA$_{Trad}$ and QA$_3$ technique (mean

(95% CI) of PWV differences = 0 (-3.24-3.24) ms^{-1}, -0.07 (-2.11-1.96) ms^{-1}, and -0.43 (-2.18-1.32) ms^{-1} for the QA$_{Trad}$, QA$_3$, and QA$_{Inv}$ of the MPA respectively; -0.5 (-3.18-2.18) ms^{-1}, -0.13 (-1.22-0.96) ms^{-1} and -0.52 (-1.46-0.43) ms^{-1} for the QA$_{Trad}$, QA$_3$, and QA$_{Inv}$ of the RPA respectively; and 0.31 (-1.51-2.14) ms^{-1}, -0.59 (-1.84-0.67) ms^{-1} and -0.24 (-1.22-0.75) ms^{-1} for the QA$_{Trad}$, QA$_3$, and QA$_{Inv}$ of the LPA respectively). A combination of a high temporal resolution sequence through the RPA combined with the QA$_{Inv}$ post processing yielded the best reproducibility.

4.2.4 Intra-observer reproducibility

Bland-Altman plots of the between scan differences are shown in Figure 4-3.

Figure 4-3: Bland-Altman plots comparing intra-observer PWV repeatability.
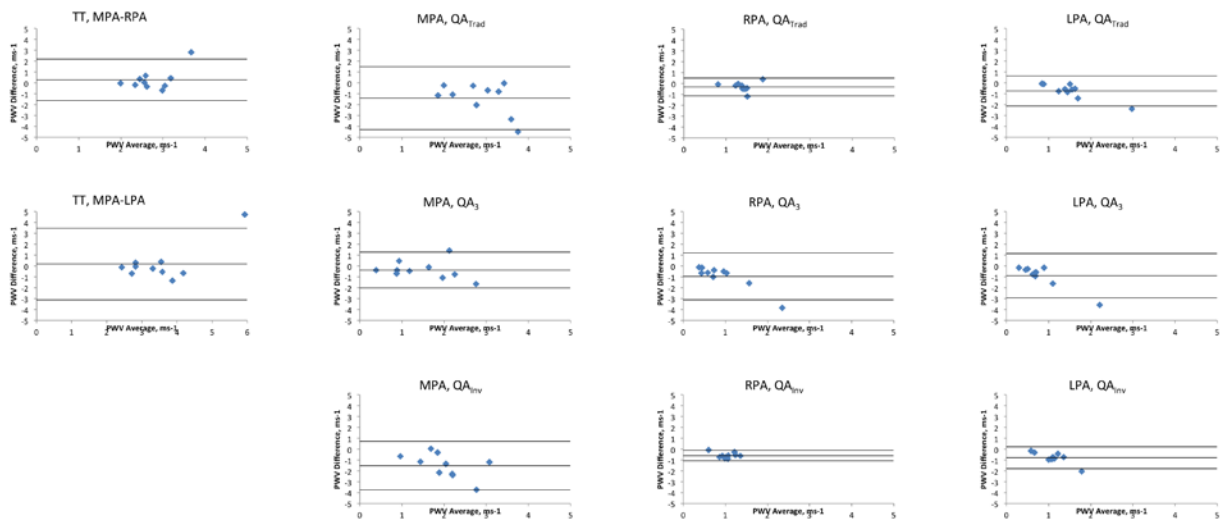
The middle line represents the mean difference while the upper and lower lines represent the $\pm$2SD limit.

Using the TT method, the MPA-RPA PWV had better precision but lower accuracy than the MPA-LPA PWV (mean (95% CI) of PWV differences = 0.28 (-1.63-2.19) ms^{-1} and 0.19 (-3.11-3.48) ms^{-1} for the MPA-RPA and MPA-LPA respectively). Using the QA technique, the QA$_{Inv}$ technique again

consistently yielded improved accuracy and precision over the QA_{Trad} and QA_3 technique (mean (95% CI) of PWV differences = -1.41 (-4.29-1.48) ms^{-1}, -0.36 (-2.01-1.28) ms^{-1}, and -1.51 (-3.74-0.73) ms^{-1} for the QA_{Trad}, QA_3, and QA_{Inv} of the MPA respectively; -0.31 (-1.12-0.5) ms^{-1}, -0.95 (-3.1-1.2) ms^{-1} and -0.58 (-1.06- -0.1) ms^{-1} for the QA_{Trad}, QA_3, and QA_{Inv} of the RPA respectively; and -0.74 (-2.12-0.64) ms^{-1}, -0.89 (-2.93-1.15) ms^{-1} and -0.78 (-1.79-0.22) ms^{-1} for the QA_{Trad}, QA_3, and QA_{Inv} of the LPA respectively). The high spatial resolution yielded better reproducibility than the high temporal resolution sequence (mean (95% CI) of QA_{Inv} PWV differences = -1.51 (-3.74-0.73) ms^{-1}, and -0.70 (-2.31-0.9) ms^{-1} for the high temporal resolution and high spatial resolution sequences respectively). A combination of a high temporal resolution sequence through the RPA combined with the QA_{Inv} post processing yielded the best intra-observer reproducibility.

4.2.5 Inter-observer reproducibility

Bland-Altman plots of the between scan differences are shown in Figure 4-4.

Figure 4-4: Bland-Altman plots comparing inter-observer PWV repeatability.
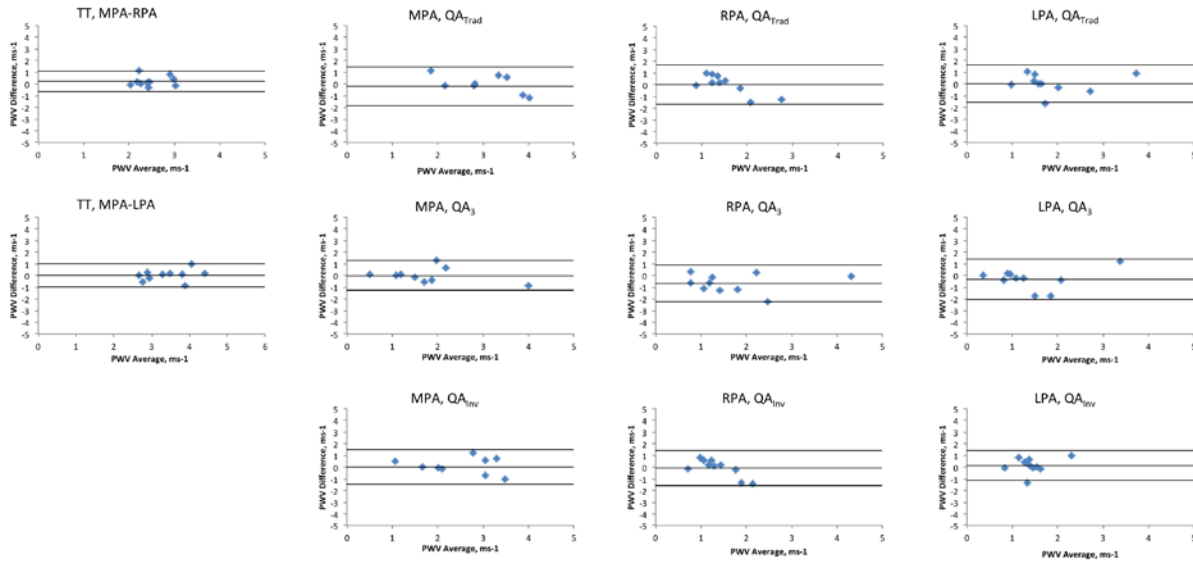
The middle line represents the mean difference while the upper and lower lines represent the $\pm 2SD$ limit.

Using the TT method, the MPA-RPA PWV had better precision but lower accuracy than the MPA-LPA PWV (mean (95% CI) of PWV differences = 0.23 (-0.64-1.1) ms^{-1} and 0.02 (-0.97-1.01) ms^{-1} for the MPA-RPA and MPA-LPA respectively). Using the QA technique, the QA$_{Inv}$ technique again consistently yielded improved accuracy and precision over the QA$_{Trad}$ and QA$_3$ technique (mean (95% CI) of PWV differences = -0.2 (-1.86-1.47) ms^{-1}, 0.02 (-1.25-1.29) ms^{-1}, and 0.01 (-1.47-1.5) ms^{-1} for the QA$_{Trad}$, QA$_3$, and QA$_{Inv}$ of the MPA respectively; 0.01 (-1.67-1.69) ms^{-1}, -0.67 (-2.24-0.9) ms^{-1} and -0.08 (-1.58-1.42) ms^{-1} for the QA$_{Trad}$, QA$_3$, and QA$_{Inv}$ of the RPA respectively; and 0.03 (-1.57-1.63) ms^{-1}, -0.32 (-2.04-1.41) ms^{-1} and 0.14 (-1.13-1.42) ms^{-1} for the QA$_{Trad}$, QA$_3$, and QA$_{Inv}$ of the LPA respectively). The high temporal resolution yielded better reproducibility than the high

spatial resolution sequence (mean (95% CI) of QA_{Inv} PWV differences = 0.01 (-1.47-1.5) ms^{-1}, and -0.18 (-2.61-2.25) ms^{-1} for the high temporal resolution and high spatial resolution sequences respectively). The TT method through the right pulmonary artery yielded the best overall inter-observer reproducibility, while the combination of a high temporal resolution sequence through the RPA combined with the QA_{Inv} post processing yielded the best inter-observer reproducibility for the QA technique.

Inter-observer and intra-observer variability account for the majority of the inter-scan variability, with the impact more pronounced in the QA technique than in the TT technique.

4.2.6 Age

There was no difference between the 2 groups in terms of age, sex, smoking status, height, weight, BMI, or resting heart rate (See Table 4-2). However the older population had a significantly higher resting systolic (YHV 113 ± 1 vs. OHV 128 ± 3 mmHg, p=0.002) and diastolic blood pressure (YHV 68 ± 2 vs. OHV 75 ± 2, p=0.028). The pulmonary PWV did not differ between the young healthy volunteers and older healthy volunteers using either the TT technique (YHV 2.4 ± 0.3 vs. OHV 2.9 ± 0.2, p=0.1) or the QA_{Inv} technique (YHV 0.95 ± 0.1 vs. OHV 1.15 ± 0.1, p=0.1). However a significant difference was observed between the two groups for the aortic arch pulse wave velocity (YHV 7.4 ± 1.6 vs. OHV 10.7 ± 1.6, p=0.014) (See Table 4-3). To further examine the results, a post hoc power calculation was performed using the reported means and standard deviations. Based on the sample size and observed variability, with a p=0.05, the study had a 80% power to detect a difference of 0.26ms^{-1} between the groups.

Table 4-2: Comparison of the demographic and anthropomorphic measures of the two

study groups

	YHV	OHV	p
Age	31.5 ± 2.4	60.1 ± 1.1	<0.001
Sex (%male)	3 (30%)	9 (45%)	0.7
Height	1.71 ± 0.02	1.73 ± 0.03	0.8
Weight	76.3 ± 6.5	73.9 ± 3.2	0.7
BMI	25.8 ± 1.9	24.6 ± 0.6	0.5
Current smoker	1 (10%)	3 (15%)	1
Ex-smoker	3 (30%)	6 (30%)	1
Never smoker	6 (60%)	11 (55%)	1
Heart rate	65.3 ± 1.9	64.4 ± 2.8	0.8
Systolic BP	113 ± 1	128 ± 3	0.002
Diastolic BP	68 ± 2	75 ± 2	0.028

Table 4-3: Effects of age on Pulmonary and Aortic PWV

	YHV	OHV	p
Pulmonary PWV			
TT (MPA-RPA)	2.4 ± 0.3	2.9 ± 0.2	0.1
TT (MPA-LPA)	3.0 ± 0.3	3.3 ± 0.3	0.5
MPA QA_{Inv}	1.0 ± 0.08	1.2 ± 0.1	0.2
RPA QA_{Inv}	1.0 ± 0.06	0.8 ± 0.07	0.1
LPA QA_{Inv}	1.0 ± 0.2	0.7 ± 0.05	0.1
Aortic PWV			
Aortic Arch PWV	7.4 ± 1.6	10.7 ± 1.6	0.014

4.2.7 Exercise

The isometric calf exercises resulted in a significant and sustained rise in heart rate from 65 ± 2 to 87 ± 3 (P<0.0001) and in blood pressure from 113/68 to 130/84 (P<0.0001). A significant increase in cardiac output was also observed from 5.5 ± 0.4 to 6.7 ± 0.6 L/min (P=0.004), which was mediated through an increase in heart rate rather than an increase in stroke volume (P=0.98). Exercise resulted in erroneous measures in 2 participants using the TT technique, and in 1 using the QA technique.

Using the TT technique: the MPA-RPA PWV changed from 2.43 ± 0.26 at rest to 2.86 ± 0.25 during exercise (mean (95% CI) of PWV differences = -0.42 (-1.2-0.4) ms^{-1}, P=0.24); while the MPA-LPA PWV changed from 3.03 ± 0.27 at rest to 3.35 ± 0.39 during exercise (mean (SD) of PWV differences = -0.32 (-1.6-1) ms^{-1}, P=0.57) (see Figure 4-5).

Using the QA$_{Inv}$ technique: the MPA PWV went from 0.95 ± 0.09 at rest to 0.91 ± 0.1 during exercise (mean (95% CI) of PWV differences = 0.03 (-0.2-0.3) ms^{-1}, P=0.77); the RPA PWV went from 1.03 ± 0.06 at rest to 0.92 ± 0.17 during exercise (mean (95% CI) of PWV differences = 0.11 (-0.3-0.5) ms^{-1}, P=0.53); the LPA PWV went from 1.03 ± 0.16 at rest to 1.05 ± 0.11 during exercise (mean (95% CI) of PWV differences = -0.02 (-0.4-0.3) ms^{-1}, P=0.9). To further examine the results, a post hoc power calculation was performed using the reported means and standard deviations. Based on the sample size and observed variability, with a p=0.05, and a study power of 80%, the study would be powered to detect a difference of 0.3ms^{-1}.

Figure 4-5: Bar and scatter plot of change of PWV with exercise
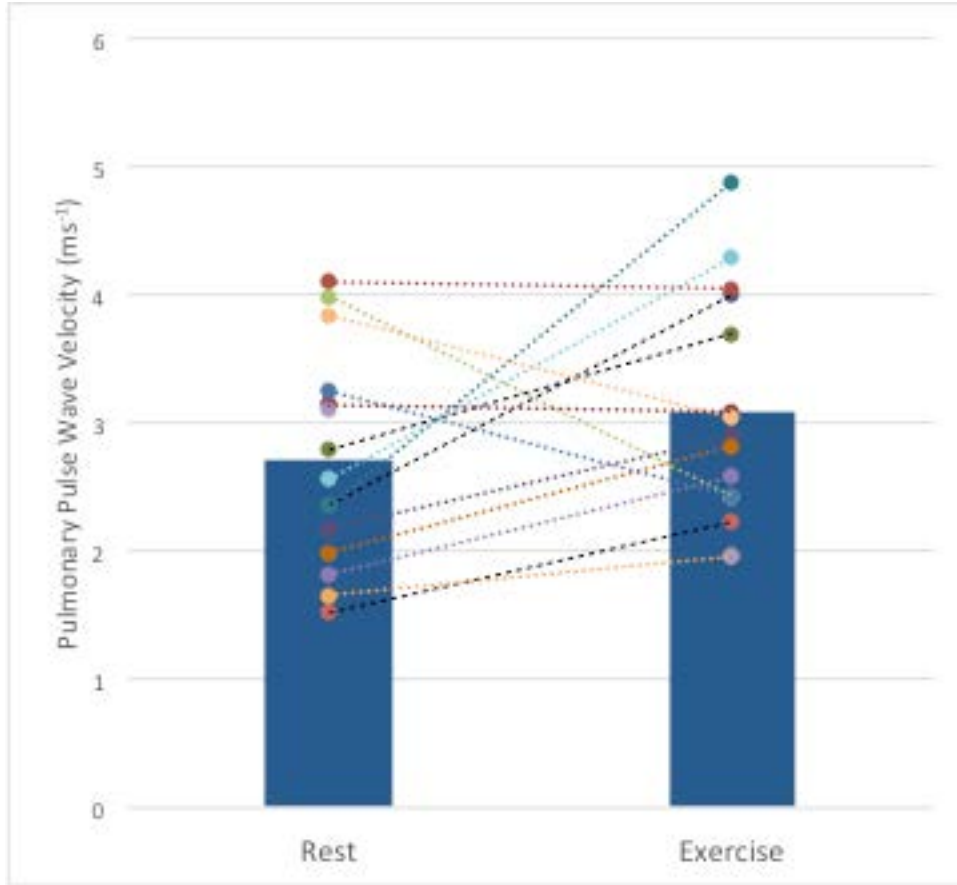
4.3 DISCUSSION

We have shown that: (i) The QA method using a high temporal resolution sequence through the right pulmonary artery using a calculation that accounts for wave reflections yields consistently better within scan, inter-scan, intra-observer and inter-observer reproducibility; (ii) Age related arterial stiffening as seen in the systemic circulation does not occur in the pulmonary vessels; (iii) Pulmonary PWV is stable and consistent at both rest and exercise.

This is the most comprehensive analysis of the techniques for measuring pulmonary PWV to date. Prior studies have either provided within scan reproducibility in n=10 using just the TT technique,(203) within and between scan reproducibility in n=17 using just the QA technique,(207)

or inter-observer comparison but without interscan assessment in n=33.(208) Thus our study of both measurement techniques as well as interrogating the effects of different acquisition sequences and different post-processing methods provides the first in depth and rigorous assessment of pulmonary PWV assessment.

It is perhaps not surprising that the RPA QA PWV measurements were the most precise as the RPA suffers from significantly less through plane motion during the cardiac cycle than the MPA as well as suffering from less respiratory variation in location. However justification of focusing on one of the branch pulmonary arteries rather than the main pulmonary artery relies on changes affecting all three arteries equally. Whilst it may be reasonable to assume this in diffuse pulmonary disease states such as COPD or idiopathic pulmonary arterial hypertension, prior work in chronic thromboembolic pulmonary hypertension (CTEPH) has demonstrated that the capacitance varies between the left and right pulmonary arteries.(267) Thus while the RPA may provide the best results in terms of reproducibility, care may have to be taken when using this in disease states, particularly CTEPH where despite its greater inter measure variability the MPA may be better suited. Further work is required in other disease states to evaluate the degree of variability in measures of pulmonary stiffness. Further consideration must be given to the fact that there appears to be a change in stiffness between the main pulmonary trunk and the branch pulmonary arteries observed in our study with both the right and left pulmonary arteries exhibiting lower stiffness than the main pulmonary artery. Current studies demonstrating prognostic significance of proximal pulmonary arterial stiffness have all focused on changes in the main pulmonary artery, thus these findings will have to be replicated in the right pulmonary artery in order to validate its usefulness as a marker of arterial stiffness of prognostic significance.

Our finding of improved reproducibility with a lower spatial resolution and higher temporal resolution is slightly counter intuitive as it has previously been thought that high spatial resolution was the more important factor in QA assessment due to the need for accurate area measurement.(193,208) However it may be that increasing the temporal resolution increases the datapoints for deriving the flow-area gradient thus improving the reproducibility. Indeed the QA_{Inv}, which uses all the points in early systole, was seen to be more precise than the QA_3 technique, which uses only the first three. The good agreement of QA_{Inv} and QA_3 compared with QA_{Trad} despite their different sampling windows and different calculations also shows the importance of correcting for the reflected wave in early systole as they both produced significantly lower results than the QA_{Trad} using both the high spatial resolution and high temporal resolution sequences. Previous animal models have shown an early expansion wave arriving during systole in the MPA,(157,195) and this becomes even more important in disease when a backward compression wave starts to arrive in systole.(189) Recently a phase contrast acquisition technique utilising a golden angle radial acquisition has been described in the pulmonary circulation which maintains high edge sharpness whilst maintaining good temporal resolution which may further improve the reproducibility of this technique.(261) Given that segmentation errors affect both the area and flow measurements it would be assumed that this would result in lower reproducibility than the TT technique, especially as previous studies in the aorta have shown exactly this.(193,208) It is likely that due to the short path length inherent in measuring pulse wave velocity in the pulmonary circulation, that small changes in RR variability and flow states result in greater impact on the short transit times compared to the relatively longer transit times in the aorta where imaging planes can be positioned significant distances apart.

In our study we found no change in pulmonary arterial PWV with exercise. This is in contradistinction to the recent findings of Forouzan et al.(268) who demonstrated an increase in

PWV on exercise in a study of n=15 using the QA technique. This previous study obtained a larger increase in cardiac output compared to our own, and was larger than our current exercise group (n=10) thus it may be that in our study the participants were insufficiently stressed to illicit a change in the proximal pulmonary arterial stiffness, or that the sample size was too small. However there are several reasons to support the accuracy of the findings of the current study. Firstly, our measures were obtained during rather than after exercise, and we have used both the TT and QA technique with a similar lack of change seen with both. Secondly, the previous study used the QA_{Trad} method for calculating the data, which we have shown provides a higher measurement of PWV than methods accounting for wave reflections. Wave reflections are known to increase substantially during exercise states thus the change in their PWV may have been due to a change in the magnitude of wave reflections rather than a change in arterial stiffness.(157) Finally our observations are in agreement with two prior invasive studies: the first of these by Laskey et al.(198) using invasive pressure and velocity wires to calculate the arterial input impedance spectrum demonstrated no change in PWV with exercise in healthy controls; and a second by Domingo et al. using right heart catheterisation and intravascular ultrasound demonstrating an increased pulsatility, but with a fall in elastic modulus and no significant change in capacitance on exercise.(269)

We have shown a lack of change in the pulmonary arterial PWV with age in comparison with the aorta where the expected increase in PWV was observed. This is in contra-distinction to a recent study by Dawes et al. which demonstrated a correlation between pulmonary PWV and age in a cohort of n=156.(270) The fact that using the same technique in the systemic circulation we were able to observe a significant change in aortic PWV suggests our technique is robust, but that the changes with age in the pulmonary circulation are far smaller than those within the aorta and thus require far larger populations to detect.

Several limitations must be mentioned regarding this study. First, no gold standard was used to compare the techniques against. The main reason for this is that the gold standard is invasive right heart catheterisation, which in a healthy population with no comorbidities would be difficult to justify. However use of the technique in patients due to undergo a clinically indicated right heart catheterisation would be a useful avenue for future work. In addition, while none were compared to the gold standard, reproducibility and reduced interscan variability is as, if not more, important than accuracy as it allows detection of smaller changes within the study group of patient cohort of interest. Secondly a high spatial resolution sequence was not applied through either the RPA or LPA, thus whilst it is unlikely given the trend of results seen in the MPA, it cannot be excluded that higher spatial resolution sequences through these regions would not result in improved reproducibility compared with the high temporal resolution sequences. Thirdly, while the number undergoing repeat measurement whilst on table was reasonably sized, those undergoing repeat measurement at 6 months was substantially smaller, however the results of this largely mirrored the results of the on-table repeat measure thus aiding in the validation of their findings.

4.4 CONCLUSION

In conclusion use of the QA technique through the right pulmonary artery combined with a high temporal resolution acquisition and a post processing technique to account for wave reflections yields the most reproducible measurements of pulmonary PWV.

CHAPTER 5: Pulmonary arterial stiffness in COPD and its role in right ventricular remodeling

5 INTRODUCTION

COPD is the second most common cause of pulmonary hypertension after left sided heart disease with the prevalence of this increasing with increasing severity of COPD.(63) In comparison to other causes of pulmonary hypertension the pulmonary pressure elevations are modest, however survival is poor and correlates better with the pulmonary pressures and pulmonary vascular resistance than with the severity of airflow obstruction.(67–70) The notion of an elevated rest pressure as a cut-off is also restrictive in evaluating the role of the pulmonary arteries and right heart as even minimal exertion causes marked elevations in mPAP and oxygen desaturation in COPD, with exercise induced pulmonary hypertension present in 35%-58% of patients with normoxaemia or mild hypoxia.(67,85–87)

The role of pulmonary arterial stiffness in COPD was highlighted in a recent study where an increase in pulmonary arterial stiffness was observed during exercise with a greater contribution from this to changes in the mean pulmonary arterial pressures (mPAP) than the peripheral vascular resistance (PVR).(65) Pulmonary arterial wall thickness is also related to exercise pulmonary pressures rather than resting pulmonary pressures, and to correlate highly with change in pressure from rest to exercise.(165)

Pulmonary PWV has been demonstrated to be feasible for the measurement of pulmonary arterial stiffness, and to be increased in those with pulmonary hypertension, however has never been used

to examine the pulmonary vasculature in COPD.(207,208,271,272) Thus the aim of the current study was to examine pulmonary arterial PWV in COPD and establish its role in right ventricular remodeling with the hypothesis that i) PWV would be elevated in those with COPD and ii) that elevated PWV would be associated with right ventricular remodeling.

5.1 MATERIAL AND METHODS

COPD and age and sex matched controls were identified and screened as described in Chapter 3. 104 COPD participants were screened with 37 excluded due to co-existent coronary artery disease, AF, prior thoracotomy, co-existent lung condition, left ventricular systolic dysfunction on echo, or no history of smoking. This left 67 in the cohort. Of these 58 were included in the final analysis (6 excluded due to incomplete scan secondary to claustrophobia, 1 due to a history of metal fragments in the orbits not picked up in screening, and 2 due to inadequate image quality for analysis).

A healthy control (HC) group was recruited to be approximately age and sex matched, with no prior history of cardiac or pulmonary pathology.

All COPD participants underwent spirometry, DLCO, body plethysmography, a 6-minute walk test, and a cardiac MRI on the same day. All study visits were coordinated so that the study participant had been free from a COPD exacerbation for 8 weeks prior to attendance for these tests. All healthy controls underwent a cardiac MRI. Spirometry, DLCO and 6MWT were performed as per ERS/ATS guidelines.(255,256)

5.1.1 MRI

All study participants underwent pulmonary phase contrast acquisition of the main pulmonary artery using the high temporal resolution sequence described in Chapter 3. These images were analysed using the Davies et al technique (QA_{INV}). The phase contrast sequence was also used for the calculation of pulmonary acceleration time. A pulmonary cine sequence was used to calculate pulmonary pulsatility. A short axis stack of the ventricles was acquired and used for the analysis of right ventricular mass, volumes and function.

5.1.2 Statistics

Descriptive statistics were used for the analysis of the demographic and clinical features of the cohorts with data expressed as mean ± SD. Normality and equality of variances of the variables was tested. An independent sample t-test was used to compare the differences in continuous variables between the HC and COPD cohort, and to compare the difference in continuous variables between the top and bottom tertiles of PWV within the COPD cohort. Chi-square, Fisher exact or Mann-Whitney U tests were used as appropriate to compare differences in ordinal and nominal data between the groups. Pearson or spearman rank co-efficients were used to assess the correlation between PWV and demographic, spirometric and MRI factors. All data were analysed using SPSS statistical package (version 21.0, SPSS Inc. Chicago, Illinois). Significance was assumed when $p < 0.05$.

5.2 RESULTS

58 COPD patients (67.4 ± 9.0 years, 55% male) and 21 healthy controls (60.4 ± 5.1, 48% male) completed the study protocol. Despite approximate age and sex matching, those with COPD were significantly older (p<0.001), had a higher BMI (COPD: 26.8 ± 5.2 kg/m^2 vs. HC: 24.7 ± 2.5 kg/m^2, p=0.02), and a higher resting heart rate (COPD: 73.8 ± 20.3 bpm vs. HC: 64.2 ± 11.8 bpm, p=0.05). Of those with COPD the majority had moderate COPD with n=12 with GOLD I, n=32 with GOLD II, n=13 with GOLD III and n=1 with GOLD IV COPD. Using the modified British Medical Research Council (mMRC) breathlessness score experienced breathlessness was also on the milder end of the spectrum with n=5 grade 0, n=26 grade 1, n=14 grade 2, n=11 grade 3 and n=2 grade 4. Full baseline characteristics are detailed in Table 5-1.

Table 5-1: Demographics of the COPD and healthy control cohorts

	Healthy controls	COPD	p
N	21	58	
Age	60.4 ± 5.1	67.5 ± 9.2	<0.001
Sex (male)	10 (48%)	30 (52%)	0.75
BMI (kg/m²)	24.7 ± 2.5	26.8 ± 5.2	0.02
Heart rate (bpm)	64.2 ± 11.8	73.8 ± 20.3	0.05
Systolic BP (mmHg)	127.6 ± 13.9	131.1 ± 20.0	0.47
Diastolic BP (mmHg)	74.7 ± 7.8	75.1 ± 8.5	0.85
Smoking status			
Current smoker	2 (10%)	17 (29%)	0.07
Ex-smoker	7 (33%)	41 (71%)	0.003
Never smoker	12 (57%)	0 (0%)	<0.001
Pack years	4.68 ± 7.4	48.5 ± 24.0	<0.001
Medications			
SABA		54 (93%)	
SAMA		1 (2%)	
LABA		8 (14%)	
LAMA		36 (62%)	
ICS		7 (12%)	
LABA/ICS combo		28 (48%)	
Oral steroid	2 (10%)	4 (7%)	
Antibiotics		2 (3%)	
Theophylline		4 (7%)	
Mucolytics		9 (16%)	
GOLD status			
I		12 (21%)	
II		32 (55%)	
III		13 (22%)	
IV		1 (2%)	
mMRC grade			
0		5 (9%)	
1		26 (45%)	
2		14 (24%)	
3		11 (19%)	
4		2 (3%)	

Those with COPD demonstrated evidence of pulmonary arterial stiffening and pulmonary vascular remodeling with higher pulmonary artery area at end diastole (COPD: 2.36 ± 0.56 cm^2/m$^{1.7}$ vs. HC: 2.14 ± 0.28 cm^2/m$^{1.7}$, p=0.027), reduced pulsatility (COPD: 24.88 ± 8.84 % vs. HC: 30.55 ± 11.28 %, p=0.021), reduced PAT (COPD: 104.0 ± 22.9 ms vs. HC: 128.1 ± 32.2 ms, p<0.001) and higher PWV (COPD: 2.62 ± 1.29 ms^{-1} vs. HC: 1.78 ± 0.72 ms^{-1}, p=0.001). Compared with the HCs those with COPD had significantly smaller right ventricular end diastolic volumes (HC: 59.9 ± 13.0 ml/m$^{1.7}$ vs. COPD: 53.6 ± 11.1 ml/m$^{1.7}$, p=0.037), stroke volume (HC: 37.1 ± 6.2 ml/m$^{1.7}$ vs. COPD: 31.9 ± 6.9 ml/m$^{1.7}$, p=0.003), and right ventricular mass:volume ratio (HC: 0.27 ± 0.04 g/ml vs. COPD: 0.31 ± 0.06 g/ml, p=0.004) (See Table 5-2 for full right ventricular and pulmonary arterial parameters).

Table 5-2: Ventricular quantification and measures of pulmonary arterial stiffness and haemodynamics in the healthy control and COPD cohort.

	Healthy controls	COPD	p
N	21	58	
Right ventricle			
RVEDV (ml/m$^{1.7}$)	59.9 ± 13.0	53.6 ± 11.1	0.037
RVESV (ml/m$^{1.7}$)	22.9 ± 8.6	21.8 ± 7.3	0.58
RVSV (ml/m$^{1.7}$)	37.1 ± 6.2	31.9 ± 6.9	0.003
RVEF (%)	63.0 ± 7.9	59.8 ± 7.8	0.10
RVM (g/m$^{1.7}$)	15.8 ± 3.2	16.3 ± 3.4	0.53
RVMVR (g/ml)	0.27 ± 0.04	0.31 ± 0.06	0.004
Pulmonary artery			
Max area (cm^2/m$^{1.7}$)	2.80 ± 0.48	2.94 ± 0.74	0.33
Min Area (cm^2/m$^{1.7}$)	2.14 ± 0.28	2.36 ± 0.56	0.027
Pulsatility (%)	30.55 ± 11.28	24.88 ± 8.84	0.021
PAT (ms)	128.1 ± 32.2	104.0 ± 22.9	<0.001
PWV (ms^{-1})	1.78 ± 0.72	2.62 ± 1.29	0.001

PWV was associated with BMI (R=-0.28, p=0.03) and diastolic blood pressure (R=0.35, p=0.009), and total lung capacity (R=0.28, p=0.039), but did not demonstrate any significant association with any right ventricular parameters (see Table 5-3). To further explore any potential relationship between right ventricular mass and end diastolic volumes, scatter plots were performed looking at linear and quadratic associations (see Figure 5-1) however neither of these revealed a significant association.

Figure 5-1: Scatter plots comparing pulmonary PWV against RVM (A and B) and RVEDV (C and D)

A.

R, Linear = 0.020

y=17.12−0.39*x

B.

R, Quadratic =0.022

y=16.56+0.06*x−0.07*x^2

C.

R, Linear = 0.015

y=58.14−1.18*x

D.

R, Quadratic =0.016

y=56.17+0.42*x−0.26*x^2
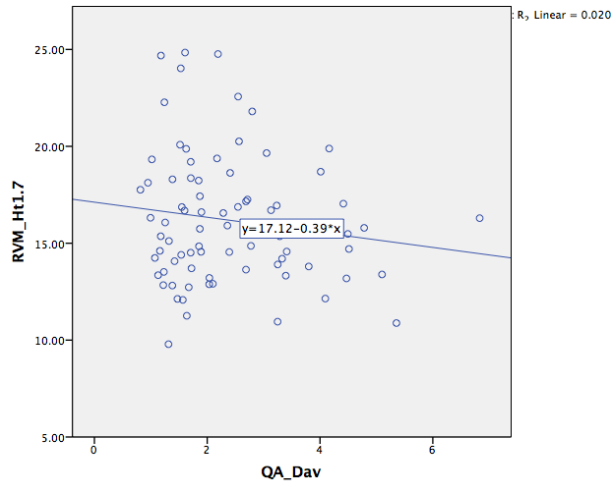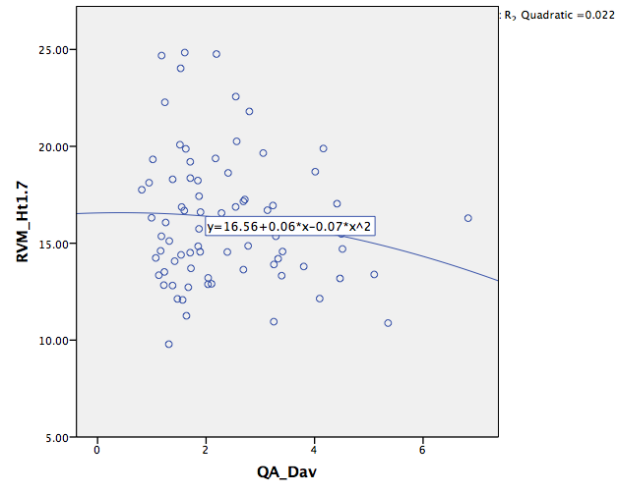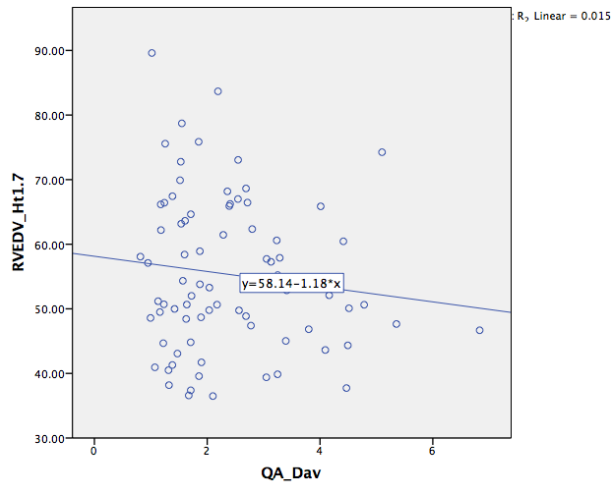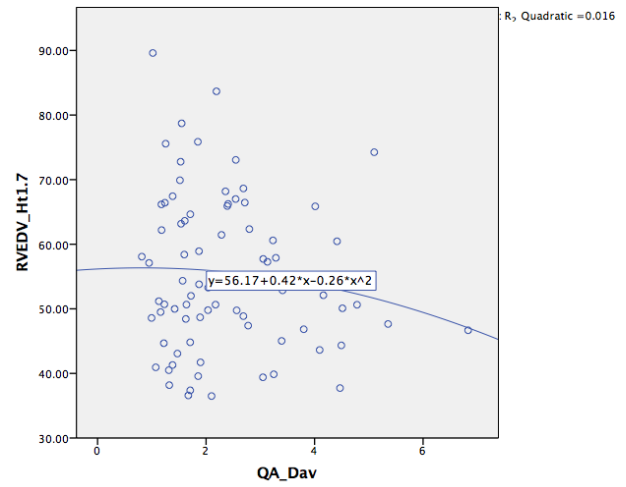
Table 5-3: Correlation co-efficients of PWV with demographic, spirometric and right ventricular measures.

	PWV	
	R	p
Age	0.04	0.15
BMI (kg/m^2)	**-0.28**	**0.03**
Heart rate (bpm)	0.20	0.14
Systolic BP (mmHg)	0.14	0.29
Diastolic BP (mmHg)	**0.35**	**0.009**
SpO2	-0.06	0.65
Pack years	0.01	0.94
FEV1, % predicted	-0.16	0.24
FVC, % predicted	-0.07	0.61
FEV1/FVC	-0.18	0.18
FEF 25-75, % predicted	-0.11	0.40
DLCO, % predicted	-0.05	0.73
DLCO/VA, % predicted	-0.07	0.60
RLV, % predicted	0.25	0.067
VC, % predicted	-0.02	0.88
TLC, % predicted	**0.28**	**0.039**
RLV /TLC	0.21	0.13
6MWT (m)	-0.17	0.20
RVEDV (ml/m$^{1.7}$)	-0.12	0.39
RVESV (ml/m$^{1.7}$)	-0.20	0.14
RVSV (ml/m$^{1.7}$)	0.02	0.86
RVEF (%)	0.18	0.18
RVM (g/m$^{1.7}$)	-0.24	0.067
RVMVR (g/ml)	-0.14	0.31

As the pulmonary stiffness did not appear to affect cardiac remodeling and the cardiac remodeling appeared to be that of a reduced preload rather than an increased afterload the determinants of the cardiac volumes were examined as detailed in Table 5-4. RVEDV and LVEDV demonstrated a strong correlation with one another (R=0.64, p<0.001). Both RVEDV and LVEDV demonstrated significant correlations with heart rate (RVEDV R=-0.41, p=0.04; LVEDV R=-0.30, p=0.02) and DLCO (RVEDV R=0.29, p=0.03; LVEDV R=0.28, p=0.03), with RVEDV also showing a significant correlation with KCO (RVEDV R=0.27, p=0.046) and BMI (RVEDV R=0.27, p=0.04).

Table 5-4: Correlation co-efficients between right and left ventricular end diastolic volumes and demographic, spirometric and pulmonary measures.

	RVEDV		LVEDV	
	r	p	r	p
Age	-0.05	0.69	-0.02	0.99
BMI (kg/m^2)	**0.27**	**0.04**	0.21	0.11
Heart rate (bpm)	**-0.41**	**0.002**	**-0.30**	**0.02**
Systolic BP (mmHg)	0.02	0.90	0.14	0.31
Diastolic BP (mmHg)	-0.13	0.35	-0.07	0.63
SpO2 (%)	-0.02	0.91	0.03	0.85
Pack years	0.11	0.41	0.05	0.69
FEV1, % predicted	0.22	0.09	0.18	0.17
FVC, % predicted	0.13	0.35	0.03	0.81
FEV1/FVC	0.21	0.12	-0.11	0.44
FEF 25-75, % predicted	0.23	0.08	0.23	0.08
DLCO, % predicted	**0.29**	**0.03**	**0.28**	**0.03**
KCO, % predicted	**0.27**	**0.046**	0.25	0.06
RLV, % predicted	-0.21	0.12	-0.02	0.91
TLC, % predicted	-0.23	0.10	0.12	0.38
VC, % predicted	0.11	0.44	0.21	0.12
RLV/TLC	-0.20	0.15	-0.17	0.23

5.3 DISCUSSION

COPD is associated with significant pulmonary arterial remodeling and stiffening, however this stiffening is not associated with adverse right ventricular remodeling. The former confirms our pre-study hypothesis but the latter goes against it thus requiring some examination.

This is the first study examining PWV in COPD, demonstrating an elevated pulmonary PWV. The fact that an increased PWV was accompanied by a fall in PAT and a fall in the pulsatility provides further confirmatory evidence that significant central pulmonary vascular remodeling is present within the COPD cohort. This is consistent with histological observation in those with severe COPD undergoing volume reduction surgery.(165) In the current study we found that while there was a significant elevation in PWV, this was not associated with right ventricular remodeling or a significant decline in functional status or performance. A previous echocardiographic study has demonstrated reduced right artery pulsatility in a cohort of 54 COPD patients, with this correlating with New York Heart Association (NYHA) functional status.(186) However the limitation of using pulsatility is that it falls as stroke volume falls independent of the vascular wall stiffness. As a reduced right ventricular function was indeed present in this prior study, with this also falling with worsening NYHA status and no multivariable analysis performed, the true impact of pulmonary stiffness on functional status cannot be determined. Another previous study in n=98 COPD patients has shown elevated pulmonary arterial stiffness on exercise with this correlating better with exercise induced pulmonary hypertension than pulmonary vascular resistance. This previous study examined the more severe end of the COPD spectrum with 62% of their cohort being either GOLD III or IV compared with only 24% in the current study. Previous work in pulmonary hypertension has demonstrated a significant increase in pulmonary arterial stiffness before a rapid decompensation occurs in right ventricular function.(141) Thus the lack of association between PWV and right ventricular function in the current study may be secondary to the milder disease

present in the current cohort with the cohort yet to enter the level of arterial stiffening associated with rapid ventricular decompensation.

In fact, despite the elevated arterial stiffness, the right ventricular remodeling evident in our study was that of a reduced preload rather than an increased afterload with evidence of smaller right ventricular volumes, smaller stroke volume and no significant increase in right ventricular mass. A similar pattern was observed in a small study of 24 COPD patients by Wells et al., where pulmonary arterial dilation was not associated with any increase in right ventricular mass despite being associated with a fall in RVEF.(273) In the current work, both right and left ventricular volumes demonstrated a moderate correlation with DLCO suggesting that emphysema is somehow causing the reduction in cardiac volumes. This observation is consistent with observations in the MESA-COPD cohort which also showed reduced right ventricular volumes with increasing emphysema burden.(274) A further argument in favour for this is the strong correlation between RVEDV and LVEDV, with both being associated with the same factors. In pulmonary hypertension the right ventricle is classically dilated and hypertrophied with the left ventricle being underfilled with a reduced mass, thus remodeling occurring in parallel between the two chambers suggests it is not the vasculature that lies between them, but a more systemic influence affecting this.(275) Thus the current study adds to the current literature that in a contemporary community population with COPD, the primary cardiac effects are those of emphysema induced preload reduction rather than that of cor pulmonale.(274,276) The precise mechanism by which emphysema results in underfilling of the ventricles remains unclear. While a single study utilising echocardiography found a significant link between hyperinflation and ventricular underfilling,(277) both this study and the MESA-COPD study utilising cardiac MRI found no link between hyperinflation and ventricular volumes. Given that MRI is the gold standard for the assessment of ventricular volumes and mass, and the agreement between these two CMR based studies the evidence would suggest

that it is not emphysema induced hyperexpansion and hyperinflation that is causing the

underfilling. Remaining possibilities are that the emphysema causes increased intra-thoracic

pressure resulting in an increased pressure gradient between the thoracic cavity and abdominal

and extra-thoracic venous return impeding the inflow to the heart. Alternately it may be that

emphysema is associated with global ventricular stiffening and diastolic dysfunction. Indeed

multiple studies have demonstrated diastolic dysfunction in COPD,(78,278,279) however others

have suggested the impaired relaxation of the ventricles is itself due to impaired venous return

rather than true ventricular stiffening.(46)

As both the MESA-COPD cohort and the current study are predominantly within the milder

spectrum of COPD, further work is required to determine if, as the disease progresses into the very

severe end of the spectrum a shift occurs from a preload driven phenotype into an afterload driven

phenotype. This is an important clinical consideration as both require different management

strategies with the former benefiting from volume reduction strategies(280), while the latter

benefits from medications targeting the pulmonary vasculature.(216) Further examination in a

more severe disease cohort is even more important as, if the same right ventricular pattern of

preload remodeling is still present, it may provide a significant explanatory factor as to the

continued failure of traditional pulmonary hypertension medications in a COPD cohort.(213–

215,217)

One final consideration must be made, and that is that central pulmonary arterial stiffening as

captured by PWV is not in fact a manifestation of pulmonary disease but that of a global arterial

stiffening affecting both the pulmonic and systemic arteries. Multiple studies have demonstrated

systemic arterial stiffening in those with COPD when compared with matched smokers, for this to

correlate with the percentage of emphysema, and to reduce with inhaler treatment for

COPD.(23,24,26) It has also been shown that those with COPD who are taking statins have lower pulmonary pressures on right heart catheterisation than those not on statins, and that statins are associated with improved functional capacity and lower mortality in COPD.(222,224,225) One supportive finding in the current study is that pulmonary PWV was associated with an elevated diastolic blood pressure which is increased in those with elevated systemic PWV.(23,281) Thus the disease process afflicting the pulmonary arteries may simply be the same pathological process underpinning the well documented systemic arterial remodeling.

There are several limitations within the current study. As previously mentioned the current cohort were predominantly earlier stage COPD, although as this is the main subtype seen in the community this more accurately reflects the clinical environment rather than a study focusing on the severe end of the spectrum. The healthy controls included smokers, with no pulmonary function tests performed within this cohort, thus subclinical COPD may have been present. However this would only have lessened any observed differences in pulmonary arterial stiffness or right ventricular remodeling, thus our observation of increased pulmonary arterial stiffness and reduced cardiac volumes in the COPD cohort remains robust to this confounder. Finally, in the previous chapter we have seen that a high temporal resolution in excess of the one used in the current study (7ms versus 12ms used in the current cohort) through the right pulmonary artery provides more reproducible measures of pulmonary arterial PWV than an acquisition through the main pulmonary artery using a slightly lower temporal resolution.(282) However, arterial stiffening is known to occur asymmetrically between the right and left pulmonary artery in some disease states,(267) thus the main pulmonary artery was chosen in the current study to ensure early remodeling was not missed or underestimated by inadvertently choosing a side with lower disease burden.

5.4 CONCLUSION

In conclusion, while pulmonary artery stiffening is present in those with COPD this has no

significant associations with right ventricular remodeling or functional capacity.

CHAPTER 6: Pulmonary arterial stiffness: Pulmonary induced or merely another manifestation of systemic atherosclerosis

6   INTRODUCTION

Despite being a disease of the pulmonary parenchyma, chronic obstructive pulmonary disease (COPD) is associated with significant cardiac morbidity and mortality, with up to 43% of mortality in COPD secondary to cardiovascular causes.(283–285)   However the precise cause of this is controversial with several mechanisms proposed.(1)   One proposed mechanism is that of COPD causing downstream inflammatory changes and resultant increased arterial stiffness – a known risk factor for future cardiovascular mortality.(199)   Indeed, multiple studies have demonstrated systemic arterial stiffening in those with COPD when compared with matched smokers, and for this to correlate with the percentage of emphysema, and for COPD therapy to result in an improvement in arterial stiffness.(23,24,26)

Another viable hypothesis is that of COPD related pulmonary vascular remodeling resulting in heart failure.   Pulmonary hypertension is prevalent in those with moderate to severe COPD, and is associated with a poor prognosis.(67,68,70)   In addition, pulmonary arterial stiffness is raised in those with pulmonary hypertension in COPD and correlates with exercise capacity.   It has also been shown that those with COPD who are taking statins have lower pulmonary pressures on right heart catheterisation than those not on statins, and that statins are associated with improved functional capacity and lower mortality in COPD.(222,224,225)   Given that statins improve systemic cardiovascular disease and mediate adverse vascular remodeling in atherosclerosis,(228,286) it

may thus be posited that the disease process afflicting the pulmonary arteries may simply be the same pathological process underpinning the well documented systemic arterial remodeling. We saw in the previous chapter that pulmonary PWV was elevated in COPD but did not correlate with right ventricular remodeling, adding further weight to this consideration.

Thus the aim of the current study was to examine the association between aortic and pulmonary arterial remodeling and their effects on cardiac remodeling with the hypothesis that i) aortic and pulmonary stiffening occur independently of each other and ii) that elevated systemic PWV would be associated with ventricular remodeling in the left but not the right ventricle.

6.1 MATERIALS AND METHODS

COPD and age and sex matched controls were identified and screened as described in Chapter 3. 104 COPD participants were screened with 37 excluded due to co-existent coronary artery disease, AF, prior thoracotomy, co-existent lung condition, left ventricular systolic dysfunction on echo, or no history of smoking. This left 67 in the cohort. Of these, 56 were included in the final analysis (6 excluded due to incomplete scan secondary to claustrophobia, 1 due to a history of metal fragments in the orbits not picked up in screening, and 4 due to inadequate image quality for analysis).

All COPD participants underwent spirometry, DLCO, a six-minute walk test (6MWT), and a cardiac MRI on the same day. All healthy controls underwent a cardiac MRI. Spirometry, DLCO and 6MWT were performed as per ERS/ATS guidelines.(255,256)

6.1.1 MRI

All study participants underwent pulmonary phase contrast acquisition of the main pulmonary artery using the high temporal resolution sequence described in Chapter 3. These images were analysed using the Davies et al technique (QA_{INV}). Similarly, the aortic PWV was calculated as previously described. A short axis stack of the ventricles was acquired and used for the analysis of right and left ventricular mass, volumes and function.

6.1.2 Statistics

Descriptive statistics were used for the analysis of the demographic and clinical features of the cohorts with data expressed as mean ± SD. Normality and equality of variances of the variables was tested. An independent sample t-test was used to compare the differences in continuous variables between the HC and COPD cohort. Chi-square, Fisher exact or Mann-Whitney U tests were used as appropriate to compare differences in ordinal and nominal data between the groups. Pearson or spearman rank co-efficients were used to assess the correlation between aortic and pulmonary PWV, and to look at the correlates of both of these with baseline demographic, spirometric and MRI factors in the COPD cohort, excluding the healthy cohort from this and the linear regression. Multiple linear regression analysis was performed with sPWV and pPWV entered separately as the dependent variable with those factors which were p<0.1 on single variable analysis entered as independent variables. All data were analysed using SPSS statistical package (version 21.0, SPSS Inc. Chicago, Illinois). Significance was assumed when p < 0.05.

6.2 RESULTS

56 COPD patients (67.4 ± 9.0 years, 55% male) and 20 healthy controls (60.4 ± 5.1, 48% male) completed the study protocol. Despite approximate age and sex matching, those with COPD were significantly older (p<0.001), had a higher BMI (COPD: 26.8 ± 5.3 kg/m^2 vs. HC: 24.6 ± 2.5 kg/m^2, p=0.02). While those with COPD had a significantly higher prevalence of hypertension, there was no significant difference in blood pressure or pulse pressure due to a higher prevalence of antihypertensive medication prescription. Full baseline characteristics are detailed in Table 6-1.

Table 6-1: Demographics of the COPD and healthy control cohorts

	Healthy controls	COPD	p
N	20	56	
Age	60.1 ± 4.9	67.5 ± 9.3	**<0.001**
Sex (male)	9 (45%)	29 (52%)	0.60
BMI (kg/m²)	24.6 ± 2.5	26.8 ± 5.3	**0.02**
Heart rate (bpm)	64.4 ± 12.1	74.0 ± 20.7	0.061
Systolic BP (mmHg)	128.5 ± 13.7	130.8 ± 20.4	0.65
Diastolic BP (mmHg)	75.0 ± 7.9	75.1 ± 8.6	0.95
Pulse Pressure (mmHg)	53.5 ± 9.4	55.7 ± 18.7	0.63
Hypertension	2 (10%)	24 (43%)	**0.012**
Hypercholesterolaemia	3 (15%)	3 (5%)	0.18
Diabetes	0 (0%)	9 (16%)	0.1
Smoking status			
Current smoker	2 (10%)	17 (30%)	0.08
Ex-smoker	7 (35%)	39 (70%)	**0.009**
Never smoker	11 (55%)	0 (0%)	**<0.001**
Pack years	4.92 ± 7.5	48.5 ± 23.6	**<0.001**
Medications			
Aspirin	1 (5%)	9 (16%)	0.28
Beta-blocker	1 (5%)	3 (5%)	1
Diuretic	0 (0%)	9 (16%)	0.10
Calcium-channel blocker	1 (5%)	15 (27%)	0.055
ACEi/AIIA	0 (0%)	8 (14%)	0.10
Statin	4 (20%)	14 (25%)	0.77
GOLD status			
I		11 (20%)	
II		31 (55%)	
III		13 (23%)	
IV		1 (2%)	
mMRC grade			
0		5 (9%)	
1		26 (46%)	
2		13 (23%)	
3		10 (18%)	
4		2 (4%)	

Those with COPD demonstrated a higher aortic PWV although this was not statistically significant (COPD: 8.7 ± 2.7 ms^{-1} vs. HC: 7.4 ± 2.1 ms^{-1}, p=0.06) and a significantly higher pulmonary PWV (COPD: 2.6 ± 1.3 ms^{-1} vs. HC: 1.8 ± 0.7 ms^{-1}, p=0.006). Compared with the HCs those with COPD had a significantly lower RV stroke volume (COPD: 31.7 ± 7.0 ml/m$^{1.7}$ vs. HC: 36.6 ± 5.9 ml/m$^{1.7}$, p=0.007), and a higher right ventricular mass:volume ratio (COPD: 0.29 ± 0.05 g/ml vs. COPD: 0.25 ± 0.04 g/ml, p=0.012). Those with COPD also had significantly higher left ventricular mass:volume ratio (COPD 0.78 ± 0.13 g/ml vs. 0.70 ± 0.09 g/ml, p=0.009). (See Table 6-2 for full ventricular and pulmonary arterial parameters).

Table 6-2: Ventricular quantification and measures of PWV in the healthy control and COPD cohort.

	Healthy controls	COPD	p
N	21	56	
Right ventricle			
RVEDV (ml/m$^{1.7}$)	58.7 ± 12.1	53.6 ± 11.2	0.09
RVESV (ml/m$^{1.7}$)	22.2 ± 8.2	21.9 ± 7.4	0.87
RVSV (ml/m$^{1.7}$)	36.6 ± 5.9	31.7 ± 7.0	**0.007**
RVEF (%)	63.3 ± 7.9	59.6 ± 7.9	0.08
RVM (g/m$^{1.7}$)	14.7 ± 2.4	15.2 ± 3.2	0.50
RVMVR (g/ml)	0.25 ± 0.04	0.29 ± 0.05	**0.012**
Left ventricle			
LVEDV (ml/m$^{1.7}$)	59.0 ± 9.2	56.1 ± 12.1	0.33
LVESV (ml/m$^{1.7}$)	23.4 ± 6.1	23.4 ± 9.4	0.99
LVSV (ml/m$^{1.7}$)	35.6 ± 4.8	32.7 ± 6.7	0.09
LVEF (%)	60.7 ± 6.0	59.1 ± 8.6	0.46
LVM (g/m$^{1.7}$)	41.0 ± 7.4	43.3 ± 9.5	0.33
LVMVR (g/ml)	0.70 ± 0.09	0.78 ± 0.13	**0.009**
Pulse wave velocity			
Aortic PWV	7.35 ± 2.1	8.67 ± 2.7	**0.06**
Pulmonary PWV	1.76 ± 0.7	2.63 ± 1.3	**0.006**

Pulmonary PWV correlated with percentage predicted total lung capacity (rho=0.28, p=0.046), inversely correlated with BMI (rho=-0.28, p=0.04) and correlated with increasing diastolic blood pressure (rho=0.36, p=0.01). See Table 6-3 for full correlates. On multiple variable backward linear regression, diastolic blood pressure (ß = 0.28, p=0.035) and percentage predicted total lung capacity (ß = 0.30, p=0.028) remained significantly associated with pPWV.

Table 6-3: Correlation co-efficients between Aortic PWV and Pulmonary PWV and demographic and ventricular measures.

	Pulmonary PWV		Aortic PWV	
	r	p	r	p
Age	0.03	0.81	**0.45**	**0.001**
BMI (kg/m^2)	-0.28	0.036	-0.04	0.78
Heart rate (bpm)	0.21	0.15	0.02	0.91
Systolic BP (mmHg)	0.15	0.29	**0.31**	**0.03**
Diastolic BP (mmHg)	**0.36**	**0.01**	0.22	0.12
Pulse Pressure (mmHg)	0.000	1	0.24	0.09
SpO2 (%)	-0.06	0.68	-0.07	0.64
Pack years	0.004	0.98	-0.13	0.36
FEV1, % predicted	-0.15	0.28	0.05	0.70
FVC, % predicted	-0.06	0.64	-0.03	0.85
FEV1/FVC	-0.17	0.21	0.07	0.64
DLCO, % predicted	-0.05	0.73	**0.30**	**0.03**
KCO, % predicted	-0.08	0.56	**0.46**	**<0.001**
RLV, % predicted	0.25	0.08	-0.10	0.50
TLC, % predicted	**0.28**	**0.046**	-0.05	0.71
VC, % predicted	-0.02	0.90	0.03	0.83
RLV/TLC	0.20	0.15	0.12	0.40
RVEDV (ml/m$^{1.7}$)	-0.12	0.39	0.08	0.59
RVESV (ml/m$^{1.7}$)	-0.21	0.13	0.19	0.17
RVSV (ml/m$^{1.7}$)	0.03	0.83	-0.07	0.62
RVEF (%)	-0.19	0.19	-0.19	0.16
RVM (g/m$^{1.7}$)	-0.25	0.067	0.19	0.18
RVMVR (g/ml)	-0.15	0.27	0.19	0.17
LVEDV (ml/m$^{1.7}$)	-0.08	0.58	-0.03	0.83
LVESV (ml/m$^{1.7}$)	-0.11	0.44	0.02	0.89
LVSV (ml/m$^{1.7}$)	0.001	0.99	-0.08	0.55
LVEF (%)	0.14	0.30	-0.06	0.67
LVM (g/m$^{1.7}$)	-0.18	0.20	0.17	0.22
LVMVR (g/ml)	-0.13	0.33	**0.34**	**0.01**
Pulmonary PWV	-	-	-0.004	0.97
Aortic PWV	-0.004	0.97	-	-

In comparison aortic PWV showed a significant association with age (rho=0.47, p<0.001), systolic blood pressure (rho=0.32, p=0.02), and percentage predicted KCO (rho=0.43, p=0.001). On linear regression, age (ß = 0.30, p=0.02), systolic blood pressure (ß = 0.27, p=0.04), and percentage predicted KCO (ß = 0.37, p=0.003) all remained significantly associated with aortic PWV.

sPWV was significantly associated with LVMVR (rho=0.34, p=0.01), while no such correlation was seen between pPWV and RVMVR (rho= -0.15, p=0.27). Similarly, there was no significant association between aortic and pulmonary PWV (rho=-0.004, p=0.97) – See Figure 6-1.

Figure 6-1: Scatterplots of (A) Aortic PWV against Pulmonary PWV; (B) Pulmonary PWV against RVMVR; and (C) Aortic PWV against LVMVR

A)
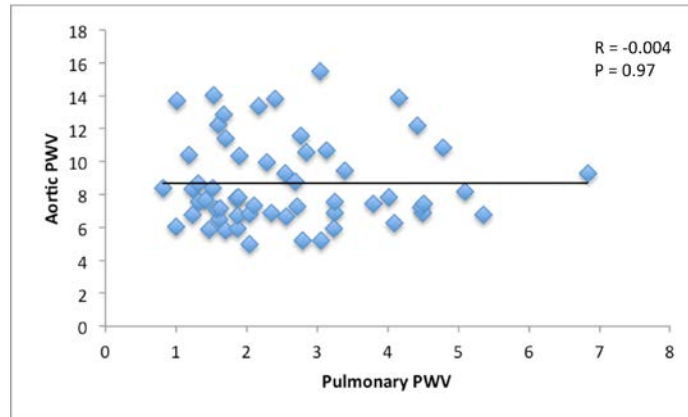
B)
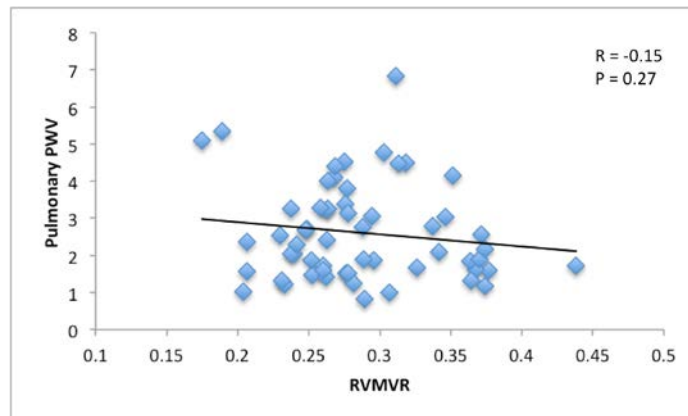
C)
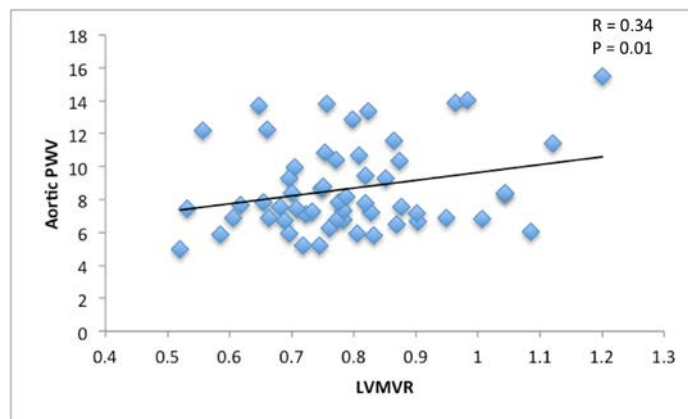
6.3 DISCUSSION

In this study we have seen that while both pulmonary and systemic arteries are stiffer in COPD compared with matched controls, these processes occur independently from one another. Not only was no correlation seen between the systemic and pulmonary PWV, but also they are associated with different risk factors from one another. While aortic PWV was associated with age and systolic blood pressure, pulmonary PWV showed an association with lung hyperexpansion, and diastolic BP. Finally while there was no significant association between pulmonary PWV and right ventricular remodeling, a correlation was seen between aortic PWV and left ventricular mass:volume ratio which is a marker of concentric myocardial remodeling.(287)

Our finding of increased aortic stiffness is consistent with previous work demonstrating increased sPWV in those with COPD. The underlying cause of the increased systemic arterial stiffness in COPD is still a topic of debate. Several groups have demonstrated an association between aortic PWV and inflammatory markers,(25) FEV1,(288) or %emphysema measured on CT,(24) while other groups have found no such correlation with any of these metrics.(25,289,290) In the current study we found that those with COPD the aortic PWV to be independently associated with age and blood pressure, but not FEV1 or measures of hyperexpansion. Of note we also observed a significant positive correlation with KCO, only one other group has simultaneously examined KCO and aortic PWV in COPD, finding no significant correlation, thus the significance of this is uncertain.(25) Our finding of a significant association between LVMVR – a marker of concentric left remodeling – and aortic PWV provides significant mechanistic insight into the interface between the pulmonary and cardiovascular disease evident in COPD. As with increased aortic PWV multiple studies have documented left ventricular hypertrophy in COPD, demonstrating both a high prevalence and with significant implications for mortality in a COPD cohort.(40,41,291) While the

association of PWV and left ventricular mass has been described in the general population,(292,293) to the best of the authors knowledge, no studies have examined the role of pulmonary arterial stiffness as a linking mechanism in COPD. Given that LVMVR is a known risk factor for future cardiovascular events this association may help explain both the increased cardiovascular risk in COPD and the beneficial effects in COPD of beta-blockers - a known regressor of left ventricular mass (albeit less pronounced than other anti-hypertensives).(43,294,295)

Pulmonary PWV was not associated with age or systolic blood pressure, but was instead associated with pulmonary hyperinflation and diastolic blood pressure. In addition it did not show any significant association with right ventricular remodeling, unlike aortic PWV. Previous work has described pulmonary arterial stiffening to be significantly associated with exercise induced elevations in pulmonary pressures,(65,165) however we found no link between this and right ventricular remodeling, therefore while the pressures may elevated in exercise the clinical significance of this is uncertain. Longitudinal studies will be required to determine the long-term implications of pulmonary arterial stiffening.

There are several limitations to the current study. Patients with known coronary artery disease were excluded, thus the results may not be representative of the wider COPD cohort in whom cardiovascular disease is common. We also used two different techniques for the MRI assessment of the aortic and pulmonary PWV, using a transit time method in the aorta and a flow-area technique within the pulmonary artery. This was done as the former is more accurate in longer vessels such as the aorta,(193) however the short pulmonary artery is less amenable to this due to the rapid transition times and prior work has shown the transit time within the pulmonary arteries to be less reproducible than the flow-area technique.(282) In addition the two techniques demonstrate reasonable agreement with one another.(296)

6.4 CONCLUSION

In conclusion, both aortic and pulmonary arterial stiffening occur in COPD, but these processes develop independent of one another with aortic but not pulmonary PWV demonstrating a significant association with remodeling in the ventricle.

CHAPTER 7: Effect of pulmonary arterial stiffness on longitudinal changes in cardiac remodeling.

7 INTRODUCTION

In the preceding chapters we have seen that pulmonary PWV is elevated in COPD but that it does not correlate with spirometric markers of COPD, right ventricular parameters, or functional capacity. However while a lack of correlation combined with a cardiac phenotype of a reduced preload rather than an increased afterload would suggest that there is no causative link between pulmonary arterial stiffness and cardiac remodeling and morbidity, longitudinal studies are required to determine these.

The aim of the current arm of the study was to answer this point, following the COPD participants up at 1 year to examine changes in right ventricular remodeling with the hypothesis that those with stiffer arteries at baseline would undergo greater cardiac remodeling evidenced by an increase in right ventricular mass.

7.1 MATERIALS AND METHODS

All participants recruited and scanned for the main study before August 2015 went on to have a 1-year follow-up scan. Of the 49 who were scanned prior to this date, 35 underwent their follow-up examination. 16 were lost due to: pacemaker insertion (n=1), lung cancer diagnosed on initial CMR and receiving treatment for this (n=2), interval diagnosis of bladder cancer (n=2), unwilling to undergo repeat CMR (n=1), recurrent chest infections (as needed to be free from exacerbations for

2 months)(n=2), withdrawal from the study (n=2), unable to contact (n=6). Of the 35 scanned, 1 had to be abandoned due to claustrophobia despite having successfully completed their CMR the preceding year, leaving 34 in the final analysis.

All participants underwent spirometry, DLCO, body plethysmography, a 6-minute walk test, and a cardiac MRI on the same day using the same techniques and machines as on the first visit. These were performed as described in chapter 3.

7.1.1 Statistics

Descriptive statistics were used for the analysis of the demographic and clinical features of the cohorts with data expressed as mean ± SD. Normality and equality of variances of the variables was tested. A paired sample t-test was used to compare baseline and 1 year follow-up metrics and to compare those that underwent follow-up imaging compared to those who only underwent a baseline visit. A bonferroni correction factor was applied to ameliorate the risk of alpha error from multiple pairwise comparisons. An independent sample t-test was used to compare the difference in continuous variables between the top and bottom tertiles of PWV within the COPD cohort. Chi-square, Fisher exact or Mann-Whitney U tests were used as appropriate to compare differences in ordinal and nominal data between the groups. Pearson or spearman rank co-efficients were used to assess the correlation between PWV and demographic, spirometric and MRI factors. All data were analysed using SPSS statistical package (version 21.0, SPSS Inc. Chicago, Illinois). Significance was assumed when $p < 0.05$.

7.2 RESULTS

32 (68.6 ± 8.2 years, 50% male) completed the full study protocol. Those who completed the study protocol had a significantly lower baseline heart rate than those who dropped out (69.1 ± 18.2 vs. 80.5 ± 21.7 bpm, p=0.039), but were otherwise matched in demographics, pulmonary function, and cardiac mass and function. The demographics and baseline characteristics of the 32 who underwent repeat CMR compared with those who only attended the baseline visit are described in Table 7-1.

At follow-up ten participants had had a serious adverse health event in the interval: Infective exacerbation of COPD, n=4; TIA, n=1, Ureteronephrectomy for urothelial malignancy n=1; Head injury, n=1; Ankle fracture, n=1, Wrist fracture, n=1; Colitis, n=1. Ten participant had had their medications changed with those pertinent to COPD being: Seretide exchanged for Fostair, n=1; Glycopyrronium started, n=2; Indacaterol started, n=1; Combined glycopyrronium/indacaterol inhaler started, n=1.

At 1 year follow up, there was no significant change in allometric measures or clinical observations. On repeat pulmonary function testing there was significant increase in KCO (from 71.4±19.8 to 78.0±19.5 % predicted, p<0.001), and a significant fall in 6MWT (from 473±97 to 445±99m, p=0.001). The pulmonary PWV also showed a significant interval increase from 2.31±1.0 to 3.4 ±1.4 ms-1 (+47%, p<0.001)(See Figure 7-1).

Table 7-1: Comparison of those who only underwent baseline scan compared with those who completed both study visits.

	Baseline only cohort	Follow-up cohort	p
N	26	32	
Age	66.1 ± 10.4	68.6 ± 8.2	0.31
Sex (male)	14 (54%)	16 (50%)	0.77
BMI (kg/m^2)	26.4 ± 5.3	27.1 ± 5.3	0.63
Heart rate (bpm)	80.5 ± 21.7	69.1 ± 18.2	**0.039**
Systolic BP (mmHg)	130 ± 24	132 ± 17	0.74
Diastolic BP (mmHg)	76 ± 9	74 ± 8	0.39
SpO2	95.9 ± 1.9	95.9 ± 1.7	0.98
Smoking status			
Current smoker	11 (42%)	6 (19%)	0.08
Ex-smoker	15 (58%)	26 (81%)	0.08
Never smoker	0	0	1
Pack years	44.0 ± 18.7	52.1 ± 27.3	0.20
Medications			
SABA	25 (96%)	29 (91%)	0.62
SAMA	1 (4%)	0	0.45
LABA	4 (15%)	4 (13%)	1
LAMA	16 (62%)	20 (77%)	0.94
ICS	1 (4%)	6 (19%)	0.12
LABA/ICS combo	15 (58%)	13 (41%)	0.20
Oral steroid	1 (4%)	3 (9%)	0.62
Antibiotics	1 (4%)	1 (3%)	1
Theophylline	2 (8%)	2 (6%)	1
Mucolytics	4 (15%)	5 (16%)	1
GOLD status			
I	4 (15%)	8 (25%)	0.61
II	16 (62%)	16 (50%)	
III	6 (23%)	7 (22%)	
IV	0	1 (3%)	
mMRC grade			
0	2 (8%)	3 (9%)	0.17
1	10 (38%)	16 (50%)	

2	9 (73%)	5 (16%)	
3	3 (12%)	8 (25%)	
4	2 (8%)	0	
Pulmonary Function tests			
FEV1, % predicted	66.9 ± 22.7	65.5 ± 21.0	0.81
FVC, % predicted	99.2 ± 21.5	100.0 ± 19.6	0.87
FEV1/FVC	53.3 ± 10.2	51.2 ± 11.6	0.49
FEF 25-75, % predicted	25.5 ± 12.1	24.2 ± 12.5	0.70
DLCO, % predicted	61.2 ± 23.5	54.5 ± 16.7	0.22
DLCO/VA, % predicted	79.4 ± 23.9	71.1 ± 19.5	0.16
RLV, % predicted	176 ± 49	176 ± 56	0.97
VC, % predicted	98.9 ± 20.0	100.6 ± 17.4	0.74
TLC, % predicted	124.2 ± 16.6	124.8 ± 22.9	0.92
RLV /TLC	0.55 ± 0.11	0.55 ± 0.11	0.92
6MWT (m)	428 ± 121	471 ± 97	0.14
CMR			
RVEDV ($ml/m^{1.7}$)	53.9 ± 12.8	53.4 ± 12.8	0.87
RVESV ($ml/m^{1.7}$)	21.9 ± 8.1	21.7 ± 6.7	0.92
RVSV ($ml/m^{1.7}$)	32.1 ± 7.0	31.7 ± 7.0	0.84
RVEF (%)	60.0 ± 7.0	59.7 ± 8.5	0.37
RVM ($g/m^{1.7}$)	16.5 ± 3.5	16.3 ± 3.4	0.83
RVMVR (g/ml)	0.31 ± 0.07	0.31 ± 0.05	0.65
LVEDV ($ml/m^{1.7}$)	57.0 ± 14.8	55.5 ± 9.4	0.66
LVESV ($ml/m^{1.7}$)	24.5 ± 12.6	22.3 ± 5.6	0.42
LVSV ($ml/m^{1.7}$)	32.5 ± 7.3	33.2 ± 6.3	0.72
LVEF (%)	58.5 ± 11.0	60.0 ± 6.0	0.53
LVM ($g/m^{1.7}$)	44.1 ± 10.2	42.9 ± 8.8	0.63
LVMVR (g/ml)	0.79 ± 0.16	0.77 ± 0.11	0.59
Pulmonary PWV	2.97 ± 1.6	2.34 ± 0.97	0.09
Pulmonary Pulsatility	25.6 ± 7.7	24.1 ± 8.7	0.50
Pulmonary acceleration time	102.8 ± 22.8	105.1 ± 23.5	0.71
Aortic PWV	9.3 ± 3.1	8.2 ± 2.2	0.13

Table 7-2 provides full details of changes between the baseline and follow-up visit. As 5 participants had an uptitring of their medications over the course of the year between the visits which could potentially skew the results, the analyses was re-run with these cases excluded. This did not result in any significant change in the results.

Figure 7-1: Bar (representing the mean) and dot (representing the individual participants) plot of the change in Right Ventricular Mass (A), PWV (B), and Six minute walk distance (C).

A.
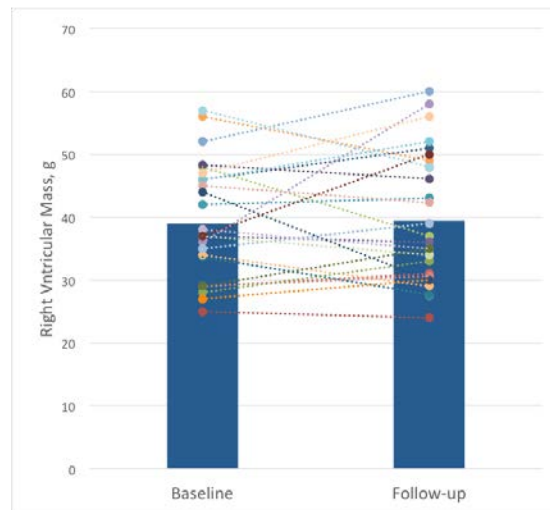
B.

C.
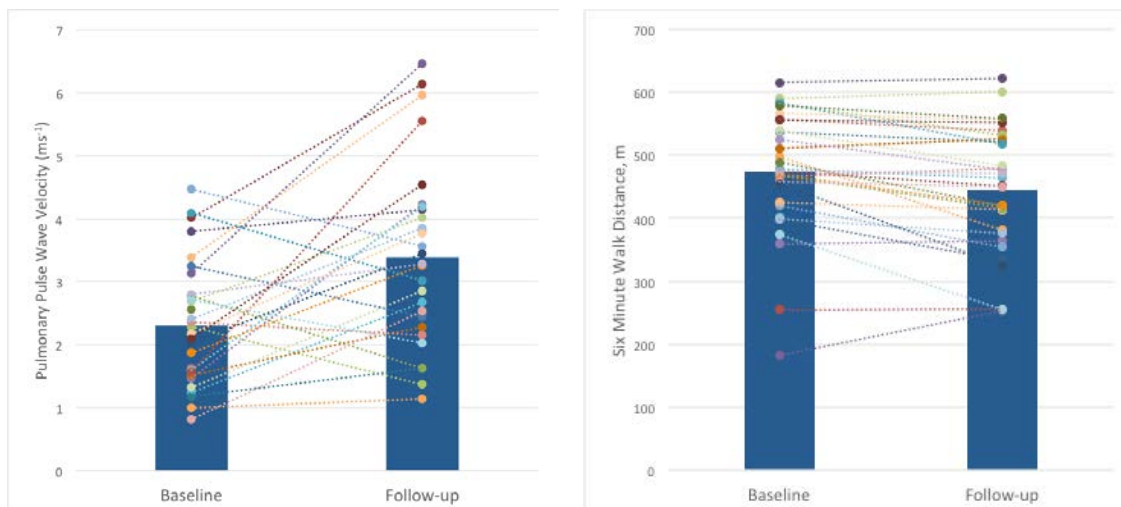
Table 7-2: Change in demographics, pulmonary function tests and CMR parameters at 1-year follow-up.

	Baseline	1 year	Interval change (%)	P*
Age	68.6 ± 8.2	69.9 ± 8.2		
BMI (kg/m^2)	27.1 ± 5.3	27.2 ± 5.2	+0.2%	0.82
Heart rate (bpm)	67.1 ± 11.2	68.2 ± 10.6	+2%	0.62
Systolic BP (mmHg)	133.4 ± 12.9	129.8 ± 18.2	-3%	0.19
Diastolic BP (mmHg)	75.8 ± 9.6	73.3 ± 9.6	-1%	0.18
SpO2	95.9 ± 1.7	96.3 ± 2.2	+0.4%	0.20
FEV1, % predicted	65.5 ± 21.0	63.6 ± 20.2	-3%	0.24
FVC, % predicted	100 ± 20	100 ± 22	0%	0.88
FEV1/FVC	51.3 ± 11.6	49.7 ± 9.9	-3%	0.05
DLCO, % predicted	54.4 ± 17.0	59.1 ± 18.1	+9%	0.002
DLCO/VA, % predicted	71.4 ± 19.8	78.0 ± 19.5	+9%	**<0.001**
6MWT (m)	473 ± 97	445 ± 99	-6%	**0.001**
RVEDV (ml/m$^{1.7}$)	53.4 ± 9.6	52.1 ± 10.8	-2%	0.37
RVESV (ml/m$^{1.7}$)	21.7 ± 6.7	21.8 ± 7.5	+3%	0.93
RVSV (ml/m$^{1.7}$)	31.7 ± 7.0	30.4 ± 7.1	-4%	0.14
RVEF (%)	59.7 ± 8.5	58.6 ± 9.2	-2%	0.37
RVM (g/m$^{1.7}$)	16.3 ± 3.4	16.4 ± 3.1	0%	0.91
RVMVR (g/ml)	0.31 ± 0.05	0.32 ± 0.05	+5%	0.19
LVEDV (ml/m$^{1.7}$)	55.5 ± 9.4	54.2 ± 9.7	-2%	0.34

LVESV (ml/m$^{1.7}$)	22.3 ± 5.6	23.6 ± 6.9	+6%	0.16
LVSV (ml/m$^{1.7}$)	33.2 ± 6.3	30.6 ± 6.8	-8%	0.028
LVEF (%)	60.0 ± 6.04	56.4 ± 9.0	-6%	0.02
LVM (g/m$^{1.7}$)	42.9 ± 8.8	43.1 ± 9.9	+1%	0.80
LVMVR (g/ml)	0.77 ± 0.11	0.80 ± 0.15	+3%	0.23
Pulmonary PWV	2.30 ± 0.97	3.39 ± 1.4	+47%	**<0.001**
Pulmonary Pulsatility	24.1 ± 8.7	26.8 ± 9.4	+11%	0.20
PAT	105.2 ± 23.5	108.8 ± 17.8	+3%	0.35
Aortic PWV	8.2 ± 2.3	8.5 ± 2.6	+4%	0.52

* Significance set at p<0.0018 after bonferroni correction for multiple comparisons

Those with the stiffest arteries at baseline (upper tertile of PWV) had no significant differences in right ventricular or left ventricular remodeling at follow-up than those with the most elastic arteries (bottom tertile of PWV). For full comparison of the change in ventricular metrics between PWV tertiles see Table 7-3.

Table 7-3: Comparison of change in 6MWT and CMR at follow up compared with baseline across baseline PWV tertiles

	Tertile			
	1	**2**	**3**	**P***
N	10	11	11	
Baseline PWV	1.31 ± 0.26	2.18 ± 0.32	3.42 ± 0.59	
Δ6MWT (m)	-38.8 ± 39.4	-22.5 ± 41.9	-26.8 ± 52.3	0.57
<u>CMR</u>				
ΔRVEDV (ml/m$^{1.7}$)	-3.9 ± 8.1	-1.6 ± 7.0	1.3 ± 8.9	0.18
ΔRVESV (ml/m$^{1.7}$)	-2.5 ± 7.0	0.6 ± 3.7	2.0 ± 5.9	0.13
ΔRVSV (ml/m$^{1.7}$)	-1.3 ± 5.6	-2.2 ± 3.9	-0.5 ± 5.9	0.75
ΔRVEF (%)	0.7 ± 8.6	-2.2 ± 3.3	-1.5 ± 7.3	0.55

ΔRVM (g/m$^{1.7}$)	-0.66 ± 2.8	0.26 ± 4.2	0.53 ± 2.3	0.29
ΔRVMVR (g/ml)	0.01 ± 0.07	0.01 ± 0.08	0.02 ± 0.07	0.71
ΔLVEDV (ml/m$^{1.7}$)	-1.1 ± 7.7	-3.8 ± 5.1	1.1 ± 8.7	0.54
ΔLVESV (ml/m$^{1.7}$)	0.54 ± 6.4	0.38 ± 4.7	3.0 ± 4.4	0.32
ΔLVSV (ml/m$^{1.7}$)	-1.7± 6.0	-4.2 ± 7.0	-1.8 ± 6.1	0.96
ΔLVEF (%)	-2.3 ± 9.5	-3.9 ± 10.2	-4.4 ± 4.4	0.52
ΔLVM (g/m$^{1.7}$)	0.55 ± 5.4	-0.38 ± 4.8	0.55 ± 5.77	0.99
ΔLVMVR (g/ml)	0.02 ± 0.13	0.05 ± 0.06	0.00 ± 0.13	0.76

*P-value is tertile 3 compared to tertile 1

Despite seeing a 54% increase in PWV between baseline and follow up visit, there was no significant correlation between baseline clinical observations or pulmonary function tests or interval change in PWV other than a negative correlation between heart rate and change in PWV (see Table 7-4). Scatter plots demonstrate a linear trend for this with no significant improvement of the R^2 on mapping a curvilinear plot (see Figure 7-2).

Table 7-4: Correlation co-efficients of ΔPWV and baseline demographic and spirometric measures.

	ΔPWV	
Baseline Variable	R	p
Age	0.07	0.72
BMI (kg/m^2)	-0.11	0.54
Heart rate (bpm)	-0.38	0.032
Systolic BP (mmHg)	0.23	0.20
Diastolic BP (mmHg)	-0.08	0.66
SpO2	-0.005	0.98
Pack years	-0.26	0.14
FEV1, % predicted	0.22	0.23

FVC, % predicted	0.10	0.59
FEV1/FVC	0.20	0.28
FEF 25-75, % predicted	0.22	0.22
DLCO, % predicted	0.20	0.26
DLCO/VA, % predicted	0.14	0.44
RLV, % predicted	-0.17	0.38
VC, % predicted	0.23	0.21
TLC, % predicted	-0.15	0.44

Figure 7-2: Scatter plots of baseline heart rate against change in PWV with linear (left) and curvilinear (right) lines of best fit applied.

R₂ Quadratic =0.148

$y=69.87-1.9*x-0.14*x^2$
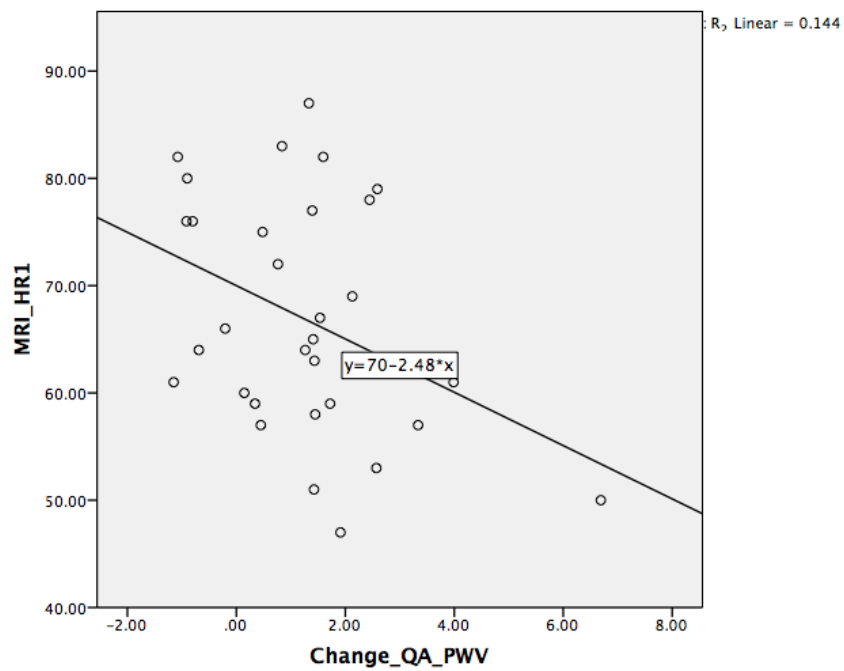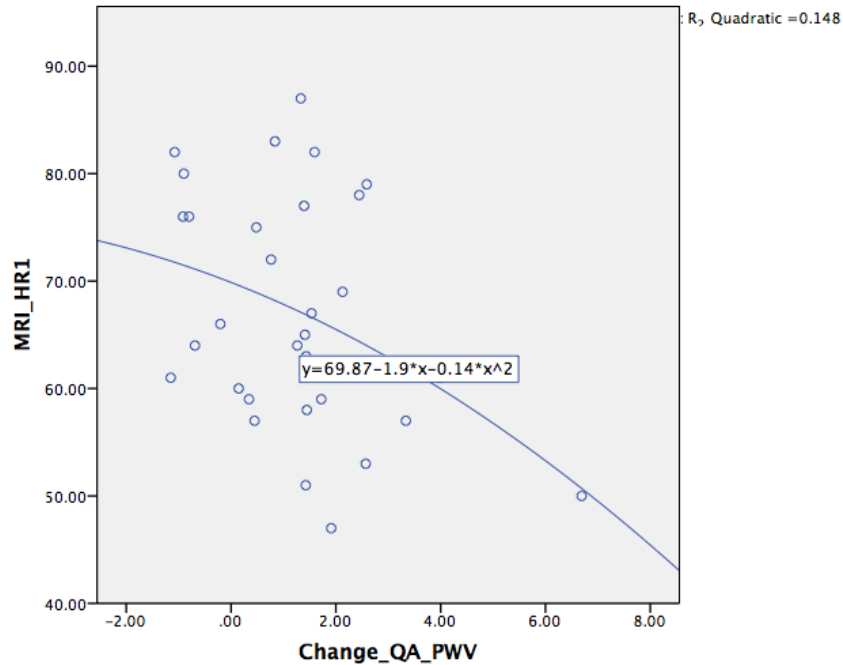
As a significant fall in 6MWT was observed an unplanned analysis of the determinants of this change was performed. 6MWT distance walked at follow-up was strongly correlated with baseline 6MWT, age, FEV1, FEV1/FVC, FEF25-75, DLCO, KCO, RLV/TLC, LVEF and pulmonary pulsatility (see Table 7-5). On backward entry linear regression, baseline FEV1 percent predicted (ß=0.44, p=0.003) and pulmonary pulsatility (ß=0.48, p=0.003) were independently associated with follow-up 6MWT. However when baseline 6MWT was included in the model, this significance was lost with only baseline 6MWT predicting 6MWT distance at 1 year (ß=0.84, p<0.001).

Previous reports have described a 30m cutoff as a clinical significant deterioration in functional performance,(297) thus a comparison was performed between those who's 6MWT distance had fallen by greater than 30m compared with those who's distance had fallen by less than 30m. Those who had a clinically significant fall in 6MWT were older (73.2±6.3 years vs. 65.1±7.7 years, p=0.005) with significantly lower pulmonary pulsatility (19.7±7.1 vs. 26.7±8.9%, p=0.028) but

were otherwise similar (See Table 7-6). After correction for multiple comparisons with a new significance threshold of $p<0.0014$, no significant difference between the groups remained.

Table 7-5: Correlation of change in 6MWT with demographic, spirometric and cardiac metrics at baseline.

	Follow-up 6MWT	
Baseline measure*	R	p
6MWT	0.9	**<0.001**
Age	-0.52	**0.003**
BMI (kg/m^2)	-0.17	0.35
Heart rate (bpm)	-0.7	0.69
Systolic BP (mmHg)	-0.21	0.26
Diastolic BP (mmHg)	-0.11	0.56
SpO2	0.17	0.36
Pack years	-0.18	0.32
FEV1, % predicted	0.39	**0.03**
FVC, % predicted	0.23	0.22
FEV1/FVC	0.44	**0.01**
FEF 25-75, % predicted	0.38	**0.04**
DLCO, % predicted	0.5	**0.004**
DLCO/VA, % predicted	0.37	**0.04**
RLV, % predicted	-0.16	0.41
VC, % predicted	0.22	0.25
TLC, % predicted	-0.08	0.69
RLV /TLC	-0.38	**0.04**
RVEDV (ml/m$^{1.7}$)	-0.04	0.82
RVESV (ml/m$^{1.7}$)	-0.29	0.11
RVSV (ml/m$^{1.7}$)	0.22	0.23
RVEF (%)	0.35	0.05
RVM (g/m$^{1.7}$)	-0.02	0.94
RVMVR (g/ml)	0.08	0.66
LVEDV (ml/m$^{1.7}$)	0.07	0.72
LVESV (ml/m$^{1.7}$)	-0.22	0.23
LVSV (ml/m$^{1.7}$)	0.30	0.10
LVEF (%)	0.41	**0.02**
LVM (g/m$^{1.7}$)	0.06	0.76
LVMVR (g/ml)	0.03	0.88
Pulmonary PWV	-0.03	0.89
Pulmonary Pulsatility	0.52	**0.003**
Pulmonary acceleration time	-0.18	0.33

Table 7-6: Comparison of the baseline demographic, pulmonary function and cardiac parameters between those with and without a clinically significant fall in 6-minute walking distance.

	Fall in 6MWT		
	< 30m	> 30m	P+
N*	19	12	
Age	65.1 ± 7.7	73.2 ± 6.3	0.005
Sex (male)	7 (37%)	9 (75%)	0.066
BMI (kg/m^2)	27.8 ± 4.7	26.2 ± 6.3	0.42
Heart rate (bpm)	68.8 ± 21.9	70.8 ± 10.8	0.77
Systolic BP (mmHg)	127 ± 18	136 ± 10	0.13
Diastolic BP (mmHg)	73 ± 9	75 ± 8	0.55
SpO2	96.1 ± 1.6	95.8 ± 2.0	0.64
Smoking status			
Current smoker	5 (26%)	1 (8%)	0.36
Ex-smoker	14 (74%)	11 (92%)	0.36
Pack years	53.9 ± 24.7	53.3 ± 29.7	0.95
COPD exacerbation since baseline	3	0	0.27
Uptitring of inhaler therapy	1	3	0.27
Pulmonary Function tests			
FEV1, % predicted	63.5 ± 18.4	65.9 ± 24.2	0.75
FVC, % predicted	101.0 ± 18.6	97.3 ± 22.1	0.62
FEV1/FVC	50.4 ± 11.6	51.3 ± 11.2	0.84
FEF 25-75, % predicted	22.4 ± 12.9	25.7 ± 11.7	0.48
DLCO, % predicted	56.4 ± 17.9	51.8 ± 15.8	0.47
DLCO/VA, % predicted	69.7 ± 17.3	72.7 ± 23.9	0.69

RLV, % predicted	178.2 ± 55	173.8 ± 58.6	0.84
VC, % predicted	98.8 ± 13.7	103.2 ± 22.2	0.50
TLC, % predicted	124.9 ± 23.3	124.6 ± 23.3	0.97

CMR

RVEDV (ml/m$^{1.7}$)	52.1 ± 10.3	56.2 ± 8.5	0.26
RVESV (ml/m$^{1.7}$)	20.1 ± 6.3	24.5 ± 6.9	0.08
RVSV (ml/m$^{1.7}$)	32.0 ± 8.4	31.7 ± 4.2	0.87
RVEF (%)	61.4 ± 9.5	57.0 ± 6.7	0.18
RVM (g/m$^{1.7}$)	15.7 ± 3.3	17.6 ± 3.5	0.14
RVMVR (g/ml)	0.31 ± 0.05	0.31 ± 0.05	0.69
LVEDV (ml/m$^{1.7}$)	54.9 ± 9.3	56.5 ± 10.2	0.64
LVESV (ml/m$^{1.7}$)	22.1 ± 4.4	22.9 ± 7.4	0.73
LVSV (ml/m$^{1.7}$)	32.8 ± 6.7	33.6 ± 6.0	0.72
LVEF (%)	59.7 ± 5.1	60.2 ± 7.7	0.81
LVM (g/m$^{1.7}$)	41.1 ± 8.5	45.5 ± 9.2	0.18
LVMVR (g/ml)	0.75 ± 0.11	0.81 ± 0.10	0.18
Pulmonary PWV	2.35 ± 0.88	2.22 ± 1.12	0.72
Pulmonary Pulsatility	26.7 ± 8.9	19.7 ± 7.1	0.028
Pulmonary acceleration time	103.0 ± 19.6	107.3 ± 30.0	0.64
Aortic PWV	8.19 ± 2.25	8.0 ± 2.22	0.81

*Total n=31 rather than 32 as one patient had had a recent ankle fracture and was therefore excluded from repeat 6MWT.

[+]Significance set at p<0.0013 after bonferroni correction for multiple comparisons.

7.3 DISCUSSION

In this chapter we have seen that the primary study outcome – change in right ventricular mass at 1 year – was negative. Thus all other comparisons must be interpreted with caution.

This is the first study to look at longitudinal changes in ventricular function in COPD. Due to this lack of prior work, the primary study outcome – change in right ventricular mass – was powered according to the placebo arms of randomised control trials in pulmonary hypertension as this was the only data available. These describe an increase in mass of 5-8g (change in right ventricular mass detected over 4-36 months in groups of 21 and 44 participants respectively).(263,264) Based on these factors, n=17 would allow detection of a 4g change with study power of 80% and a p=0.05. The rationale for this was that all the cardiac MRI studies at the time of the study design had described right ventricular hypertrophy, with the severity of this increasing with COPD severity.(79–81,298) However, as we have seen in chapter 4, we found a pattern of reduced ventricular volumes with no evidence of right ventricular hypertrophy, with our results mirroring those of the MESA-COPD study.(274) Our observed right ventricular mass of 39g is also significantly lower than the mass of 74-102g seen in the pulmonary hypertension interventional trials. Thus it is perhaps not surprising that at one-year follow-up we detected no significant interval change in right ventricular mass. Given that the change in absolute RV mass only equated to an increase of 0.44g, with a similarly small change in other ventricular metrics, this suggests that cardiac remodeling occurs slowly and can largely be considered stable over the usual time period used in interventional studies. As a result we are unable to examine the longitudinal effects of pulmonary PWV on ventricular remodeling other than to say that if it is present it is likely small and beyond the power of this study to detect it.

The change in pulmonary arterial stiffness in the follow-up appears disproportionate to the findings of the changes or lack thereof of the remainder of the metrics. Indeed if one were to consider a 50% increment in pulmonary PWV per year, one would very rapidly see end stage pulmonary vascular changes with inordinately high PWV values. However this was not the case with pulmonary PWV remaining significantly lower than the aortic values. Therefore the inverse correlation between the heart rate and change in pulse wave velocity must also be viewed with caution and will require replication in future studies. If validated it would however raise an interesting facet of pulmonary vascular remodeling. Sympathetic over activation is common in COPD(299), with increased sympathetic activation associated with increased arterial stiffening.(300) However hypercapnia and metabolic acidosis are associated with increased parasympathetic activation, thus those with a reduced heart rate may represent a subset with more severe disease leading to more rapid pulmonary remodeling.(301)

The observed rapid shift in PWV requires exploration. While all visits were coordinated to occur 8 weeks or more after an acute exacerbation it is not entirely inconceivable that patients could have been in the earliest stages of developing an exacerbation during one or both of their visits. While pulmonary arterial stiffness has not been directly assessed in the acute exacerbation phase of COPD, it is known that these are associated with a transient dilation of the main pulmonary artery during the acute episode.(302) Thus an early exacerbation of COPD could potentially cause an acute rise in arterial stiffness and thus PWV. However in a cohort of 32, it is unlikely that enough people would develop early acute exacerbations at the time of their second visit but not their first in order to skew the results in such a fashion. In addition the pulmonary pulsatility and pulmonary acceleration time - both metrics of pulmonary vascular status - remained stable, making significant interval changes in PWV somewhat less likely. Thus the technique itself must be examined. We saw in chapter 4 that the mean interscan difference for the QA-PWV was 0.43ms^{-1} with limits of

agreement of -2.18 - 1.32ms^{-1}. Therefore the observed rise in pulmonary PWV of 1.2ms^{-1} may be possibly be attributable to these rather wide limits of agreement producing a Type 1 error. Given the width of the limits of agreement a similar consideration must also be made for the lack of observation of significant correlation between the pulmonary PWV and clinical and spirometric variables due to this providing a significant level of 'noise' thereby potentially obscuring significant associations. Further work to improve pulmonary PWV measurement repeatability will allow for smaller temporal changes to be observed over time and greater accuracy of the determinants and associations of this. Potential avenues for this include new phase contrast sequences using 'radial' and 'stack of stars' k-space acquisition which have been described to provide greater edge definition – an important factor in the flow-area PWV calculation.(261) 4D flow techniques may also allow more accurate measurements or arterial stiffening. While these suffer from poor temporal resolution this is offset by a simultaneous acquisition of the flow information at multiple sites therefore reducing the effect of interscan r-r variability on wave arrival time, and also allows multiple regions of interest to be applied along a vessels length irrespective of its geometry with these multiple sampling points improving the accuracy of the timing of the transit of the pulse wave throughout the vessel.(303,304)

We have shown that while the cardiac metrics remained stable a significant deterioration in the six-minute walk test occurred. Our finding of a significant correlation between baseline FEV1 and pulmonary pulsatility is interesting. The finding of a significant correlation between FEV1 and decline in exercise capacity is consistent with prior work in the ECLIPSE multinational study.(297) A previous study using echocardiography found that pulmonary pulsatility significantly correlated with NYHA status, so a concordance with exercise capacity would fit with this.(186) In addition, in COPD increased pulmonary arterial diameters (typically seen with reduced pulsatility) have been demonstrated to be associated with reduced six minute walk test, increased incidence of acute

exacerbations and increased prevalence of pulmonary hypertension.(126,127,273) Given the findings of our current study and these prior studies, further work is warranted to better examine the implications of pulmonary pulsatility in exercise capacity.

The main limitation of the current study other than those mentioned above is the small sample size that returned for the final study visit. This was largely due to the time constraints of the PhD meaning that those recruited after the end of the second year could not be brought back for a repeat visit. This reduces the effect size between study visits that can be detected and also increases the risk of both type I and type II errors when conducting multiple analyses within a small cohort.

7.4 CONCLUSION

In this chapter we have seen that there was no significant interval change in right ventricular mass or function. As a result we are unable to examine the longitudinal effects of pulmonary PWV on ventricular remodeling other than to say that if it is present it is likely small and beyond the power of this study to detect it.

CHAPTER 8: Discussion and Further Work

We have seen in Chapter 1 that there are four broad prevailing mechanisms potentially linking COPD with the markedly elevated cardiovascular risk profile in those suffering this condition. This thesis was designed and centered on the role of pulmonary hypertension in COPD, and more specifically, the role of pulmonary arterial stiffening. This was based on extensive evidence of a relatively common prevalence of this complication, its occurrence early in COPD and links to poorer outcome. A technique for the measurement of pulse wave velocity in the pulmonary arteries was developed and its reproducibility was assessed. This technique was then applied in a COPD cohort and age and sex matched healthy cohort. We observed the expected stiffening of the pulmonary arteries in the COPD cohort, but contrary to the original hypothesis and expectations, found that it did not correlate either with baseline or follow-up right ventricular mass. In fact the pattern of ventricular remodeling was instead that of an underfilled state rather than a pressure overloaded state, with the left ventricle demonstrating similar remodeling to the right.

Future work in this area needs to focus on two aspects. First, what is the cause for this underfilling? We have previously discussed the competing theories for the underfilling of the ventricles of increased intra-thoracic pressure impeding venous return versus myocardial stiffening with impaired relaxation. These questions could potentially be answered using a combination of cross-sectional/volumetric quantification of the SVC and IVC for evidence of compression/collapse, and advanced cardiac imaging techniques of

feature-tracking/tagging of the myocardium to examine systolic and diastolic strain and relaxation rates to examine for myocardial stiffening.

The second question to be examined is, what are the clinical implications of this underfilling, and does this explain the disproportionate cardiovascular risk profile of this group of patients? While utilisation of existing echo databases can give some insight into this, looking at historical ventricular volumes and associated mortality risk in those with COPD. Prospective longitudinal follow-up of a large cohort of COPD patients to determine causative deterministics of reduced ventricular volumes on cardiovascular morbidity or mortality will be ultimately required.

In the current study we found that pulmonary PWV could indeed pick up differences between populations but its repeatability needs further improvement and to date, this technique has still not been validated against the gold standard of invasive PWV measurement. Thus further work is needed exploring the potential utility of both faster acquisition sequences using non-Cartesian k-space sampling and 4D acquisition techniques. Assessment of this in a population due to undergo right heart catheterisation would be ideal as it would allow acquisition of an invasive PWV without necessitating any additional procedures to then compare against these competing techniques.

REFERENCES

1.   Stone IS, Barnes NC, Petersen SE. Chronic obstructive pulmonary disease: a modifiable risk factor for cardiovascular disease? Heart 2012;98:1055–62. doi:10.1136/heartjnl-2012-301759.
2.   Vestbo J, Hurd SS, Agustí AG, et al. Global strategy for the diagnosis, management, and prevention of chronic obstructive pulmonary disease: GOLD executive summary. Am J Respir Crit Care Med 2013;187:347–65. doi:10.1164/rccm.201204-0596PP.
3.   National Institute for Clinical Excellence. Chronic obstructive pulmonary disease: Management of chronic obstructive pulmonary disease in adults in primary and secondary care 2010.
4.   Ford ES, Mannino DM, Zhao G, Li C, Croft JB. Changes in mortality among US adults with COPD in two national cohorts recruited from 1971-1975 and 1988-1994. Chest 2012;141:101–10. doi:10.1378/chest.11-0472.
5.   McCullough P a, Hollander JE, Nowak RM, et al. Uncovering heart failure in patients with a history of pulmonary disease: rationale for the early use of B-type natriuretic peptide in the emergency department. Acad Emerg Med 2003;10:198–204.
6.   Rutten FH, Cramer M-JM, Grobbee DE, et al. Unrecognized heart failure in elderly patients with stable chronic obstructive pulmonary disease. Eur Heart J 2005;26:1887–94. doi:10.1093/eurheartj/ehi291.
7.   Hole DJ, Watt GC, Davey-Smith G, et al. Impaired lung function and mortality risk in men and women: findings from the Renfrew and Paisley prospective population study. BMJ 1996;313:711-5-6.
8.   Engström G, Wollmer P, Hedblad B, et al. Occurrence and prognostic significance of ventricular arrhythmia is related to pulmonary function: a study from "men born in 1914," Malmö, Sweden. Circulation 2001;103:3086–91. doi:10.1161/01.CIR.103.25.3086.
9.   Curkendall SM, DeLuise C, Jones JK, et al. Cardiovascular disease in patients with chronic obstructive pulmonary disease, Saskatchewan Canada cardiovascular disease in COPD patients. Ann Epidemiol 2006;16:63–70. doi:10.1016/j.annepidem.2005.04.008.
10.   Rodriguez BL, Masaki K, Burchfiel C, et al. Pulmonary function decline and 17-year total mortality: the Honolulu Heart Program. Am J Epidemiol 1994;140:398–408.
11.   Tockman MS, Pearson JD, Fleg JL, et al. Rapid decline in FEV1. A new risk factor for coronary heart disease mortality. Am J Respir Crit Care Med 1995;151:390–8. doi:10.1164/ajrccm.151.2.7842197.
12.   Voelkel NF, Gomez-Arroyo J, Mizuno S. COPD/emphysema: The vascular story. Pulm Circ 2013;1:320–6. doi:10.4103/2045-8932.87295.
13.   Sinden NJ, Stockley R a. Systemic inflammation and comorbidity in COPD: a result of "overspill" of inflammatory mediators from the lungs? Review of the evidence. Thorax 2010;65:930–6. doi:10.1136/thx.2009.130260.
14.   Cockayne DA, Cheng DT, Waschki B, et al. Systemic biomarkers of neutrophilic inflammation, tissue injury and repair in COPD patients with differing levels of

disease severity. PLoS One 2012;7:e38629. doi:10.1371/journal.pone.0038629.

15.   de Godoy I, Donahoe M, Calhoun WJ, Mancino J, Rogers RM. Elevated TNF-alpha production by peripheral blood monocytes of weight-losing COPD patients. Am J Respir Crit Care Med 1996;153:633–7. doi:10.1164/ajrccm.153.2.8564110.

16.   Valipour A, Schreder M, Wolzt M, et al. Circulating vascular endothelial growth factor and systemic inflammatory markers in patients with stable and exacerbated chronic obstructive pulmonary disease. Clin Sci (Lond) 2008;115:225–32. doi:10.1042/CS20070382.

17.   Donaldson GC, Seemungal TAR, Patel IS, et al. Airway and systemic inflammation and decline in lung function in patients with COPD. Chest 2005;128:1995–2004. doi:10.1378/chest.128.4.1995.

18.   Man SFP, Connett JE, Anthonisen NR, et al. C-reactive protein and mortality in mild to moderate chronic obstructive pulmonary disease. Thorax 2006;61:849–53. doi:10.1136/thx.2006.059808.

19.   Hubbard RC, Brantly ML, Sellers SE, Mitchell ME, Crystal RG. Anti-neutrophil-elastase defenses of the lower respiratory tract in alpha 1-antitrypsin deficiency directly augmented with an aerosol of alpha 1-antitrypsin. Ann Intern Med 1989;111:206–12.

20.   Smith RM, Traber LD, Traber DL, Spragg RG. Pulmonary deposition and clearance of aerosolized alpha-1-proteinase inhibitor administered to dogs and to sheep. J Clin Invest 1989;84:1145–54. doi:10.1172/JCI114278.

21.   Potocka E, Amin N, Cassidy J, et al. Insulin pharmacokinetics following dosing with Technosphere insulin in subjects with chronic obstructive pulmonary disease. Curr Med Res Opin 2010;26:2347–53. doi:10.1185/03007995.2010.511971.

22.   Zhang Q, Kandic I, Kutryk MJ. Dysregulation of angiogenesis-related microRNAs in endothelial progenitor cells from patients with coronary artery disease. Biochem Biophys Res Commun 2011;405:42–6. doi:10.1016/j.bbrc.2010.12.119.

23.   Mills NL, Miller JJ, Anand A, et al. Increased arterial stiffness in patients with chronic obstructive pulmonary disease: a mechanism for increased cardiovascular risk. Thorax 2008;63:306–11. doi:10.1136/thx.2007.083493.

24.   McAllister D a, Maclay JD, Mills NL, et al. Arterial stiffness is independently associated with emphysema severity in patients with chronic obstructive pulmonary disease. Am J Respir Crit Care Med 2007;176:1208–14. doi:10.1164/rccm.200707-1080OC.

25.   Sabit R, Bolton CE, Edwards PH, et al. Arterial stiffness and osteoporosis in chronic obstructive pulmonary disease. Am J Respir Crit Care Med 2007;175:1259–65. doi:10.1164/rccm.200701-067OC.

26.   Dransfield MT, Cockcroft JR, Townsend RR, et al. Effect of fluticasone propionate/salmeterol on arterial stiffness in patients with COPD. Respir Med 2011;105:1322–30. doi:10.1016/j.rmed.2011.05.016.

27.   Laurent S, Cockcroft J, Van Bortel L, et al. Expert consensus document on arterial stiffness: methodological issues and clinical applications. Eur Heart J 2006;27:2588–605. doi:10.1093/eurheartj/ehl254.

28.   O'Rourke MF, Safar ME. Relationship between aortic stiffening and microvascular disease in brain and kidney: cause and logic of therapy. Hypertension 2005;46:200–4. doi:10.1161/01.HYP.0000168052.00426.65.

29.   Harris B, Klein R, Jerosch-Herold M, et al. The association of systemic microvascular changes with lung function and lung density: a cross-sectional study. PLoS One 2012;7:e50224. doi:10.1371/journal.pone.0050224.

30.   Barr RG, Mesia-Vela S, Austin JHM, et al. Impaired flow-mediated dilation is associated with low pulmonary function and emphysema in ex-smokers: the Emphysema and Cancer Action Project (EMCAP) Study. Am J Respir Crit Care Med 2007;176:1200–7. doi:10.1164/rccm.200707-980OC.

31.   Eickhoff P, Valipour A, Kiss D, et al. Determinants of systemic vascular function in patients with stable chronic obstructive pulmonary disease. Am J Respir Crit Care Med 2008;178:1211–8. doi:10.1164/rccm.200709-1412OC.

32.   Anderson TJ, Uehata A, Gerhard MD, et al. Close relation of endothelial function in the human coronary and peripheral circulations. J Am Coll Cardiol 1995;26:1235–41. doi:10.1016/0735-1097(95)00327-4.

33.   Takase B, Hamabe A, Satomura K, et al. Close relationship between the vasodilator response to acetylcholine in the brachial and coronary artery in suspected coronary artery disease. Int J Cardiol 2005;105:58–66. doi:10.1016/j.ijcard.2004.12.021.

34.   Bøttcher M, Madsen MM, Refsgaard J, et al. Peripheral flow response to transient arterial forearm occlusion does not reflect myocardial perfusion reserve. Circulation 2001;103:1109–14. doi:10.1161/01.CIR.103.8.1109.

35.   Scholtens AM, Tio RA, Willemsen A, et al. Myocardial perfusion reserve compared with peripheral perfusion reserve: a [13N]ammonia PET study. J Nucl Cardiol 2011;18:238–46. doi:10.1007/s12350-011-9339-2.

36.   Lerman A, Zeiher AM. Endothelial function: cardiac events. Circulation 2005;111:363–8. doi:10.1161/01.CIR.0000153339.27064.14.

37.   Barr RG, Ahmed FS, Carr JJ, et al. Subclinical atherosclerosis, airflow obstruction and emphysema: the MESA Lung Study. Eur Respir J 2012;39:846–54. doi:10.1183/09031936.00165410.

38.   Timmins SC, Diba C, Farrow CE, et al. The relationship between airflow obstruction, emphysema extent, and small airways function in COPD. Chest 2012;142:312–9. doi:10.1378/chest.11-2169.

39.   Tschernko EM, Gruber EM, Jaksch P, et al. Ventilatory mechanics and gas exchange during exercise before and after lung volume reduction surgery. Am J Respir Crit Care Med 1998;158:1424–31.

40.   Anderson WJ, Lipworth BJ, Rekhraj S, Struthers AD, George J. Left ventricular hypertrophy in COPD without hypoxemia: the elephant in the room? Chest 2013;143:91–7. doi:10.1378/chest.12-0775.

41.   Smith BM, Kawut SM, Bluemke DA, et al. Pulmonary hyperinflation and left ventricular mass: the Multi-Ethnic Study of Atherosclerosis COPD Study. Circulation 2013;127:1503–11, 1511-6. doi:10.1161/CIRCULATIONAHA.113.001653.

42.   Scharf SM, Brown R, Saunders N, Green LH. Effects of normal and loaded spontaneous inspiration on cardiovascular function. J Appl Physiol 1979;47:582–90.

43.   Bluemke D a, Kronmal R a, Lima JAC, et al. The relationship of left ventricular mass and geometry to incident cardiovascular events: the MESA (Multi-Ethnic Study of Atherosclerosis) study. J Am Coll Cardiol 2008;52:2148–55. doi:10.1016/j.jacc.2008.09.014.

44.   Jörgensen K, Houltz E, Westfelt U, et al. Effects of lung volume reduction surgery on

left ventricular diastolic filling and dimensions in patients with severe emphysema. Chest 2003;124:1863–70.

45. Jörgensen K, Müller MF, Nel J, et al. Reduced intrathoracic blood volume and left and right ventricular dimensions in patients with severe emphysema: an MRI study. Chest 2007;131:1050–7. doi:10.1378/chest.06-2245.

46. Smith BM, Prince MR, Hoffman E a, et al. Impaired left ventricular filling in COPD and emphysema: is it the heart or the lungs? The Multi-Ethnic Study of Atherosclerosis COPD Study. Chest 2013;144:1143–51. doi:10.1378/chest.13-0183.

47. Jörgensen K, Houltz E, Westfelt U, Ricksten S-E. Left ventricular performance and dimensions in patients with severe emphysema. Anesth Analg 2007;104:887–92. doi:10.1213/01.ane.0000258020.27849.6b.

48. Casanova C, Cote C, de Torres JP, et al. Inspiratory-to-total lung capacity ratio predicts mortality in patients with chronic obstructive pulmonary disease. Am J Respir Crit Care Med 2005;171:591–7. doi:10.1164/rccm.200407-867OC.

49. Moore AJ, Soler RS, Cetti EJ, et al. Sniff nasal inspiratory pressure versus IC/TLC ratio as predictors of mortality in COPD. Respir Med 2010;104:1319–25. doi:10.1016/j.rmed.2010.03.001.

50. Boutou AK, Shrikrishna D, Tanner RJ, et al. Lung function indices for predicting mortality in COPD. Eur Respir J 2013;42:616–25. doi:10.1183/09031936.00146012.

51. Makita H, Nasuhara Y, Nagai K, et al. Characterisation of phenotypes based on severity of emphysema in chronic obstructive pulmonary disease. Thorax 2007;62:932–7. doi:10.1136/thx.2006.072777.

52. Guerassimov A, Hoshino Y, Takubo Y, et al. The development of emphysema in cigarette smoke-exposed mice is strain dependent. Am J Respir Crit Care Med 2004;170:974–80. doi:10.1164/rccm.200309-1270OC.

53. Shifren A, Mecham RP. The stumbling block in lung repair of emphysema: elastic fiber assembly. Proc Am Thorac Soc 2006;3:428–33. doi:10.1513/pats.200601-009AW.

54. Zieman SJ, Melenovsky V, Kass DA. Mechanisms, pathophysiology, and therapy of arterial stiffness. Arterioscler Thromb Vasc Biol 2005;25:932–43. doi:10.1161/01.ATV.0000160548.78317.29.

55. Pyeritz RE. The Marfan syndrome. Annu Rev Med 2000;51:481–510. doi:10.1146/annurev.med.51.1.481.

56. Dyhdalo K, Farver C. Pulmonary histologic changes in Marfan syndrome: a case series and literature review. Am J Clin Pathol 2011;136:857–63. doi:10.1309/AJCP79SNDHGKQFIN.

57. Patel BD, Loo WJ, Tasker AD, et al. Smoking related COPD and facial wrinkling: is there a common susceptibility? Thorax 2006;61:568–71. doi:10.1136/thx.2005.053827.

58. Kuro-o M, Matsumura Y, Aizawa H, et al. Mutation of the mouse klotho gene leads to a syndrome resembling ageing. Nature 1997;390:45–51. doi:10.1038/36285.

59. Roberts R, Stewart AFR. Genes and coronary artery disease: where are we? J Am Coll Cardiol 2012;60:1715–21. doi:10.1016/j.jacc.2011.12.062.

60. Todd JL, Goldstein DB, Ge D, Christie J, Palmer SM. The state of genome-wide association studies in pulmonary disease: a new perspective. Am J Respir Crit Care Med 2011;184:873–80. doi:10.1164/rccm.201106-0971PP.

61.   Natoli G, Ghisletti S, Barozzi I. The genomic landscapes of inflammation. Genes Dev 2011;25:101–6. doi:10.1101/gad.2018811.
62.   Cho MH, Boutaoui N, Klanderman BJ, et al. Variants in FAM13A are associated with chronic obstructive pulmonary disease. Nat Genet 2010;42:200–2. doi:10.1038/ng.535.
63.   Hyduk A, Croft JB, Ayala C, et al. Pulmonary hypertension surveillance--United States, 1980-2002. MMWR Surveill Summ 2005;54:1–28.
64.   Thabut G, Dauriat G, Stern JB, et al. Pulmonary hemodynamics in advanced COPD candidates for lung volume reduction surgery or lung transplantation. Chest 2005;127:1531–6. doi:10.1378/chest.127.5.1531.
65.   Hilde JM, Skjørten I, Hansteen V, et al. Haemodynamic responses to exercise in patients with COPD. Eur Respir J 2013;41:1031–41. doi:10.1183/09031936.00085612.
66.   Minai OA, Chaouat A, Adnot S. Pulmonary hypertension in COPD: epidemiology, significance, and management: pulmonary vascular disease: the global perspective. Chest 2010;137:39S–51S. doi:10.1378/chest.10-0087.
67.   Kessler R, Faller M, Weitzenblum E, et al. "Natural history" of pulmonary hypertension in a series of 131 patients with chronic obstructive lung disease. Am J Respir Crit Care Med 2001;164:219–24. doi:10.1164/ajrccm.164.2.2006129.
68.   Oswald-Mammosser M, Weitzenblum E, Quoix E, et al. Prognostic factors in COPD patients receiving long-term oxygen therapy. Importance of pulmonary artery pressure. Chest 1995;107:1193–8.
69.   Weitzenblum E, Hirth C, Ducolone A, et al. Prognostic value of pulmonary artery pressure in chronic obstructive pulmonary disease. Thorax 1981;36:752–8.
70.   Cuttica MJ, Kalhan R, Shlobin OA, et al. Categorization and impact of pulmonary hypertension in patients with advanced COPD. Respir Med 2010;104:1877–82. doi:10.1016/j.rmed.2010.05.009.
71.   Galiè N, Hoeper MM, Humbert M, et al. Guidelines for the diagnosis and treatment of pulmonary hypertension: the Task Force for the Diagnosis and Treatment of Pulmonary Hypertension of the European Society of Cardiology (ESC) and the European Respiratory Society (ERS), endorsed by the Internat. Eur Heart J 2009;30:2493–537. doi:10.1093/eurheartj/ehp297.
72.   Kiely DG, Elliot CA, Sabroe I, Condliffe R. Pulmonary hypertension: diagnosis and management. Bmj 2013;346:f2028–f2028. doi:10.1136/bmj.f2028.
73.   Nogami M, Ohno Y, Koyama H, et al. Utility of phase contrast MR imaging for assessment of pulmonary flow and pressure estimation in patients with pulmonary hypertension: comparison with right heart catheterization and echocardiography. J Magn Reson Imaging 2009;30:973–80. doi:10.1002/jmri.21935.
74.   Arcasoy SM, Christie JD, Ferrari VA, et al. Echocardiographic assessment of pulmonary hypertension in patients with advanced lung disease. Am J Respir Crit Care Med 2003;167:735–40. doi:10.1164/rccm.200210-1130OC.
75.   Iyer AS, Wells JM, Vishin S, et al. CT scan-measured pulmonary artery to aorta ratio and echocardiography for detecting pulmonary hypertension in severe COPD. Chest 2014;145:824–32. doi:10.1378/chest.13-1422.
76.   Devaraj A, Wells AU, Meister MG. Detection of pulmonary hypertension with multidetector CT and echocardiography alone and in combination. Japanese J Chest

Dis 2010;69:570. doi:10.1148/radiol.09090548.

77.   Peinado VI, Barberá JA, Abate P, et al. Inflammatory reaction in pulmonary muscular arteries of patients with mild chronic obstructive pulmonary disease. Am J Respir Crit Care Med 1999;159:1605–11. doi:10.1164/ajrccm.159.5.9807059.

78.   Hilde JM, Skjørten I, Grøtta OJ, et al. Right ventricular dysfunction and remodeling in chronic obstructive pulmonary disease without pulmonary hypertension. J Am Coll Cardiol 2013;62:1103–11. doi:10.1016/j.jacc.2013.04.091.

79.   Vonk-Noordegraaf A, Marcus JT, Holverda S, Roseboom B, Postmus PE. Early changes of cardiac structure and function in COPD patients with mild hypoxemia. Chest 2005;127:1898–903. doi:10.1378/chest.127.6.1898.

80.   Gao Y, Du X, Qin W, Li K. Assessment of the right ventricular function in patients with chronic obstructive pulmonary disease using MRI. Acta Radiol 2011;52:711–5. doi:10.1258/ar.2011.100449.

81.   Pattynama PM, Willems LN, Smit AH, van der Wall EE, de Roos A. Early diagnosis of cor pulmonale with MR imaging of the right ventricle. Radiology 1992;182:375–9. doi:10.1148/radiology.182.2.1531092.

82.   Seimetz M, Parajuli N, Pichl A, et al. Inducible NOS inhibition reverses tobacco-smoke-induced emphysema and pulmonary hypertension in mice. Cell 2011;147:293–305. doi:10.1016/j.cell.2011.08.035.

83.   Wright JL, Churg A. Effect of long-term cigarette smoke exposure on pulmonary vascular structure and function in the guinea pig. Exp Lung Res 1991;17:997–1009.

84.   Ferrer E, Peinado VI, Castañeda J, et al. Effects of cigarette smoke and hypoxia on pulmonary circulation in the guinea pig. Eur Respir J 2011;38:617–27. doi:10.1183/09031936.00105110.

85.   Holverda S, Rietema H, Westerhof N, et al. Stroke volume increase to exercise in chronic obstructive pulmonary disease is limited by increased pulmonary artery pressure. Heart 2009;95:137–41. doi:10.1136/hrt.2007.138172.

86.   Christensen CC, Ryg MS, Edvardsen A, Skjønsberg OH. Relationship between exercise desaturation and pulmonary haemodynamics in COPD patients. Eur Respir J 2004;24:580–6. doi:10.1183/09031936.04.00118303.

87.   Skjørten I, Hilde JM, Melsom MN, et al. Pulmonary artery pressure and PaO2 in chronic obstructive pulmonary disease. Respir Med 2013;107:1271–9. doi:10.1016/j.rmed.2013.03.021.

88.   Barberà JA, Riverola A, Roca J, et al. Pulmonary vascular abnormalities and ventilation-perfusion relationships in mild chronic obstructive pulmonary disease. Am J Respir Crit Care Med 1994;149:423–9. doi:10.1164/ajrccm.149.2.8306040.

89.   Magee F, Wright JL, Wiggs BR, Paré PD, Hogg JC. Pulmonary vascular structure and function in chronic obstructive pulmonary disease. Thorax 1988;43:183–9.

90.   Santos S, Peinado VI, Ramírez J, et al. Characterization of pulmonary vascular remodelling in smokers and patients with mild COPD. Eur Respir J 2002;19:632–8. doi:10.1183/09031936.02.00245902.

91.   Barberà JA. Mechanisms of development of chronic obstructive pulmonary disease-associated pulmonary hypertension. Pulm Circ 2013;3:160–4. doi:10.4103/2045-8932.109949.

92.   Peinado VI, Barbera JA, Ramirez J, et al. Endothelial dysfunction in pulmonary arteries of patients with mild COPD. Am J Physiol 1998;274:L908-13.

93.   Chen S-L, Zhang Y-J, Zhou L, et al. Percutaneous pulmonary artery denervation completely abolishes experimental pulmonary arterial hypertension in vivo. EuroIntervention 2013;9:269–76. doi:10.4244/EIJV9I2A43.

94.   Baylen BG, Emmanouilides GC, Juratsch CE, et al. Main pulmonary artery distention: a potential mechanism for acute pulmonary hypertension in the human newborn infant. J Pediatr 1980;96:540–4.

95.   Juratsch CE, Jengo JA, Castagna J, Laks MM. Experimental pulmonary hypertension produced by surgical and chemical denervation of the pulmonary vasculature. Chest 1980;77:525–30.

96.   Osorio J, Russek M. Reflex changes on the pulmonary and systemic pressures elicited by stimulation of baroreceptors in the pulmonary artery. Circ Res 1962;10:664–7.

97.   Chen S-L, Zhang F-F, Xu J, et al. Pulmonary artery denervation to treat pulmonary arterial hypertension: the single-center, prospective, first-in-man PADN-1 study (first-in-man pulmonary artery denervation for treatment of pulmonary artery hypertension). J Am Coll Cardiol 2013;62:1092–100. doi:10.1016/j.jacc.2013.05.075.

98.   Galiè N, Manes A. New treatment strategies for pulmonary arterial hypertension: hopes or hypes? J Am Coll Cardiol 2013;62:1101–2. doi:10.1016/j.jacc.2013.06.032.

99.   Starr I, Jeffers WA, Jr. RHM. The absence of conspicuous increments of venous pressure after severe damage to the right ventricle of the dog, with a discussion of the relation between clinical congestive failure and heart disease. Am Heart J 1943;26:291–301. doi:http://dx.doi.org/10.1016/S0002-8703(43)90325-4.

100.   Bakos ACP. The Question of the Function of the Right Ventricular Myocardium: An Experimental Study. Circulation 1950;1:724–32. doi:10.1161/01.CIR.1.4.724.

101.   Kagan A. Dynamic responses of the right ventricle following extensive damage by cauterization. Circulation 1952;5:816–23. doi:10.1161/01.CIR.5.6.816.

102.   Goldstein J a, Vlahakes GJ, Verrier ED, et al. The role of right ventricular systolic dysfunction and elevated intrapericardial pressure in the genesis of low output in experimental right ventricular infarction. Circulation 1982;65:513–22.

103.   Vonk-Noordegraaf A, Marcus JT, Gan CT, Boonstra A, Postmus PE. Interventricular mechanical asynchrony due to right ventricular pressure overload in pulmonary hypertension plays an important role in impaired left ventricular filling. Chest 2005;128:628S–630S. doi:10.1378/chest.128.6_suppl.628S.

104.   Marcus JT, Gan CT-J, Zwanenburg JJM, et al. Interventricular mechanical asynchrony in pulmonary arterial hypertension: left-to-right delay in peak shortening is related to right ventricular overload and left ventricular underfilling. J Am Coll Cardiol 2008;51:750–7. doi:10.1016/j.jacc.2007.10.041.

105.   Vonk Noordegraaf a, Marcus JT, Roseboom B, et al. The effect of right ventricular hypertrophy on left ventricular ejection fraction in pulmonary emphysema. Chest 1997;112:640–5.

106.   Shehata ML, Harouni AA, Skrok J, et al. Regional and global biventricular function in pulmonary arterial hypertension: a cardiac MR imaging study. Radiology 2013;266:114–22. doi:10.1148/radiol.12111599.

107.   Hardziyenka M, Campian ME, Reesink HJ, et al. Right ventricular failure following chronic pressure overload is associated with reduction in left ventricular mass: evidence for atrophic remodeling. J Am Coll Cardiol 2011;57:921–8. doi:10.1016/j.jacc.2010.08.648.

108. Boussuges A, Pinet C, Molenat F, et al. Left atrial and ventricular filling in chronic obstructive pulmonary disease. An echocardiographic and Doppler study. Am J Respir Crit Care Med 2000;162:670–5. doi:10.1164/ajrccm.162.2.9908056.

109. Aaron CP, Tandri H, Barr RG, et al. Physical activity and right ventricular structure and function. The MESA-Right Ventricle Study. Am J Respir Crit Care Med 2011;183:396–404. doi:10.1164/rccm.201003-0469OC.

110. Chahal H, Johnson C, Tandri H, et al. Relation of cardiovascular risk factors to right ventricular structure and function as determined by magnetic resonance imaging (results from the multi-ethnic study of atherosclerosis). Am J Cardiol 2010;106:110–6. doi:10.1016/j.amjcard.2010.02.022.

111. Chahal H, McClelland RL, Tandri H, et al. Obesity and right ventricular structure and function: the MESA-Right Ventricle Study. Chest 2012;141:388–95. doi:10.1378/chest.11-0172.

112. Kaufmann MR, Barr RG, Lima J a C, et al. Right ventricular morphology and the onset of dyspnea: the MESA-right ventricle study. PLoS One 2013;8:e56826. doi:10.1371/journal.pone.0056826.

113. Kawut SM, Barr RG, Lima J a C, et al. Right ventricular structure is associated with the risk of heart failure and cardiovascular death: the Multi-Ethnic Study of Atherosclerosis (MESA)--right ventricle study. Circulation 2012;126:1681–8. doi:10.1161/CIRCULATIONAHA.112.095216.

114. Cuttica MJ, Shah SJ, Rosenberg SR, et al. Right heart structural changes are independently associated with exercise capacity in non-severe COPD. PLoS One 2011;6:e29069. doi:10.1371/journal.pone.0029069.

115. Burgess MI, Mogulkoc N, Bright-Thomas RJ, et al. Comparison of echocardiographic markers of right ventricular function in determining prognosis in chronic pulmonary disease. J Am Soc Echocardiogr 2002;15:633–9.

116. Vivodtzev I, Tamisier R, Baguet J-P, et al. Arterial Stiffness in COPD. Chest 2014;145:861–75. doi:10.1378/chest.13-1809.

117. Fourie PR, Coetzee AR, Bolliger CT. Pulmonary artery compliance: its role in right ventricular-arterial coupling. Cardiovasc Res 1992;26:839–44.

118. Dalen JE, Haynes FW, Jr. FGH, et al. Cardiovascular responses to experimental pulmonary embolism. Am J Cardiol 1967;20:3–9. doi:http://dx.doi.org/10.1016/0002-9149(67)90104-X.

119. Lankhaar J-W, Westerhof N, Faes TJC, et al. Quantification of right ventricular afterload in patients with and without pulmonary hypertension. Am J Physiol Heart Circ Physiol 2006;291:H1731-7. doi:10.1152/ajpheart.00336.2006.

120. Piene H. Pulmonary arterial impedance and right ventricular function. Physiol Rev 1986;66:606–52.

121. O'Rourke MF. Vascular impedance in studies of arterial and cardiac function. Physiol Rev 1982;62:570–623.

122. Piene H, Sund T. Flow and power output of right ventricle facing load with variable input impedance. Am J Physiol 1979;237:H125–30.

123. Chemla D, Castelain V, Zhu K, et al. Estimating right ventricular stroke work and the pulsatile work fraction in pulmonary hypertension. Chest 2013;143:1343–50. doi:10.1378/chest.12-1880.

124. Saouti N, Westerhof N, Helderman F, et al. Right ventricular oscillatory power is a

constant fraction of total power irrespective of pulmonary artery pressure. Am J Respir Crit Care Med 2010;182:1315–20. doi:10.1164/rccm.200910-1643OC.

125.   Shin S, King CS, Brown a W, et al. Pulmonary artery size as a predictor of pulmonary hypertension and outcomes in patients with chronic obstructive pulmonary disease. Respir Med 2014;108:1626–32. doi:10.1016/j.rmed.2014.08.009.

126.   Wells JM, Washko GR, Han MK, et al. Pulmonary arterial enlargement and acute exacerbations of COPD. N Engl J Med 2012;367:913–21. doi:10.1056/NEJMoa1203830.

127.   Iyer AS, Wells JM, Vishin S, et al. CT Scan-Measured Pulmonary Artery to Aorta Ratio and Echocardiography for Detecting Pulmonary Hypertension in Severe COPD. Chest 2014;145:824–32. doi:10.1378/chest.13-1422.

128.   Wells JM, Iyer a. S, Rahaghi FN, et al. Pulmonary Artery Enlargement Is Associated With Right Ventricular Dysfunction and Loss of Blood Volume in Small Pulmonary Vessels in Chronic Obstructive Pulmonary Disease. Circ Cardiovasc Imaging 2015;8:e002546–e002546. doi:10.1161/CIRCIMAGING.114.002546.

129.   Tan W, Madhavan K, Hunter KS, Park D, Stenmark KR. Vascular stiffening in pulmonary hypertension: cause or consequence? (2013 Grover Conference series). Pulm Circ 2014;4:560–80. doi:10.1086/677370.

130.   Safar ME, Levy BI, Struijker-Boudier H. Current perspectives on arterial stiffness and pulse pressure in hypertension and cardiovascular diseases. Circulation 2003;107:2864–9. doi:10.1161/01.CIR.0000069826.36125.B4.

131.   Gorgulu S, Eren M, Uslu N, Ozer O, Nurkalem Z. The determinants of right ventricular function in patients with atrial septal defect. Int J Cardiol 2006;111:127–30. doi:10.1016/j.ijcard.2005.07.037.

132.   Scott D, Tan Y, Shandas R, Stenmark KR, Tan W. High pulsatility flow stimulates smooth muscle cell hypertrophy and contractile protein expression. Am J Physiol Lung Cell Mol Physiol 2013;304:L70-81. doi:10.1152/ajplung.00342.2012.

133.   Li M, Scott DE, Shandas R, Stenmark KR, Tan W. High pulsatility flow induces adhesion molecule and cytokine mRNA expression in distal pulmonary artery endothelial cells. Ann Biomed Eng 2009;37:1082–92. doi:10.1007/s10439-009-9684-3.

134.   Kang K-W, Chang H-J, Kim Y-J, et al. Cardiac magnetic resonance imaging-derived pulmonary artery distensibility index correlates with pulmonary artery stiffness and predicts functional capacity in patients with pulmonary arterial hypertension. Circ J 2011;75:2244–51. doi:10.1253/circj.CJ-10-1310.

135.   Gan CT-J, Lankhaar J-W, Westerhof N, et al. Noninvasively assessed pulmonary artery stiffness predicts mortality in pulmonary arterial hypertension. Chest 2007;132:1906–12. doi:10.1378/chest.07-1246.

136.   Mahapatra S, Nishimura R a, Sorajja P, Cha S, McGoon MD. Relationship of pulmonary arterial capacitance and mortality in idiopathic pulmonary arterial hypertension. J Am Coll Cardiol 2006;47:799–803. doi:10.1016/j.jacc.2005.09.054.

137.   Mahapatra S, Nishimura R a, Oh JK, McGoon MD. The prognostic value of pulmonary vascular capacitance determined by Doppler echocardiography in patients with pulmonary arterial hypertension. J Am Soc Echocardiogr 2006;19:1045–50. doi:10.1016/j.echo.2006.03.008.

138.   Rodés-Cabau J, Domingo E, Román A, et al. Intravascular ultrasound of the elastic

pulmonary arteries: a new approach for the evaluation of primary pulmonary hypertension. Heart 2003;89:311–5.

139. Dupont M, Mullens W, Skouri HN, et al. Prognostic role of pulmonary arterial capacitance in advanced heart failure. Circ Heart Fail 2012;5:778–85. doi:10.1161/CIRCHEARTFAILURE.112.968511.

140. Zuckerman BD, Orton EC, Stenmark KR, et al. Alteration of the pulsatile load in the high-altitude calf model of pulmonary hypertension. J Appl Physiol 1991;70:859–68.

141. Stevens GR, Garcia-Alvarez A, Sahni S, et al. RV dysfunction in pulmonary hypertension is independently related to pulmonary artery stiffness. JACC Cardiovasc Imaging 2012;5:378–87. doi:10.1016/j.jcmg.2011.11.020.

142. Castelain V, Hervé P, Lecarpentier Y, et al. Pulmonary artery pulse pressure and wave reflection in chronic pulmonary thromboembolism and primary pulmonary hypertension. J Am Coll Cardiol 2001;37:1085–92.

143. Sanz J, Kariisa M, Dellegrottaglie S, et al. Evaluation of pulmonary artery stiffness in pulmonary hypertension with cardiac magnetic resonance. JACC Cardiovasc Imaging 2009;2:286–95. doi:10.1016/j.jcmg.2008.08.007.

144. Lau EMT, Iyer N, Ilsar R, et al. Abnormal pulmonary artery stiffness in pulmonary arterial hypertension: in vivo study with intravascular ultrasound. PLoS One 2012;7:e33331. doi:10.1371/journal.pone.0033331.

145. Pasierski TJ, Starling RC, Binkley PF, Pearson AC. Echocardiographic evaluation of pulmonary artery distensibility. Chest 1993;103:1080–3.

146. Chantler PD, Lakatta EG, Najjar SS. Arterial-ventricular coupling: mechanistic insights into cardiovascular performance at rest and during exercise. J Appl Physiol 2008;105:1342–51. doi:10.1152/japplphysiol.90600.2008.

147. Kass DA. Age-related changes in venticular-arterial coupling: pathophysiologic implications. Heart Fail Rev 2002;7:51–62. doi:10.1023/A:1013749806227.

148. Sunagawa K, Maughan WL, Burkhoff D, Sagawa K. Left ventricular interaction with arterial load studied in isolated canine ventricle. Am J Physiol 1983;245:H773-80.

149. Kelly RP, Ting CT, Yang TM, et al. Effective arterial elastance as index of arterial vascular load in humans. Circulation 1992;86:513–21. doi:10.1161/01.CIR.86.2.513.

150. Kussmaul WG, Noordergraaf A, Laskey WK. Right ventricular-pulmonary arterial interactions. Ann Biomed Eng 1992;20:63–80. doi:10.1007/BF02368506.

151. Laffon E, Bernard V, Montaudon M, et al. Tuning of pulmonary arterial circulation evidenced by MR phase mapping in healthy volunteers. J Appl Physiol 2001;90:469–74.

152. Kuehne T, Yilmaz S, Steendijk P, et al. Magnetic resonance imaging analysis of right ventricular pressure-volume loops: in vivo validation and clinical application in patients with pulmonary hypertension. Circulation 2004;110:2010–6. doi:10.1161/01.CIR.0000143138.02493.DD.

153. Burkhoff D, Sagawa K. Ventricular efficiency predicted by an analytical model. Am J Physiol 1986;250:R1021–7.

154. Suga H, Igarashi Y, Yamada O, Goto Y. Mechanical efficiency of the left ventricle as a function of preload, afterload, and contractility. Heart Vessels 1985;1:3–8. doi:10.1007/BF02066480.

155. Najjar SS, Schulman SP, Gerstenblith G, et al. Age and gender affect ventricular-vascular coupling during aerobic exercise. J Am Coll Cardiol 2004;44:611–7.

doi:10.1016/j.jacc.2004.04.041.

156. Starling MR. Left ventricular-arterial coupling relations in the normal human heart. Am Heart J 1993;125:1659–66. doi:10.1016/0002-8703(93)90756-Y.

157. Hollander EH, Wang JJ, Dobson GM, Parker KH, Tyberg J V. Negative wave reflections in pulmonary arteries. Am J Physiol Heart Circ Physiol 2001;281:H895-902.

158. Little WC, Cheng CP. Left ventricular-arterial coupling in conscious dogs. Am J Physiol 1991;261:H70–6.

159. van den Horn GJ, Westerhof N, Elzinga G. Optimal power generation by the left ventricle. A study in the anesthetized open thorax cat. Circ Res 1985;56:252–61. doi:10.1161/01.RES.56.2.252.

160. Otsuki T, Maeda S, Iemitsu M, et al. Contribution of systemic arterial compliance and systemic vascular resistance to effective arterial elastance changes during exercise in humans. Acta Physiol (Oxf) 2006;188:15–20. doi:10.1111/j.1748-1716.2006.01596.x.

161. Otsuki T, Maeda S, Iemitsu M, et al. Systemic arterial compliance, systemic vascular resistance, and effective arterial elastance during exercise in endurance-trained men. Am J Physiol Regul Integr Comp Physiol 2008;295:R228-35. doi:10.1152/ajpregu.00009.2008.

162. Lalande S, Yerly P, Faoro V, Naeije R. Pulmonary vascular distensibility predicts aerobic capacity in healthy individuals. J Physiol 2012;590:4279–88. doi:10.1113/jphysiol.2012.234310.

163. Lankhaar J-W, Westerhof N, Faes TJC, et al. Pulmonary vascular resistance and compliance stay inversely related during treatment of pulmonary hypertension. Eur Heart J 2008;29:1688–95. doi:10.1093/eurheartj/ehn103.

164. Park S, Ha J-W, Shim CY, et al. Gender-related difference in arterial elastance during exercise in patients with hypertension. Hypertension 2008;51:1163–9. doi:10.1161/HYPERTENSIONAHA.107.106690.

165. Kubo K, Ge RL, Koizumi T, et al. Pulmonary artery remodeling modifies pulmonary hypertension during exercise in severe emphysema. Respir Physiol 2000;120:71–9.

166. Wang Z, Chesler NC. Pulmonary vascular wall stiffness: An important contributor to the increased right ventricular afterload with pulmonary hypertension. Pulm Circ 2011;1:212–23. doi:10.4103/2045-8932.83453.

167. Dias CA, Assad RS, Caneo LF, et al. Reversible pulmonary trunk banding. II. An experimental model for rapid pulmonary ventricular hypertrophy. J Thorac Cardiovasc Surg 2002;124:999–1006. doi:10.1067/mtc.2002.124234.

168. Nitenberg A, Antony I, Loiseau A. Left ventricular contractile performance, ventriculoarterial coupling, and left ventricular efficiency in hypertensive patients with left ventricular hypertrophy. Am J Hypertens 1998;11:1188–98. doi:10.1097/00004872-199917060-00025.

169. Bellofiore A, Roldán-Alzate A, Besse M, et al. Impact of acute pulmonary embolization on arterial stiffening and right ventricular function in dogs. Ann Biomed Eng 2013;41:195–204. doi:10.1007/s10439-012-0635-z.

170. Nitenberg A, Loiseau A, Antony I. Left ventricular mechanical efficiency in hypertensive patients with and without increased myocardial mass and with normal pump function. Am J Hypertens 2001;14:1231–8.

171. Sanz J, García-Alvarez A, Fernández-Friera L, et al. Right ventriculo-arterial coupling

in pulmonary hypertension: a magnetic resonance study. Heart 2012;98:238–43. doi:10.1136/heartjnl-2011-300462.

172.   Swift AJ, Rajaram S, Condliffe R, et al. Pulmonary artery relative area change detects mild elevations in pulmonary vascular resistance and predicts adverse outcome in pulmonary hypertension. Invest Radiol 2012;47:571–7. doi:10.1097/RLI.0b013e31826c4341.

173.   Kroeker EJ, Wood EH. Comparison of simultaneously recorded central and peripheral arterial pressure pulses during rest, exercise and tilted position in man. Circ Res 1955;3:623–32. doi:10.1161/01.RES.3.6.623.

174.   Laffon E, Laurent F, Bernard V, et al. Noninvasive assessment of pulmonary arterial hypertension by MR phase-mapping method. J Appl Physiol 2001;90:2197–202.

175.   Reiter G, Reiter U, Kovacs G, et al. Magnetic resonance-derived 3-dimensional blood flow patterns in the main pulmonary artery as a marker of pulmonary hypertension and a measure of elevated mean pulmonary arterial pressure. Circ Cardiovasc Imaging 2008;1:23–30. doi:10.1161/CIRCIMAGING.108.780247.

176.   Saba TS, Foster J, Cockburn M, Cowan M, Peacock AJ. Ventricular mass index using magnetic resonance imaging accurately estimates pulmonary artery pressure. Eur Respir J 2002;20:1519–24. doi:10.1183/09031936.02.00014602.

177.   Swift AJ, Rajaram S, Hurdman J, et al. Noninvasive estimation of PA pressure, flow, and resistance with CMR imaging: derivation and prospective validation study from the ASPIRE registry. JACC Cardiovasc Imaging 2013;6:1036–47. doi:10.1016/j.jcmg.2013.01.013.

178.   Roeleveld RJ, Marcus JT, Boonstra A, et al. A comparison of noninvasive MRI-based methods of estimating pulmonary artery pressure in pulmonary hypertension. J Magn Reson Imaging 2005;22:67–72. doi:10.1002/jmri.20338.

179.   Fisher MR, Forfia PR, Chamera E, et al. Accuracy of Doppler echocardiography in the hemodynamic assessment of pulmonary hypertension. Am J Respir Crit Care Med 2009;179:615–21. doi:10.1164/rccm.200811-1691OC.

180.   Pienn M, Kovacs G, Tscherner M, et al. Non-invasive determination of pulmonary hypertension with dynamic contrast-enhanced computed tomography: a pilot study. Eur Radiol 2014;24:668–76. doi:10.1007/s00330-013-3067-8.

181.   Muthurangu V, Taylor A, Andriantsimiavona R, et al. Novel method of quantifying pulmonary vascular resistance by use of simultaneous invasive pressure monitoring and phase-contrast magnetic resonance flow. Circulation 2004;110:826–34. doi:10.1161/01.CIR.0000138741.72946.84.

182.   Kuehne T, Yilmaz S, Schulze-Neick I, et al. Magnetic resonance imaging guided catheterisation for assessment of pulmonary vascular resistance: in vivo validation and clinical application in patients with pulmonary hypertension. Heart 2005;91:1064–9. doi:10.1136/hrt.2004.038265.

183.   Moral S, Fernández-Friera L, Stevens G, et al. New index α improves detection of pulmonary hypertension in comparison with other cardiac magnetic resonance indices. Int J Cardiol 2012;161:25–30. doi:10.1016/j.ijcard.2011.04.024.

184.   Sanz J, Kuschnir P, Rius T, et al. Pulmonary arterial hypertension: noninvasive detection with phase-contrast MR imaging. Radiology 2007;243:70–9. doi:10.1148/radiol.2431060477.

185.   Jardim C, Rochitte CE, Humbert M, et al. Pulmonary artery distensibility in

pulmonary arterial hypertension: an MRI pilot study. Eur Respir J 2007;29:476–81. doi:10.1183/09031936.00016806.

186.   Ertan C, Tarakci N, Ozeke O, Demir AD. Pulmonary artery distensibility in chronic obstructive pulmonary disease. Echocardiography 2013;30:940–4. doi:10.1111/echo.12170.

187.   Liu C-Y, Parikh M, Gomes AS, et al. Chronic Obstructive Pulmonary Disease (COPD) is associated with pulmonary artery stiffness - the MESA COPD study. J Cardiovasc Magn Reson 2013;15:O62. doi:10.1186/1532-429X-15-S1-O62.

188.   Milnor WR, Conti CR, Lewis KB, O'Rourke MF. Pulmonary arterial pulse wave velocity and impedance in man. Circ Res 1969;25:637–49. doi:10.1161/01.RES.25.6.637.

189.   Nakayama Y, Nakanishi N, Hayashi T, et al. Pulmonary artery reflection for differentially diagnosing primary pulmonary hypertension and chronic pulmonary thromboembolism. J Am Coll Cardiol 2001;38:214–8.

190.   Muthurangu V, Atkinson D, Sermesant M, et al. Measurement of total pulmonary arterial compliance using invasive pressure monitoring and MR flow quantification during MR-guided cardiac catheterization. Am J Physiol Heart Circ Physiol 2005;289:H1301-6. doi:10.1152/ajpheart.00957.2004.

191.   Kopeć G, Moertl D, Jankowski P, et al. Pulmonary artery pulse wave velocity in idiopathic pulmonary arterial hypertension. Can J Cardiol 2013;29:683–90. doi:10.1016/j.cjca.2012.09.019.

192.   Lau EMT, Abelson D, Dwyer N, et al. Assessment of ventriculo-arterial interaction in pulmonary arterial hypertension using wave intensity analysis. Eur Respir J 2014;43:1804–7. doi:10.1183/09031936.00148313.

193.   Ibrahim E-SH, Johnson KR, Miller AB, Shaffer JM, White RD. Measuring aortic pulse wave velocity using high-field cardiovascular magnetic resonance: comparison of techniques. J Cardiovasc Magn Reson 2010;12:26. doi:10.1186/1532-429X-12-26.

194.   Caro CG, Harrison GK. Observations on pulse wave velocity and pulsatile blood pressure in the human pulmonary circulation. Clin Sci 1962;23:317–29.

195.   Dwyer N, Yong AC, Kilpatrick D. Variable open-end wave reflection in the pulmonary arteries of anesthetized sheep. J Physiol Sci 2012;62:21–8. doi:10.1007/s12576-011-0182-7.

196.   Furuno Y, Nagamoto Y, Fujita M, et al. Reflection as a cause of mid-systolic deceleration of pulmonary flow wave in dogs with acute pulmonary hypertension: comparison of pulmonary artery constriction with pulmonary embolisation. Cardiovasc Res 1991;25:118–24.

197.   Grignola JC, Ginés F, Bia D, Armentano R. Improved right ventricular-vascular coupling during active pulmonary hypertension. Int J Cardiol 2007;115:171–82. doi:10.1016/j.ijcard.2006.03.007.

198.   Laskey WK, Ferrari VA, Palevsky HI, Kussmaul WG. Pulmonary artery hemodynamics in primary pulmonary hypertension. J Am Coll Cardiol 1993;21:406–12.

199.   Ben-Shlomo Y, Spears M, Boustred C, et al. Aortic pulse wave velocity improves cardiovascular event prediction: An individual participant meta-analysis of prospective observational data from 17,635 subjects. J Am Coll Cardiol 2014;63:636–46. doi:10.1016/j.jacc.2013.09.063.

200.   Asmar R, Benetos A, Topouchian J, et al. Assessment of arterial distensibility by automatic pulse wave velocity measurement. Validation and clinical application studies. Hypertension 1995;26:485–90. doi:10.1161/01.HYP.26.3.485.

201.   van der Heijden-Spek JJ, Staessen JA, Fagard RH, et al. Effect of age on brachial artery wall properties differs from the aorta and is gender dependent: a population study. Hypertension 2000;35:637–42. doi:10.1161/01.HYP.35.2.637.

202.   Cruickshank K, Riste L, Anderson SG, et al. Aortic pulse-wave velocity and its relationship to mortality in diabetes and glucose intolerance: an integrated index of vascular function? Circulation 2002;106:2085–90. doi:10.1161/01.CIR.0000033824.02722.F7.

203.   Bradlow WM, Gatehouse PD, Hughes RL, et al. Assessing normal pulse wave velocity in the proximal pulmonary arteries using transit time: a feasibility, repeatability, and observer reproducibility study by cardiovascular magnetic resonance. J Magn Reson Imaging 2007;25:974–81. doi:10.1002/jmri.20888.

204.   Westenberg JJM, van Poelgeest EP, Steendijk P, et al. Bramwell-Hill modeling for local aortic pulse wave velocity estimation: a validation study with velocity-encoded cardiovascular magnetic resonance and invasive pressure assessment. J Cardiovasc Magn Reson 2012;14:2. doi:10.1186/1532-429X-14-2.

205.   Joly L, Perret-Guillaume C, Kearney-Schwartz A, et al. Pulse wave velocity assessment by external noninvasive devices and phase-contrast magnetic resonance imaging in the obese. Hypertension 2009;54:421–6. doi:10.1161/HYPERTENSIONAHA.109.133645.

206.   Dogui A, Kachenoura N, Frouin F, et al. Consistency of aortic distensibility and pulse wave velocity estimates with respect to the Bramwell-Hill theoretical model: a cardiovascular magnetic resonance study. J Cardiovasc Magn Reson 2011;13:11. doi:10.1186/1532-429X-13-11.

207.   Peng H-H, Chung H-W, Yu H-Y, Tseng W-YI. Estimation of pulse wave velocity in main pulmonary artery with phase contrast MRI: preliminary investigation. J Magn Reson Imaging 2006;24:1303–10. doi:10.1002/jmri.20782.

208.   Ibrahim E-SH, Shaffer JM, White RD. Assessment of pulmonary artery stiffness using velocity-encoding magnetic resonance imaging: evaluation of techniques. Magn Reson Imaging 2011;29:966–74. doi:10.1016/j.mri.2011.04.012.

209.   Bogren HG, Klipstein RH, Mohiaddin RH, et al. Pulmonary artery distensibility and blood flow patterns: a magnetic resonance study of normal subjects and of patients with pulmonary arterial hypertension. Am Heart J 1989;118:990–9.

210.   Paz R, Mohiaddin RH, Longmore DB. Magnetic resonance assessment of the pulmonary arterial trunk anatomy, flow, pulsatility and distensibility. Eur Heart J 1993;14:1524–30.

211.   Stevens GR, Lala A, Sanz J, et al. Exercise performance in patients with pulmonary hypertension linked to cardiac magnetic resonance measures. J Heart Lung Transplant 2009;28:899–905. doi:10.1016/j.healun.2009.05.004.

212.   Revel M-P, Faivre J-B, Remy-Jardin M, et al. Pulmonary hypertension: ECG-gated 64-section CT angiographic evaluation of new functional parameters as diagnostic criteria. Radiology 2009;250:558–66. doi:10.1148/radiol.2502080315.

213.   Blanco I, Santos S, Gea J, et al. Sildenafil to improve respiratory rehabilitation outcomes in COPD: a controlled trial. Eur Respir J 2013;42:982–92.

doi:10.1183/09031936.00176312.

214.   Stolz D, Rasch H, Linka A, et al. A randomised, controlled trial of bosentan in severe COPD. Eur Respir J 2008;32:619–28. doi:10.1183/09031936.00011308.

215.   Badesch DB, Feldman J, Keogh A, et al. ARIES-3: ambrisentan therapy in a diverse population of patients with pulmonary hypertension. Cardiovasc Ther 2012;30:93–9. doi:10.1111/j.1755-5922.2011.00279.x.

216.   Goudie AR, Lipworth BJ, Hopkinson PJ, Wei L, Struthers AD. Tadalafil in patients with chronic obstructive pulmonary disease: a randomised, double-blind, parallel-group, placebo-controlled trial. Lancet Respir Med 2014;2:293–300. doi:10.1016/S2213-2600(14)70013-X.

217.   Blanco I, Gimeno E, Munoz PA, et al. Hemodynamic and gas exchange effects of sildenafil in patients with chronic obstructive pulmonary disease and pulmonary hypertension. Am J Respir Crit Care Med 2010;181:270–8. doi:10.1164/rccm.200907-0988OC.

218.   Toyama K, Sugiyama S, Oka H, et al. Combination treatment of rosuvastatin or atorvastatin, with regular exercise improves arterial wall stiffness in patients with coronary artery disease. PLoS One 2012;7:e41369. doi:10.1371/journal.pone.0041369.

219.   Rizos EC, Agouridis AP, Elisaf MS. The effect of statin therapy on arterial stiffness by measuring pulse wave velocity: a systematic review. Curr Vasc Pharmacol 2010;8:638–44. doi:10.2174/157016110792006950.

220.   Wright JL, Zhou S, Preobrazhenska O, et al. Statin reverses smoke-induced pulmonary hypertension and prevents emphysema but not airway remodeling. Am J Respir Crit Care Med 2011;183:50–8. doi:10.1164/rccm.201003-0399OC.

221.   Lee J-H, Lee D-S, Kim E-K, et al. Simvastatin inhibits cigarette smoking-induced emphysema and pulmonary hypertension in rat lungs. Am J Respir Crit Care Med 2005;172:987–93. doi:10.1164/rccm.200501-041OC.

222.   Reed RM, Iacono A, DeFilippis A, et al. Statin therapy is associated with decreased pulmonary vascular pressures in severe COPD. COPD 2011;8:96–102. doi:10.3109/15412555.2011.558545.

223.   Janda S, Park K, FitzGerald JM, Etminan M, Swiston J. Statins in COPD: a systematic review. Chest 2009;136:734–43. doi:10.1378/chest.09-0194.

224.   Lawes CMM, Thornley S, Young R, et al. Statin use in COPD patients is associated with a reduction in mortality: a national cohort study. Prim Care Respir J 2012;21:35–40. doi:10.4104/pcrj.2011.00095.

225.   Lee T-M, Lin M-S, Chang N-C. Usefulness of C-reactive protein and interleukin-6 as predictors of outcomes in patients with chronic obstructive pulmonary disease receiving pravastatin. Am J Cardiol 2008;101:530–5. doi:10.1016/j.amjcard.2007.09.102.

226.   Mascitelli L, Pezzetta F, Goldstein MR. Statins, vitamin D, and COPD. Chest 2010;137:742–3; author reply 743. doi:10.1378/chest.09-2219.

227.   Pearson M. Statins for COPD: a challenge to conventional beliefs? Prim Care Respir J 2012;21:5–7. doi:10.4104/pcrj.2012.00020.

228.   Kao MP, Ang DS, Gandy SJ, et al. Allopurinol benefits left ventricular mass and endothelial dysfunction in chronic kidney disease. J Am Soc Nephrol 2011;22:1382–9. doi:10.1681/ASN.2010111185.

229.   Kostka-Jeziorny K, Uruski P, Tykarski A. Effect of allopurinol on blood pressure and aortic compliance in hypertensive patients. Blood Press 2011;20:104–10. doi:10.3109/08037051.2010.532323.

230.   Khan F, George J, Wong K, et al. Allopurinol treatment reduces arterial wave reflection in stroke survivors. Cardiovasc Ther 2008;26:247–52. doi:10.1111/j.1755-5922.2008.00057.x.

231.   Butler R, Morris AD, Belch JJF, Hill A, Struthers AD. Allopurinol Normalizes Endothelial Dysfunction in Type 2 Diabetics With Mild Hypertension. Hypertension 2000;35:746–51. doi:10.1161/01.HYP.35.3.746.

232.   Cardillo C, Kilcoyne CM, Cannon RO, Quyyumi AA, Panza JA. Xanthine oxidase inhibition with oxypurinol improves endothelial vasodilator function in hypercholesterolemic but not in hypertensive patients. Hypertension 1997;30:57–63. doi:10.1161/01.HYP.30.1.57.

233.   Guthikonda S. Xanthine Oxidase Inhibition Reverses Endothelial Dysfunction in Heavy Smokers. Circulation 2003;107:416–21. doi:10.1161/01.CIR.0000046448.26751.58.

234.   Guthikonda S, Woods K, Sinkey CA, Haynes WG. Role of xanthine oxidase in conduit artery endothelial dysfunction in cigarette smokers. Am J Cardiol 2004;93:664–8. doi:10.1016/j.amjcard.2003.11.046.

235.   El Solh a a, Saliba R, Bosinski T, et al. Allopurinol improves endothelial function in sleep apnoea: a randomised controlled study. Eur Respir J 2006;27:997–1002. doi:10.1183/09031936.06.00101005.

236.   Sharma B, Neilan TG, Kwong RY, et al. Evaluation of right ventricular remodeling using cardiac magnetic resonance imaging in co-existent chronic obstructive pulmonary disease and obstructive sleep apnea. COPD 2013;10:4–10. doi:10.3109/15412555.2012.719050.

237.   Hoshikawa Y, Ono S, Suzuki S, et al. Generation of oxidative stress contributes to the development of pulmonary hypertension induced by hypoxia. J Appl Physiol 2001;90:1299–306.

238.   Jankov RP, Kantores C, Pan J, Belik J. Contribution of xanthine oxidase-derived superoxide to chronic hypoxic pulmonary hypertension in neonatal rats. Am J Physiol Lung Cell Mol Physiol 2008;294:L233-45. doi:10.1152/ajplung.00166.2007.

239.   Dopp JM, Philippi NR, Marcus NJ, et al. Xanthine oxidase inhibition attenuates endothelial dysfunction caused by chronic intermittent hypoxia in rats. Respiration 2011;82:458–67. doi:10.1159/000329341.

240.   Williams AL, Chen L, Scharf SM. Effects of allopurinol on cardiac function and oxidant stress in chronic intermittent hypoxia. Sleep Breath 2010;14:51–7. doi:10.1007/s11325-009-0279-x.

241.   Kjaeve J, Veel T, Bjertnaes L. Allopurinol inhibits hypoxic pulmonary vasoconstriction. Role of toxic oxygen metabolites. Acta Anaesthesiol Scand 1990;34:384–8.

242.   Ichinose M, Sugiura H, Yamagata S, et al. Xanthine oxidase inhibition reduces reactive nitrogen species production in COPD airways. Eur Respir J 2003;22:457–61. doi:10.1183/09031936.03.00052002.

243.   Takeda Y, Miyamori I, Yoneda T, et al. Regulation of aldosterone synthase in human vascular endothelial cells by angiotensin II and adrenocorticotropin. J Clin

Endocrinol Metab 1996;81:2797–800.

244. Davies J, Gavin A, Band M, Morris A, Struthers A. Spironolactone reduces brachial pulse wave velocity and PIIINP levels in hypertensive diabetic patients. Br J Clin Pharmacol 2005;59:520–3. doi:10.1111/j.1365-2125.2005.02363.x.

245. Edwards NC, Steeds RP, Stewart PM, Ferro CJ, Townend JN. Effect of spironolactone on left ventricular mass and aortic stiffness in early-stage chronic kidney disease: a randomized controlled trial. J Am Coll Cardiol 2009;54:505–12. doi:10.1016/j.jacc.2009.03.066.

246. Maron BA, Zhang Y-Y, White K, et al. Aldosterone Inactivates the Endothelin-B Receptor via a Cysteinyl Thiol Redox Switch to Decrease Pulmonary Endothelial Nitric Oxide Levels and Modulate Pulmonary Arterial Hypertension. Circulation 2012;126:963–74. doi:10.1161/CIRCULATIONAHA.112.094722.

247. Elinoff JM, Rame JE, Forfia PR, et al. A pilot study of the effect of spironolactone therapy on exercise capacity and endothelial dysfunction in pulmonary arterial hypertension: study protocol for a randomized controlled trial. Trials 2013;14:91. doi:10.1186/1745-6215-14-91.

248. Timms RM, Khaja FU, Williams GW. Hemodynamic response to oxygen therapy in chronic obstructive pulmonary disease. Ann Intern Med 1985;102:29–36.

249. Bartels MN, Jelic S, Basner RC, et al. Supplemental oxygen increases arterial stiffness in chronic obstructive pulmonary disease. Respir Med 2004;98:84–9.

250. Pfeifer H. A short history of nuclear magnetic resonance spectroscopy and of its early years in Germany. Magn Reson Chem 1999;159:154–9. doi:10.1002/(SICI)1097-458X(199912)37:13<S154::AID-MRC571>3.0.CO;2-0.

251. Ridgway JP. Cardiovascular magnetic resonance physics for clinicians: part I. J Cardiovasc Magn Reson 2010;12:71. doi:10.1186/1532-429X-12-71.

252. McRobbie DW, Moore E a, Graves MJ, Prince MR. MRI : From Picture to Proton. 2nd ed. Cambridge University Press; 2007. doi:http://dx.doi.org/10.1017/CBO9780511545405.

253. Alfakih K, Plein S, Thiele H, et al. Normal human left and right ventricular dimensions for MRI as assessed by turbo gradient echo and steady-state free precession imaging sequences. J Magn Reson Imaging 2003;17:323–9. doi:10.1002/jmri.10262.

254. Nayak KS, Nielsen J-F, Bernstein M a., et al. Cardiovascular magnetic resonance phase contrast imaging. J Cardiovasc Magn Reson 2015;17:71. doi:10.1186/s12968-015-0172-7.

255. Miller MR, Hankinson J, Brusasco V, et al. Standardisation of spirometry. Eur Respir J 2005;26:319–38. doi:10.1183/09031936.05.00034805.

256. Crapo R, Casaburi R, Coates A. ATS statement: guidelines for the six-minute walk test. Am J Respir Crit Care Med 2002;166:111–7. doi:10.1164/ajrccm.166.1.at1102.

257. Sciurba F, Criner GJ, Lee SM, et al. Six-Minute Walk Distance in Chronic Obstructive Pulmonary Disease: Reproducibility and Effect of Walking Course Layout and Length. Am J Respir Crit Care Med 2003;167:1522–7. doi:10.1164/rccm.200203-166OC.

258. Schulz-Menger J, Bluemke D a, Bremerich J, et al. Standardized image interpretation and post processing in cardiovascular magnetic resonance: Society for Cardiovascular Magnetic Resonance (SCMR) board of trustees task force on standardized post processing. J Cardiovasc Magn Reson 2013;15:35.

doi:10.1186/1532-429X-15-35.

259.   van de Veerdonk MC, Dusoswa S a, Tim Marcus J, et al. The importance of trabecular hypertrophy in right ventricular adaptation to chronic pressure overload. Int J Cardiovasc Imaging 2013;30:357–65. doi:10.1007/s10554-013-0338-z.

260.   Dogui A, Redheuil A, Lefort M, et al. Measurement of aortic arch pulse wave velocity in cardiovascular MR: Comparison of transit time estimators and description of a new approach. J Magn Reson Imaging 2011;33:1321–9. doi:10.1002/jmri.22570.

261.   Quail MA, Knight DS, Steeden J a, et al. Noninvasive pulmonary artery wave intensity analysis in pulmonary hypertension. Am J Physiol Heart Circ Physiol 2015;308:H1603-11. doi:10.1152/ajpheart.00480.2014.

262.   Davies JE, Whinnett ZI, Francis DP, et al. Use of simultaneous pressure and velocity measurements to estimate arterial wave speed at a single site in humans. Am J Physiol Heart Circ Physiol 2006;290:H878–85. doi:10.1152/ajpheart.00751.2005.

263.   van der Bom T, Winter MM, Bouma BJ, et al. Effect of valsartan on systemic right ventricular function: a double-blind, randomized, placebo-controlled pilot trial. Circulation 2013;127:322–30. doi:10.1161/CIRCULATIONAHA.112.135392.

264.   Wilkins MR, Ali O, Bradlow W, et al. Simvastatin as a Treatment for Pulmonary Hypertension Trial (SiPHT). Am J Respir Crit Care Med 2010;181:1106–13. doi:10.1164/rccm.200911-1699OC.

265.   Bradlow WM, Hughes ML, Keenan NG, et al. Measuring the heart in pulmonary arterial hypertension (PAH): implications for trial study size. J Magn Reson Imaging 2010;31:117–24. doi:10.1002/jmri.22011.

266.   Weir-McCall JR, Struthers AD, Lipworth BJ, Houston JG. The role of pulmonary arterial stiffness in COPD. Respir Med 2015;109:1381–90. doi:10.1016/j.rmed.2015.06.005.

267.   Saouti N, Westerhof N, Helderman F, et al. RC time constant of single lung equals that of both lungs together: a study in chronic thromboembolic pulmonary hypertension. Am J Physiol Heart Circ Physiol 2009;297:H2154-60. doi:10.1152/ajpheart.00694.2009.

268.   Forouzan O, Warczytowa J, Wieben O, François CJ, Chesler NC. Non-invasive measurement using cardiovascular magnetic resonance of changes in pulmonary artery stiffness with exercise. J Cardiovasc Magn Reson 2015;17:109. doi:10.1186/s12968-015-0213-2.

269.   Domingo E, Grignola JC, Aguilar R, et al. Impairment of pulmonary vascular reserve and right ventricular systolic reserve in pulmonary arterial hypertension. BMC Pulm Med 2014;14:69. doi:10.1186/1471-2466-14-69.

270.   Dawes TJW, Gandhi A, de Marvao A, et al. Pulmonary Artery Stiffness Is Independently Associated with Right Ventricular Mass and Function: A Cardiac MR Imaging Study. Radiology 2016;280:398–404. doi:10.1148/radiol.2016151527.

271.   Poon CY, Edwards JM, Evans CJ, et al. Assessment of pulmonary artery pulse wave velocity in children: an MRI pilot study. Magn Reson Imaging 2013;31:1690–4. doi:10.1016/j.mri.2013.08.006.

272.   Poon CY, Watkins WJ, Evans CJ, et al. Pulmonary arterial response to hypoxia in survivors of chronic lung disease of prematurity. Arch Dis Child - Fetal Neonatal Ed 2015:fetalneonatal-2015-309015. doi:10.1136/archdischild-2015-309015.

273.   Wells JM, Iyer AS, Rahaghi FN, et al. Pulmonary artery enlargement is associated

with right ventricular dysfunction and loss of blood volume in small pulmonary vessels in chronic obstructive pulmonary disease. Circ Cardiovasc Imaging 2015;8. doi:10.1161/CIRCIMAGING.114.002546.

274.   Kawut SM, Poor HD, Parikh M a., et al. Cor Pulmonale Parvus in Chronic Obstructive Pulmonary Disease and Emphysema. J Am Coll Cardiol 2014;64:2000–9. doi:10.1016/j.jacc.2014.07.991.

275.   Swift AJ, Rajaram S, Condliffe R, et al. Diagnostic accuracy of cardiovascular magnetic resonance imaging of right ventricular morphology and function in the assessment of suspected pulmonary hypertension results from the ASPIRE registry. J Cardiovasc Magn Reson 2012;14:40. doi:10.1186/1532-429X-14-40.

276.   Grau M, Barr RG, Lima J a, et al. Percent emphysema and right ventricular structure and function: the Multi-Ethnic Study of Atherosclerosis-Lung and Multi-Ethnic Study of Atherosclerosis-Right Ventricle Studies. Chest 2013;144:136–44. doi:10.1378/chest.12-1779.

277.   Watz H, Waschki B, Meyer T, et al. Decreasing cardiac chamber sizes and associated heart dysfunction in COPD: Role of hyperinflation. Chest 2010;138:32–8. doi:10.1378/chest.09-2810.

278.   Fenster BE, Holm KE, Weinberger HD, et al. Right ventricular diastolic function and exercise capacity in COPD. Respir Med 2015;109:1287–92. doi:10.1016/j.rmed.2015.09.003.

279.   López-Sánchez M, Muñoz-Esquerre M, Huertas D, et al. High Prevalence of Left Ventricle Diastolic Dysfunction in Severe COPD Associated with A Low Exercise Capacity: A Cross-Sectional Study. PLoS One 2013;8:e68034. doi:10.1371/journal.pone.0068034.

280.   Stone IS, Barnes NC, James W-Y, et al. Lung Deflation and Cardiovascular Structure and Function in Chronic Obstructive Pulmonary Disease. A Randomized Controlled Trial. Am J Respir Crit Care Med 2016;193:717–26. doi:10.1164/rccm.201508-1647OC.

281.   Kaess BM, Rong J, Larson MG, et al. Aortic stiffness, blood pressure progression, and incident hypertension. JAMA 2012;308:875–81. doi:10.1001/2012.jama.10503.

282.   Weir-McCall JR, Kamalasanan A, Cassidy DB, et al. Assessment of proximal pulmonary arterial stiffness using magnetic resonance imaging: effects of technique, age and exercise. BMJ Open Respir Res 2016;3:e000149. doi:10.1136/bmjresp-2016-000149.

283.   Anthonisen NR, Skeans MA, Wise RA, et al. The effects of a smoking cessation intervention on 14.5-year mortality: a randomized clinical trial. Ann Intern Med 2005;142:233–9.

284.   McGarvey LP, John M, Anderson JA, Zvarich M, Wise RA. Ascertainment of cause-specific mortality in COPD: operations of the TORCH Clinical Endpoint Committee. Thorax 2007;62:411–5. doi:10.1136/thx.2006.072348.

285.   Vestbo J, Anderson JA, Brook RD, et al. Fluticasone furoate and vilanterol and survival in chronic obstructive pulmonary disease with heightened cardiovascular risk (SUMMIT): a double-blind randomised controlled trial. Lancet 2016;387:1817–26. doi:10.1016/S0140-6736(16)30069-1.

286.   Taylor F, Huffman MD, Macedo AF, et al. Statins for the primary prevention of cardiovascular disease. Cochrane Database Syst Rev 2013;1:CD004816.

doi:10.1002/14651858.CD004816.pub5.

287.   Rodrigues JCL, Amadu AM, Dastidar AG, et al. Comprehensive characterisation of hypertensive heart disease left ventricular phenotypes. Heart 2016;0:1–9. doi:10.1136/.

288.   Cinarka H, Kayhan S, Gumus A, et al. Arterial Stiffness Measured Via Carotid Femoral Pulse Wave Velocity Is Associated With Disease Severity in COPD. Respir Care 2014;59:274–80. doi:10.4187/respcare.02621.

289.   Vanfleteren LEGW, Spruit MA, Groenen MTJ, et al. Arterial stiffness in patients with COPD: the role of systemic inflammation and the effects of pulmonary rehabilitation. Eur Respir J 2014;43:1306–15. doi:10.1183/09031936.00169313.

290.   Bhatt SP, Cole AG, Wells JM, et al. Determinants of arterial stiffness in COPD. BMC Pulm Med 2014;14:1. doi:10.1186/1471-2466-14-1.

291.   Short PM, Anderson WJ, Elder DHJ, Struthers AD, Lipworth BJ. Impact of Left Ventricular Hypertrophy on Survival in Chronic Obstructive Pulmonary Disease. Lung 2015;193:487–95. doi:10.1007/s00408-015-9724-8.

292.   Brandts A, van Elderen SGC, Westenberg JJM, et al. Association of aortic arch pulse wave velocity with left ventricular mass and lacunar brain infarcts in hypertensive patients: assessment with MR imaging. Radiology 2009;253:681–8. doi:10.1148/radiol.2533082264.

293.   Schillaci G, Mannarino MR, Pucci G, et al. Age-specific relationship of aortic pulse wave velocity with left ventricular geometry and function in hypertension. Hypertension 2007;49:317–21. doi:10.1161/01.HYP.0000255790.98391.9b.

294.   Short PM, Lipworth SIW, Elder DHJ, Schembri S, Lipworth BJ. Effect of beta blockers in treatment of chronic obstructive pulmonary disease: a retrospective cohort study. BMJ 2011;342:d2549. doi:10.1136/bmj.d2549.

295.   Bhatt SP, Wells JM, Kinney GL, et al. β-Blockers are associated with a reduction in COPD exacerbations. Thorax 2016;71:8–14. doi:10.1136/thoraxjnl-2015-207251.

296.   Vulliémoz S, Stergiopulos N, Meuli R. Estimation of local aortic elastic properties with MRI. Magn Reson Med 2002;47:649–54. doi:10.1002/mrm.10100.

297.   Polkey MI, Spruit MA, Edwards LD, et al. Six-Minute-Walk Test in Chronic Obstructive Pulmonary Disease. Am J Respir Crit Care Med 2013;187:382–6. doi:10.1164/rccm.201209-1596OC.

298.   Marcus JT, Vonk Noordegraaf A, De Vries PM, et al. MRI evaluation of right ventricular pressure overload in chronic obstructive pulmonary disease. J Magn Reson Imaging 1998;8:999–1005.

299.   van Gestel AJR, Steier J. Autonomic dysfunction in patients with chronic obstructive pulmonary disease (COPD). J Thorac Dis 2010;2:215–22. doi:10.3978/j.issn.2072-1439.2010.02.04.5.

300.   Harvey RE, Barnes JN, Hart ECJ, et al. Influence of Sympathetic Nerve Activity on Aortic Hemodynamics and Pulse Wave Velocity in Women. Am J Physiol - Hear Circ Physiol 2016.

301.   Sasano N, Vesely AE, Hayano J, et al. Direct effect of Pa(CO2) on respiratory sinus arrhythmia in conscious humans. Am J Physiol Heart Circ Physiol 2002;282:H973-6. doi:10.1152/ajpheart.00554.2001.

302.   Michael Wells J, Morrison JB, Bhatt SP, Nath H, Dransfield MT. Pulmonary artery enlargement is associated with cardiac injury during severe exacerbations of COPD.

Chest 2016;149:1197–204. doi:10.1378/chest.15-1504.

303.   Markl M, Wallis W, Brendecke S, et al. Estimation of global aortic pulse wave velocity by flow-sensitive 4D MRI. Magn Reson Med 2010;63:1575–82. doi:10.1002/mrm.22353.

304.   Markl M, Schnell S, Wu C, et al. Advanced flow MRI: Emerging techniques and applications. Clin Radiol 2016;71. doi:10.1016/j.crad.2016.01.011.

Conference Presentations and Publications

Weir-McCall JR, Struthers AD, Lipworth BJ, Houston JG. Cardiac remodeling in COPD: An effect of reduced preload or increased afterload?

    ECR, Vienna 2017

Weir-McCall JR, Kamalasanan A, Cassidy DB, Struthers AD, Lipworth BJ, Houston JG. Assessment of proximal pulmonary arterial stiffness using magnetic resonance imaging: Effects of technique, age and exercise

    ESCR, Krakow 2016

Weir-McCall JR, Struthers AD, Lipworth BJ, Houston JG. The role of pulmonary arterial stiffness in COPD. *Respir Med*. 2015 Jun 12. pii: S0954-6111(15)30008-1. doi: 10.1016/j.rmed.2015.06.005

Weir-McCall JR, Kamalasanan A, Cassidy DB, Struthers AD, Lipworth BJ, Houston JG. Assessment of proximal pulmonary arterial stiffness using magnetic resonance imaging: Effects of technique, age and exercise. *BMJ Open Resp Res* 2016;3:e000149 doi:10.1136/bmjresp-2016-00014

APPENDIX A: MRI STUDY PROTOCOLS

Localisers.
To repeat localisers with the patient in the isocentre.
Further localisers: VLA, HLA, SAX
HASTE: Axial and coronal, free breathing
Cine imaging using trueFISP. Matrix 256 x 80% All images to be slice thickness of 8 mm, 25% distance factor. Field of view altered to minimum, according to patient's size in all scans. Segments altered according to heart rate: <70 beats per minute, 14 segments, 70 to 80 beats per minute, 12 segments, 80 to 100 beats per minute, 11 segments. Number of phases for image construction=30. 4 chamber view. 2 chamber view. Complete ventricular short axis coverage. First slice planned at mitral valve annulus, perpendicular to inter-ventricular septum passing through the atrioventricular grooves. Ensure also covers from tricuspid valve to apex of right ventricle, not just left ventricle.
TAGGING: (3 short axis + 1 long axis 4C) Sequence is Grid, 3 slices using single breath hold sequence Segments 7-11 depending on heart rate (TR 35-50ms) IPAT factor 2 unless poor signal to noise 3 short axis planned in mid-systole from the 4/3 chambers. Mid-slice to be planned at mid-point between mitral valve tips and apex. Basal slice should be below the tips of the mitral valve and does not include any left ventricular outflow tract. Distance factor altered to apical slice below papillary muscles in diastole,

distance factor approximately 100 to 200%. 1 long-axis (4C view)
Cine imaging using trueFISP. Matrix 256 x 80% All images to be slice thickness of 8 mm. Field of view altered to minimum, according to patient's size in all scans. Segments altered according to heart rate: <70 beats per minute, 14 segments, 70 to 80 beats per minute, 12 segments, 80 to 100 beats per minute, 11 segments. Number of phases for image construction=30.   RVOT cine RVOT orthogonal view RV free wall   Main PA short axis (planned from RVOT and ortho view above valve leaflet tips)

High temporal resolution phase contrast images:
 	
Main PA using position from the main PA cine sequence
 	
    - High temporal resolution
 	
    - Repeat same sequence with 5ms delay
 	
Basal ventricular short axis through the tricuspid and mitral valve
 	
Free breathing. Venc 150cm/s. **Document HR.**

Sagittal oblique to include ascending aorta, aortic arch and descending aorta If artefact switch to FLASH/gradient echo
High temporal resolution aortic cine at PA bifurcation. **Simultaneous BP and document pulse pressure**.
Aorta flow measured at level of pulmonary artery bifurcation Venc 150cm/s.
Aorta flow measured at diaphragm just below level of the heart.

FLASH rest perfusion.

Check perfusion scan without contrast for optimised field of view/artefact.

Smallest field of view without any wrap.

Contrast to be injected at 0.04mmol/kg, 5 ml per second, followed by a 20 ml flush. Injection to commence after giving breathe IN instruction.

Inject, then breathe out. Acquisition starts.

3 short axis slices depending on heart rate:

Matrix 224 x 80%, parallel imaging factor x 2

<70 beats per minute 40 acquisitions

70-90 beats per minute 50 acquisitions

>90 beats per minute 60 acquisitions.

NB If HR > 110 may default to 2 beat trigger- reduce matrix to 192

The patient is instructed to breathe quietly, when they can no longer hold their breath.

Repeat ventricular short axis coverage.

First slice planned at mitral valve annulus, perpendicular to inter-ventricular septum passing through the atrioventricular grooves. Ensure also covers tricuspid valve.

Repeat Aorta flow - measured at pulmonary artery bifurcation, descending aorta. Copy slice position 14. Venc 150cm/s.

Repeat Aorta flow measured at diaphragm just below level of the heart.

Delayed contrast imaging inversion recovery flash sequence.

TI scout copying mid sax image position.

Complete short axis coverage copy in image positions from SAX cines.

Use phase-sensitive sequence.

Capture RR interval. Set TR ~100 msec less than RR interval.

Alter TI by 10 msec approximately every 1 to 2 slices.

If slice shows doubtful enhancement, repeat slice, and swap phase encoding direction. Also plan modified 2- chamber through inferior insertion point and anterior insertion point of RV to septum if LGE seen here

4 chamber, 2 chamber, 3 chamber, SAX stack.

Appendix B: Patient Information Sheet

PARTICIPANT INFORMATION SHEET

Title: **The role of pulmonary arterial stiffness on right ventricular remodeling in COPD.**

Chief Investigator: Prof Graeme Houston

Prinicipal Investigator: Dr Jonathan Weir-McCall

Department of Clinical Radiology

Diagnostic Group

We invite you to participate in a study looking at blood vessel stiffness within the blood vessels supplying the lungs. This study forms the core part of Dr Weir-McCall's PhD research. Before you decide whether or not you wish to participate, we are providing you with the following information. Please read it carefully and do not hesitate to ask any questions you may have. We will provide you with any further information you may ask for now and later. You may also wish to discuss taking part in the study with friends or relatives before deciding whether to take part. If you agree to take part, your GP will be informed of your participation as long as you are happy for this to be done.

Thank you for reading this.

What is the purpose of this study?

Objectives: To investigate the ability of MRI to assess the heart and blood vessels supplying the lung (pulmonary arteries) in patients with smoking induced lung disease (chronic obstructive pulmonary disease), and to improve the accuracy of this assessment.

Design: We will use MRI to compare the heart muscle and the blood flow within the blood vessels which supply the lungs in patients with and without lung disease. 30 healthy volunteers and 90 participants with lung disease will be scanned at baseline with a second scan at 1 year.

Expected outcomes: The pulmonary arteries will be stiffer in patients with COPD. Injected contrast will improve visualisation of the heart muscle and therefore improve the accuracy of MRI assessment.

Anticipated healthcare outcomes: Increased knowledge about the blood vessels in COPD could allow earlier detection of heart disease and provide new avenues of treatment for this difficult to treat disease.

Do I have to take part in this study?

It is up to you to decide whether or not to take part. You can refuse to take part and this will not affect your treatment in any way. If you agree to take part but change your mind at a later date you can withdraw immediately and do not have to give a reason for doing so. You can do this by contacting Dr Jonathan Weir-McCall. Should you withdraw from the study, all identifiable data collected would be withdrawn and destroyed. Data which is not identifiable to the research team may be retained. Please keep this information sheet. If you have any questions or doubts, please contact us.

Why have I been chosen?

You have been chosen to take part in this study as you have been previously diagnosed with COPD, which we are interested in investigating further to discover its effects on blood vessel stiffness.

What will happen to me if I take part?

If after reading through this information sheet you are happy to take part in the study please return a reply slip indicating whether or not you would be interested in taking part in the study. If you are interested, the researcher will contact you to discuss the study further and invite you to attend a screening visit, after which, if both you and the researchers are happy to progress, you will be asked to attend two further visits with a 1 year gap between these. All visits will be held at Ninewells Hospital.

Visit 1: At this visit we will talk through the project, answer any questions you might have and obtain your written permission to take part in this study. After this we will take a thorough medical history, and do a simple assessment of the heart using ultrasound (also called an echocardiogram). This visit is to make sure you are happy to take part in the study, and to make sure there are no conditions that might mean we cannot include you in the study.

Visit 2: This will be shortly after Visit 1. This will take about half a day, and will occur at Ninewells Hospital. This will involve a lung function test, an exercise test (how far you can walk in 6 minutes), blood tests and a MRI exam of the heart (which is the crucial part of the study). Some of the blood taken will be stored and used for future analysis as long as you are happy for this to occur.

Visit 3: This will occur 1 year after Visit 2, and will involve exactly the same tests. This is to see how the heart adapts over time, and whether any of the blood tests, or the stiffness of the arteries to the lungs, helps us predict this.

If further information about your condition is revealed it will be passed to the doctor who looks after your COPD.

The data held on the Study Database will be analysed by statistics to assess the factors affecting blood vessel stiffness and how this affects cardiovascular disease.

Reasonable travel expenses will be reimbursed, should you need to travel to take part in the study.

What will the MRI scan involve
The MRI scan will be performed at the Clinical Research Centre at Ninewells Hospital. Each examination takes approximately 60-75 minutes, and involves lying on a table that slides into the scanner. Prior to the scan, we will place a cannula into a vein in your

arm, this is to allow an injection of contrast during the scan to help acquire some of the images. The cannula insertion is often experienced as a sharp scratch as it goes into the vein after which the pain settles. Occasionally this will leave a bruise at this site. We will also take some blood from the cannula at the same time as this. As this is a study of your heart we will monitor your heart rate during the procedure, and this would require us to attach three small leads to your chest along with an MRI coil which is placed over the chest that collects the images. We will discuss this in detail with you beforehand. This equipment does not hurt you or cause you pain in anyway.

Volunteer with an MRI coil on their chest about to go into the MRI scanner

During the scan you will be asked to remain very still, and as the process can be noisy you will be given ear protection in the form of headphones. The headphones will also allow you to listen to some music during the scan as an aid to relaxation. The scan is painless, although it is possible that you might experience a minor amount of discomfort such as minor 'pins and needles' as a result of lying still on the MRI table. The results of your MRI examinations will be confidential. It is unlikely, but possible, that these images will reveal an abnormality that you were unaware of. Should this happen, the Consultant Radiologist will discuss the findings with you, request your permission to inform your GP and recommend whether further investigations are appropriate or not. Thereafter your MRI scan will be irreversibly anonymised once the Radiologist has checked it.

Some of the scans will involve you having to hold your breath for short periods of time. In these instances, full breathing instructions will be provided to you by the radiographers during the MRI scan.

Are there any safety implications?

MRI is recognized as a safe imaging modality and there are no known biological or health safety concerns surrounding its use. However you will be asked whether you are (or might be) pregnant, and if you are (or think you might be) then we would not include you in this study.

A member of staff will ask you a series of important questions to ensure that you have no metallic implants (e.g. pacemaker, internal clips, or other similar devices) inside your body before you enter the strong magnetic field. You will also be instructed to remove all metal objects such as watches, keys, coins etc, and we will also ask you to change into a hospital gown for the duration of the examination.

The contrast used in the study is widely used in routine clinical MRI scans. Most people experience no side effects from this, but some can experience a slight discomfort at the injection site, and a small number of people will have side effects including itchiness, headache or nausea.

Incidental findings

Since this research involves MRI scans it is quite possible that it may show up findings other than those under investigation. These are what we call "incidental findings" the significance of which is often unclear or, indeed, something that the researchers themselves are not qualified to interpret or act upon, if that is the case, expert advice will be sought. It is very important that you understand how "incidental findings" will be dealt with in this research and you will be asked to give your specific consent to this in the Consent Form that you will sign if you agree to take part.

It is normal practice for us to inform your GP of your participation in this study. Further, in the event that we find an incidental finding in your images we would wish to provide you and your GP with this information in order to plan further medical care. By signing the informed consent declaration you agree to us taking this course of action should this unlikely situation arise.

It is important that you understand what is intended before you sign the Consent Form in which case you may wish to discuss this further with a member of the research team or with other independent parties before proceeding.

What if I am harmed by taking part?

This study is sponsored by the University of Dundee and NHS Tayside.

If you have a complaint about your participation in the study you should first talk to a researcher involved in your care. You can ask to speak to a senior member of the research team or the Complaints Officer for NHS Tayside.

In the event that something goes wrong and you are harmed during the study there are no special compensation arrangements. If you are harmed and this is due to someone's negligence then you may have grounds for a legal action for compensation against the University of Dundee or NHS Tayside but you may have to pay your legal costs. The normal National Health Service complaints mechanisms will still be available to you (if appropriate):

Complaints and Claims Manager

Complaints and Advice Team

Level 7, Ninewells Hospital

Dundee DD1 9SY

Freephone: 0800 027 5507

Email: nhstaysidecomplaints@thb.scot.nhs.uk

Will I receive any payment?

Reasonable travel costs will be reimbursed, but no extra payments are provided for assistance with this study, even if the images or data are used in research that leads to an important new MRI development.

What are the advantages of taking part?

There are no direct benefits to taking part, but the information we obtain will add to our understanding of the lungs and heart, and will be be used to optimize the scanner performance in support of better clinical practice and future patient studies. If the results of the studies are sufficiently interesting to us, we may publish the results in journals or present them at conferences. You will not be identified in any of the published information.

Insurance Implications

Some insurance companies consider that participation in medical research such as this is a 'material fact' which should be mentioned in any proposal for health-related insurance, or which could influence their judgment in consideration of claims made under existing insurance policies. You should check that participation in this research does not affect any policy that you might be thinking about taking out or any existing policy.

What confidential data may be collected, and how will it be used?

We will need to record certain personal details such as your name, gender, height, weight, medical number (CHI), and date of birth in addition to the MR images that we acquire. NHS Tayside MRI Radiologists,Radiographers and Clinical Scientists will have controlled access to this information.   Your data will be allocated a study identifier, and will be anonymised for subsequent research analysis. It is standard procedure for your resulting MR images to be stored securely for a period of at least 5 years, and we will request informed consent from you to use the images anonymously during this time for research, education, technical development and quality control at NHS Tayside, University of Dundee or at other collaborative NHS or University institutions within the

United Kingdom. External collaborators will be required to sign a code of conduct to guarantee that any data received will be kept fully confidential and secure.

Your MR images will only be used for the above purposes if approved by a Data Access Committee made up of local scientists, clinicians, and managers together with input from the regional ethics committee

In addition to the above, we will also ask you to inform us whether you have recently participated in or are currently involved in other research prior to this study.

Examples of how your anonymised images might be used in the future

Research: Your anonymised images could be scientifically reviewed and then compared to images from people who have a health condition. The results of this work might be published in a scientific journal, but your identity would never be disclosed.

Education: Your anonymised images could be used in visual presentations for student teaching or for presenting work at scientific meetings. Again, your identity would never be disclosed.

Technical Development: Your anonymised images could be used to demonstrate that a new piece of MRI equipment or computer software is working well. This might require us to send the images to a UK collaborator, but your identity would never be disclosed.

Quality Control: Your anonymised images could be compared with older or newer images taken on the same or other MRI scanners to ensure that optimal imaging standards are maintained.

Will my GP be informed?

It is normal practice for us to inform your GP of your participation in this study as long as you are happy for this to occur. Further, in the event that we find an incidental finding in your images we would wish to provide you and your GP with this information in order to plan further medical care. By signing the informed consent declaration you agree to us taking this course of action should this unlikely situation arise.

Your rights:

Participation in this study is entirely voluntary and you are free to refuse to take part or withdraw from the study at any time without having to give any reason.

Who has reviewed the study?

The East of Scotland Research Ethics Committee which has responsibility for scrutinising all proposals for human research in Tayside has examined this proposal and has raised no objections from the point of view of medical ethics. The study is sponsored and overseen by the University of Dundee and NHS Tayside in collaboration. It is a requirement that your records in this research, together with any relevant medical records, be made available for scrutiny by monitors from NHS Tayside and the University of Dundee, whose role is to check that research is properly conducted and the interests of those taking part are adequately protected. All information will be strictly confidential, anonymised and coded, and will be stored electronically on a database that will only be accessible by the current investigators. The information will be kept for 5 years after which it will be destroyed.

Contact for further information?

For further information or help regarding this study please contact:

Principal Investigator:
Dr Jonathan Weir-McCall
Clinical Radiology
Ninewells Hospital
Dundee
DD1 9SY
Tel: 01382 660111 Bleep. 3188

Chief Investigator:
Prof Graeme Houston
Clinical Radiology
Ninewells Hospital
Dundee
DD1 9SY
Tel: 01382 632651

Thank you for taking the time to consider taking part in this study.

Appendix C: Consent Form

NHS Tayside

Title of Study: **The role of pulmonary arterial stiffness on right ventricular remodeling in COPD.**

Name of CI: **Prof. Graeme Houston**

Name of PI: **Dr Jonathan Weir-McCall**

Please initial box

1. I confirm that I have read and understood the information sheet dated …. (Version …) for the above study. I have had the opportunity to consider the information, ask questions and have had these answered satisfactorily.

2. I understand that my participation is voluntary and that I am free to withdraw at any time without giving any reason, without any medical care or legal rights being affected.

3. I agree that I will not be informed of any incidental findings such as set out in the Information Sheet unless the researcher decides that such findings may have an important bearing on my future medical care.

4. I understand that relevant sections of my medical notes and data collected during the study may be looked at by individuals from NHS Tayside, University of Dundee or other collaborative EU Healthcare or University Organisations where it is relevant to my taking part in this research. I give permission for these individuals to have access to my records.

5.   I consent to my images being used anonymously for purposes research, education, technical development and quality control at NHS Tayside, University of Dundee or at other collaborative NHS or University institutions within the United Kingdom   ☐

6.   I agree to my blood samples being stored for future research use. I agree to the use of this for future biomarker and genomic research.   ☐

7.   I agree to my GP being informed of my participation in the study.   ☐

8.   I agree to take part in the above study.   ☐

_____   _____   _____

Name of participant   Date   Signature

_____   _____   _____

Name of person taking consent   Date   Signature

Appendix D: Case Report Forms

PARTICIPANT ID: |___|___|___|

The role of pulmonary arterial stiffness on right ventricular remodeling in COPD.

———————

**The trial is sponsored by
NHS Tayside**

Principal Investigator: Graeme Houston
Clinical Radiology
Ninewells Hospital
Dundee DD1 9SY
Tel: 01382 632651
Email: ghouston@nhs.net

GENERAL GUIDELINES FOR THE CASE REPORT FORM COMPLETION

All clinical data collected during the study has to be documented in this case report form.

Please use a black ball-point pen for filling in the case report form.

Incorrect entries should be deleted with a single line. The original entry must be kept legible. All changes and/or corrections made to the case report form must be initialled and dated by the investigator or by another responsible person of the respective study centre.

Please answer all questions and write clearly.

Identification of patients throughout the study is done by patient number only.

Please enter only one digit in one box. Data should be entered at the right hand margin. If not enough digits are available to fill all fields, please prefix the number by recording "0".

Please enter complete dates wherever possible. If day or month of a date should be unknown, please enter "NK" in the respective fields. e.g.: NK/MAY/2004

Times should be entered using the 24-hour clock. Please enter times from 00:00 to 23:59. Do not use 24:00.

If a question is not applicable, please record "NA" for "not applicable".

If an examination was not done, please record "ND" for "not done".

If a result is zero, please enter "0".

If a page has not been used, please enter the patient number and cross out the page.

Comments should be as short as possible. Please do not enter comments outside the predefined areas (Final Comment Page).

The case report form has to be signed by the investigator. If a premature termination of the trial occurs in a patient, the case report form should be completed up to this day and the termination form (page XX) must be filled in.

Date of Visit

D D M M M Y Y Y Y

Date of Birth   Age [ ] yrs

D D M M M Y Y Y Y

Sex   ☐ Male   ☐ Female

Consent obtained   ☐ Yes   ☐ No   Date of Consent

D D M M M Y Y Y Y

_____

INCLUSION CRITERIA   YES   NO

Male and female aged 40-85 inclusive   ☐   ▣

COPD GOLD grade 2-4   ☐   ▣

FEV1 <80% predicted and FEV1/FVC ratio <70%   ☐   ▣

Smoking history ≥10 pack years   ☐   ▣

No exacerbation in the past 2 months   ☐   ▣

EXCLUSION CRITERIA   YES   NO

History of significant cardiac condition   ▣   ☐

Previous cardiac or thoracic operation   ▣   ☐

History of other primary or obstructive lung disease   ▣   ☐

Connective tissue disease or systemic vasculitis.   ▣   ☐

Moderate or severe LV systolic dysfunction (EF <40%)   ▣   ☐

Currently participating in an interventional clinical trial   ▣   ☐

Pregnancy   ▣   ☐

Inability to provide informed consent   ▣   ☐

☞ **If any of the shaded boxes is ticked, patient is not eligible for the study**

MRI ELIGIBILITY

Does the subject currently have   YES   NO

eGFR <30mls/min   ▣   ☐

Claustrophobia   ▣   ☐

Any metal implants or pacemaker   ▣   ☐

Patient eligible for MRI   ☐   ▣

OTHER MEDICAL HISTORY

Give brief details of all significant illnesses or operations with dates

Body System	Normal	Abnormal	Details
Cardiovascular	☐	☐	
Respiratory	☐	☐	
Gastrointestinal	☐	☐	
Genitourinary	☐	☐	
Endocrine/Metabolic	☐	☐	
CNS	☐	☐	
Dermatological	☐	☐	
HEENT	☐	☐	
Psychiatric	☐	☐	
Locomotor	☐	☐	
Haematological	☐	☐	
Other	☐	☐	

Any illnesses which would compromise the patient's safety or ability to complete the study   ☐Yes ☐No

CONCOMITANT MEDICATION PRESENT   ☐Yes ☐No

☞ If yes, please complete concomitant medication page

CONCOMITANT MEDICATION

Any Concomitant Medication Reported ☐Yes ☐No

Drug Name (Trade Name preferred)	Dose	Unit	Route	Freq.	Indication	Start Da (DD-MMM-Y
1.						|⌊⌊⌊⌊⌊⌊|
2.						|⌊⌊⌊⌊⌊⌊|
3.						|⌊⌊⌊⌊⌊⌊|
4.						|⌊⌊⌊⌊⌊⌊|
5.						|⌊⌊⌊⌊⌊⌊|
6.						|⌊⌊⌊⌊⌊⌊|
7.						|⌊⌊⌊⌊⌊⌊|
8.						|⌊⌊⌊⌊⌊⌊|
9.						|⌊⌊⌊⌊⌊⌊|
10.						|⌊⌊⌊⌊⌊⌊|
11.						|⌊⌊⌊⌊⌊⌊|

Route of Administration: 1=Oral, 2=Subcutaneous, 3=Intramuscular, 4=Intravenous, 5=Rectal, 6=Topical, 7=Inhaled, 8=Other

Frequency: 1=1/day, 2=2/day, 3=3/day, 4=4/day, 5=prn, 6=Other

CONCOMITANT MEDICATION CONTINUED

Repeat Page Number ☐

Drug Name (Trade Name preferred)	Dose	Unit	Route	Freq.	Indication	Start Date (DD-MMM-Y
1.						└┴┴┴┴┘
2.						└┴┴┴┴┘
3.						└┴┴┴┴┘
4.						└┴┴┴┴┘
5.						└┴┴┴┴┘
6.						└┴┴┴┴┘
7.						└┴┴┴┴┘
8.						└┴┴┴┴┘
9.						└┴┴┴┴┘
10.						└┴┴┴┴┘
11.						└┴┴┴┴┘

Route of Administration: 1=Oral, 2=Subcutaneous, 3=Intramuscular, 4=Intravenous, 5=Rectal, 6=Topical, 7=Inhaled, 8=Other

Frequency: 1=1/day, 2=2/day, 3=3/day, 4=4/day, 5=prn, 6=Other

COPD INFORMATION

Date of diagnosis |___|___|___|___|___|___|___|___|

Smoking status

Never Smoked   ☐

Ex Smoker   ☐

Current Smoker   ☐

If Current or Ex Smoker, please indicate the average amount/ day:

Cigarettes |___|___|

Cigars |___|

Pipes |___|

If Ex-Smoker, Date stopped |___|___|___|___|___|___|___|___|
                            D   D   M   M   M   Y   Y   Y   Y

Number of years smoked |___|___|

Screening PFTs   ☐ Yes ☐ No Date |___|___|___|___|___|___|___|___|

   FEV1/FVC |_._|___|___|

   FEV1 (% predicited) |_._|___|___|

Symptom severity

   mMRC dyspnea grade: |___|___|

Grade	Description of Breathlessness
0	I only get breathless with strenuous exercise.
1	I get short of breath when hurrying on level ground or walking up a slight hill.
2	On level ground, I walk slower than people of the same age because of breathlessness, or have to stop for breath when walking at my own pace.
3	I stop for breath after walking about 100 yards or after a few minutes on level ground.
4	I am too breathless to leave the house or I am breathless when dressing.

Exacerbations

COPD exacerbation in the last year   ☐Yes ☐No

    Requiring antibiotics/steroids   ☐Yes ☐No

    Requiring hospital admission   ☐Yes ☐No
    Date of most recent exacerbation

          |__|__|__|__|__|__|__|__|

Combined COPD assessment:

Score: |__|__|
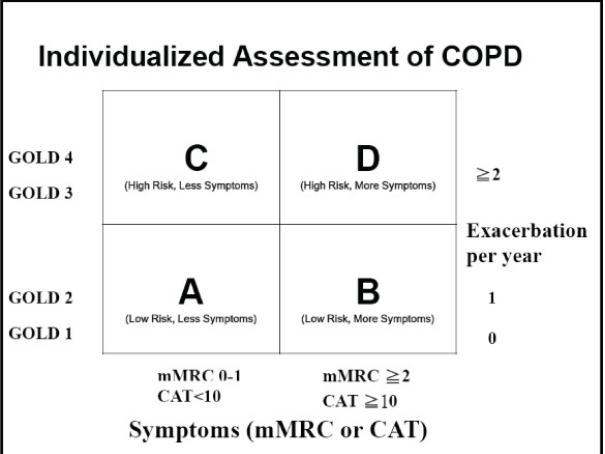
Individualized Assessment of COPD

	C (High Risk, Less Symptoms)	D (High Risk, More Symptoms)	≥2
GOLD 4 / GOLD 3			
GOLD 2 / GOLD 1	A (Low Risk, Less Symptoms)	B (Low Risk, More Symptoms)	1 / 0
	mMRC 0-1 CAT<10	mMRC ≥2 CAT ≥10	Exacerbation per year

Symptoms (mMRC or CAT)

VITAL SIGNS

Blood Pressure: Systolic | mmHg   Diastolic | mmHg   Pulse | per minute

Height   cm.   Weight . kg   BMI   .

☞ *Measured after 5 minutes rest, sitting, on the dominant arm*

_____

Echo

LVIDd   . mm

LVIDs   . mm

LVFS   . %

LVEF   . %

RAP   . %

TRV   . m/s

Pulmonary PAT   . ms

_____

ELIGIBILITY

Is the Patient eligible to participate in the study   ☐ Yes ☐ No

If no, please comment:_____ _____

_____

BLOOD TESTS

Date of Blood Samples taken

D   D   M   M   M   Y   Y   Y   Y

eGFR ☐ Yes ☐ No

Result __._ ml/min/m²

Samples stored ☐ Yes ☐ No By: _____

Date Sample stored

D   D   M   M   M   Y   Y   Y   Y

_____

Practice 6MWT

Pre   SpO2_____   Pre walk dyspnoea _____   Pre walk fatigue_____

Pre-   BP 1 _____/_____ HR_____

6 MWT distance: _____m

Post   SpO2_____   Post walk dyspnoea_____   Post walk fatigue   _____

Post-   BP 1 _____/_____ HR_____

_____

COMMENTS

Any Comments Present? ☐Yes ☐No

Page No	Field	Comment

VISIT 2

Date agreed for second visit? ☐ Yes
                                ☐ No

Date of next visit |___|___|___|___|___|___|___|___|

INVESTIGATOR STATEMENT

I hereby certify that all information entered by myself or my team is, to the best of my knowledge, correct.

Signature: _____ Date: _____

Main Visits:

Participant ID: ☐ ☐ ☐

The role of pulmonary arterial stiffness on right ventricular remodeling in COPD.
VISIT 2
_____

The trial is sponsored by
NHS Tayside

Principal Investigator: Graeme Houston
Clinical Radiology
Ninewells Hospital
Dundee DD1 9SY
Tel: 01382 632651
Email: ghouston@nhs.net

GENERAL GUIDELINES FOR THE CASE REPORT FORM COMPLETION

All clinical data collected during the study has to be documented in this case report form.

Please use a black ball-point pen for filling in the case report form.

Incorrect entries should be deleted with a single line. The original entry must be kept legible. All changes and/or corrections made to the case report form must be initialled and dated by the investigator or by another responsible person of the respective study centre.

Please answer all questions and write clearly.

Identification of patients throughout the study is done by patient number only.

Please enter only one digit in one box. Data should be entered at the right hand margin. If not enough digits are available to fill all fields, please prefix the number by recording "0".

Please enter complete dates wherever possible. If day or month of a date should be unknown, please enter "NK" in the respective fields. e.g.: NK/MAY/2004

Times should be entered using the 24-hour clock. Please enter times from 00:00 to 23:59. Do not use 24:00.

If a question is not applicable, please record "NA" for "not applicable".

If an examination was not done, please record "ND" for "not done".

If a result is zero, please enter "0".

If a page has not been used, please enter the patient number and cross out the page.

Comments should be as short as possible. Please do not enter comments outside the predefined areas (Final Comment Page).

The case report form has to be signed by the investigator. If a premature termination of the trial occurs in a patient, the case report form should be completed up to this day and the termination form (page XX) must be filled in.

Date of Visit	⊔⊔⊔⊔⊔⊔⊔⊔	
	D D M M M Y Y Y Y	

Date of Birth	⊔⊔⊔⊔⊔⊔⊔⊔	Age ⊔⊔ yrs
	D D M M M Y Y Y Y	

Sex ☐ Male ☐ Female

Consent obtained ☐ Yes ☐ No   Date of Consent ⊔⊔⊔⊔⊔⊔⊔⊔

D D M M M Y Y Y Y

_____

INCLUSION CRITERIA

	YES	NO
Male and female aged 40-85 inclusive	☐	▨
COPD GOLD grade 2-4	☐	▨
FEV1 <80% predicted and FEV1/FVC ratio <70%	☐	▨
Smoking history ≥10 pack years	☐	▨
No exacerbation in the past 2 months	☐	▨

EXCLUSION CRITERIA

	YES	NO
History of significant cardiac condition	▨	☐
Previous cardiac or thoracic operation	▨	☐
History of other primary or obstructive lung disease	▨	☐
Connective tissue disease or systemic vasculitis.	▨	☐
Moderate or severe LV systolic dysfunction (EF <40%)	▨	☐
Currently participating in an interventional clinical trial	▨	☐
Pregnancy	▨	☐
Inability to provide informed consent	▨	☐

☞ **If any of the shaded boxes is ticked, patient is not eligible for the study**

MRI ELIGIBILITY
Does the subject currently have

	YES	NO
eGFR <30mls/min	▨	☐
Claustrophobia	▨	☐
Any metal implants or pacemaker	▨	☐
Patient eligible for MRI	☐	▨

ADVERSE EVENTS REMINDER

Did any Adverse Events occur since the last visit ☐Yes ☐No

☞ **If yes, please fill in the Adverse Events Page**

CONCOMITANT MEDICATIONS REMINDER

Where there any changes to Concomitant Medication since the last visit ☐Yes ☐No

☞ **If yes, please fill in the Concomitant Medications Page**

_____

ELIGIBILITY

Is the Patient eligible to participate in the study ☐Yes ☐No

If no, please comment:_____ _____

_____

ADVERSE EVENTS

Any Adverse Events Reported ☐Yes ☐No

Adverse Event	Serious 1=Yes 2=No	Start Date (DD-MMM-YYYY)	Stop Date (DD-MMM-YYYY)	Ongoing 1=Yes 2=No	Sev
1.					
2.					
3.					
4.					
5.					
6.					

Severity: 1=Mild, 2=Moderate, 3=Severe

Relationship: 1=None, 2=Possible, 3=Probable, 4=Likely, 5=Unknown

Action taken: 1=None, 2=Medication, 3=Treatment, 4=Other

Outcome: 1=Not Yet Recovered , 2=Resolved without sequelae, 3=Resolved with sequelae, 4=Worsened, 5=Death

☞ *If Outcome is Resolved with sequelae, Worsened or Death, please complete a Serious Adverse Event/ Serious Adverse Reaction Notification Form*

CONCOMITANT MEDICATION CONTINUED

Repeat Page Number ☐

Drug Name (Trade Name preferred)	Dose	Unit	Route	Freq.	Indication	Start Date (DD-MMM-Y...
1.						⌊_⌊_⌊_⌊_⌊
2.						⌊_⌊_⌊_⌊_⌊
3.						⌊_⌊_⌊_⌊_⌊
4.						⌊_⌊_⌊_⌊_⌊
5.						⌊_⌊_⌊_⌊_⌊
6.						⌊_⌊_⌊_⌊_⌊
7.						⌊_⌊_⌊_⌊_⌊
8.						⌊_⌊_⌊_⌊_⌊
9.						⌊_⌊_⌊_⌊_⌊
10.						⌊_⌊_⌊_⌊_⌊
11.						⌊_⌊_⌊_⌊_⌊

Route of Administration: 1=Oral, 2=Subcutaneous, 3=Intramuscular, 4=Intravenous, 5=Rectal, 6=Topical, 7=Inhaled, 8=Other

Frequency: 1=1/day, 2=2/day, 3=3/day, 4=4/day, 5=prn, 6=Other

STUDY PFTs

pirometry	1	% Pred	2	% Pred	3	% Pred	Highest	Highest % pred
VC								
EV$_1$								
FVC								
EF								
EV$_1$ FVC								

EF 2575								

IOS   ☐ *Keep print outs in patients' folders*

Body Plethysmography   ☐ *Keep print outs in patients' folders*

6 MWT

Pre SpO2 _____ Pre walk dyspnoea _____ Pre walk fatigue _____

Pre-
BP 1 _____/_____ HR_____ BP 2 _____/_____ HR_____ BP 3_____/_____HR_____ **Average BP 1 _____/_____ HR_____**

6 MWT distance: _____m

Post SpO2 _____ Post walk dyspnoea _____ Post walk fatigue _____

Post-
BP 1 _____/_____ HR_____ BP 2 ____/____ HR_____ BP **3**____/_____HR_____ **Average BP 1 _____/_____ HR_____**

COPD INFORMATION

St George's COPD questionnaire completed: ☐ Yes ☐ No

VITAL SIGNS

Blood Pressure: Systolic └──┴──┴──┘ mmHg   Diastolic └──┴──┴──┘ mmHg   Pulse └──┴──┴──┘ per minute

Height └──┴──┴──┘ cm.   Weight └──┴──┴──┘.└──┘ kg   BMI └──┴──┘.└──┘

☞ *Measured after 5 minutes rest, sitting, on the dominant arm*

BLOOD TESTS

Date of Blood Samples taken └──┴──┴──┴──┴──┴──┴──┴──┘

D   D   M   M   M   Y   Y   Y   Y

eGFR   ☐ Yes ☐ No

Result └──┴──┴──┘.└──┘ ml/min/m²

Samples stored   ☐ Yes ☐ No By: _____

Date Sample stored   └──┴──┴──┴──┴──┴──┴──┴──┘

D   D   M   M   M   Y   Y   Y   Y

MRI

Date of MRI |___|___|___|___|___|___|___|___|

D   D   M   M   M   Y   Y   Y   Y

Safety checks for MRI performed ☐ Yes ☐ No

Patient eligible for MRI ☐ Yes ☐ No

If no, please comment:_____

_____

MRI RESULTS

<u>Blood Pressure:</u>

PWV1 measurement: Systolic |___|___|___| mmHg   Diastolic |___|___|___| mmHg

PWV2 measurement: Systolic |___|___|___| mmHg   Diastolic |___|___|___| mmHg

CARDIAC FUNCTION

	Results
LV EF (%)	
LVEDV (ml)	
LVESV (ml)	
LVSV (ml)	
Cardiac output (CO) (min/ml)	
Left ventricular mass (LVM) (g)	
RVEF (%)	
RVEDV (ml/m^2)	
RVESV (ml/m^2)	
RVSV (ml/m^2)	
RVM (g/m^2)	

Pulmonary Pulse Wave Velocity:

PWV |___|___| |___|.___| m/s

Pulsatility |___|___|___| |___|.___| %

Aortic Pulse Wave Velocity:

PWV |___|___| |___|.___| m/s

Compliance |___|___|___| |___|.___| cm Hg

Delayed Gadolinium   YES ☐   NO ☐

		A	AS	S	I	IL	AL
If Yes, Segmental Enhancement:	Basal	☐	☐	☐	☐	☐	☐
Mid		☐	☐	☐	☐	☐	☐

	A	S	I	L
Apical	☐	☐	☐	☐

A=Anterior, AS=Anteroseptal, S=Septal, I=Inferior, L=Lateral

Subendocardial   YES ☐   NO ☐

Maximal Wall Thickness Enhancement: ☐

| 0 = nil |
| 1 < 50% |
| 2 > 50% |

Endocardial   YES ☐   NO ☐

Focal   YES ☐   NO ☐

Generalised   YES ☐   NO ☐

COMMENTS

Any Comments Present? ☐ Yes ☐ No

Page No	Field	Comment

VISIT COMPLETION

Did the patient complete the visit as planned ☐ Yes

☐ No ☞ *Please state reason below*

Date of last study procedure |___|___|___|___|___|___|___|___|
D D M M M Y Y Y Y

_____
_____

If the visit was not completed as planned, please state the reason for study termination:

Patient withdrawal of consent ☐

Investigator's discretion ☐

Intercurrent illness ☐ ☞ *Please document under Adverse Events*

Changes in the patient's condition ☐

Noncompliance with study procedures ☐

Termination of the clinical trial ☐

Other ☐ Please describe
_____

_____
_____

_____
_____

INVESTIGATOR STATEMENT

I hereby certify that all information entered by myself or my team is, to the best of my knowledge, correct.

Signature: _____   Date:_____

Appendix E: Ethics Approval

East of Scotland Research Ethics Service (EoSRES) REC 1
Tayside Medical Sciences Centre (TASC)
Residency Block C, Level 3
Ninewells Hospital & Medical School
George Pirie Way
Dundee DD1 9SY

Professor Graeme Houston
Chair of Clinical Imaging
University of Dundee
Ninewells Hospital & Medical School
Dundee
DD1 9SY

Approved documents

The final list of documents reviewed and approved by the Committee is as follows:

Document	Version	Date
Advertisement	1	14 January 2014
Evidence of insurance or indemnity		01 August 2013
GP/Consultant Information Sheets	1.0	13 January 2014
Investigator CV		
Letter from Sponsor		21 January 2014
Letter of invitation to participant from clinic	1	13 January 2014
Letter of invitation to participant from GP	1	17 January 2014
Letter of invitation to participant – previous study participant	1	17 January 2014
Other: Letter from funder		22 July 2013
Other: CV - Dr Jonathan Weir-McCall		
Other: Reply Slip	1.0	13 January 2014
Other: Email covering letter		07 April 2014
Participant Consent Form: highlighted changes	1.1	07 April 2014
Participant Information Sheet: Healthy Volunteers – highlighted changes	1.1	07 April 2014
Participant Information Sheet: COPD - highlighted changes	1.1	25 March 2014
Protocol	1.1	07 April 2014
Questionnaire: SGRQ-COPD		01 September 2005
REC application	130196/569854/1/760	18 February 2014
Response to Request for Further Information		

Statement of compliance

The Committee is constituted in accordance with the Governance Arrangements for Research Ethics Committees and complies fully with the Standard Operating Procedures for Research Ethics Committees in the UK.

After ethical review

Reporting requirements

The attached document *"After ethical review – guidance for researchers"* gives detailed guidance on reporting requirements for studies with a favourable opinion, including:

- Notifying substantial amendments
- Adding new sites and investigators
- Notification of serious breaches of the protocol
- Progress and safety reports
- Notifying the end of the study

The NRES website also provides guidance on these topics, which is updated in the light of changes in reporting requirements or procedures.

Feedback

You are invited to give your view of the service that you have received from the National Research Ethics Service and the application procedure. If you wish to make your views known please use the feedback form available on the website.

Further information is available at National Research Ethics Service website > After Review

14/ES/0034:	Please quote this number on all correspondence

We are pleased to welcome researchers and R & D staff at our NRES committee members' training days – see details at http://www.hra.nhs.uk/hra-training/

Yours sincerely

pp
Dr Carol Macmillan
Chair

eosres.tayside@nhs.net

 Enclosures:

Conditions of the favourable opinion

The favourable opinion is subject to the following conditions being met prior to the start of the study.

- **Under "What will the MRI scan involve?" in the Participant Information Sheet – please include bruising as a complication to taking blood samples.**

Send updated information sheets with new version number and full date as a footer.

You should notify the REC in writing once all conditions have been met (except for site approvals from host organisations) and provide copies of any revised documentation with updated version numbers. The REC will acknowledge receipt and provide a final list of the approved documentation for the study, which can be made available to host organisations to facilitate their permission for the study. Failure to provide the final versions to the REC may cause delay in obtaining permissions.

Management permission or approval must be obtained from each host organisation prior to the start of the study at the site concerned.

Management permission ("R&D approval") should be sought from all NHS organisations involved in the study in accordance with NHS research governance arrangements.

Guidance on applying for NHS permission for research is available in the Integrated Research Application System or at http://www.rdforum.nhs.uk.

Where a NHS organisation's role in the study is limited to identifying and referring potential participants to research sites ("participant identification centre"), guidance should be sought from the R&D office on the information it requires to give permission for this activity.

For non-NHS sites, site management permission should be obtained in accordance with the procedures of the relevant host organisation.

Sponsors are not required to notify the Committee of approvals from host organisations

Registration of Clinical Trials

All clinical trials (defined as the first four categories on the IRAS filter page) must be registered on a publically accessible database within 6 weeks of recruitment of the first participant (for medical device studies, within the timeline determined by the current registration and publication trees).

There is no requirement to separately notify the REC but you should do so at the earliest opportunity e.g when submitting an amendment. We will audit the registration details as part of the annual progress reporting process.

To ensure transparency in research, we strongly recommend that all research is registered but for non clinical trials this is not currently mandatory.

If a sponsor wishes to contest the need for registration they should contact Catherine Blewett (catherineblewett@nhs.net), the HRA does not, however, expect exceptions to be made. Guidance on where to register is provided within IRAS.

It is the responsibility of the sponsor to ensure that all the conditions are complied with before the start of the study or its initiation at a particular site (as applicable).